ASSESSMENT OF GROUNDWATER INGRESS INTO MINE WORKINGS FROM THE DEEP-SEATED FRACTURED ROCK AQUIFER IN THE BUSHVELD IGNEOUS COMPLEX AT DISHABA MINE

Sbusiso Kwanda Dumakude

Submitted in fulfilment of the requirements for the degree

Magister Scientiae in Geohydrology

in the

Faculty of Natural and Agricultural Sciences

(Institute for Groundwater Studies)

at the

University of the Free State

Supervisor: Prof Francois Fourie

November 2023

DECLARATION

I, Sbusiso DUMAKUDE, hereby declare that the dissertation hereby submitted by me to the Institute for Groundwater Studies in the Faculty of Natural and Agricultural Sciences at the University of the Free State, in fulfilment of the degree of Magister Scientiae, is my own independent work. It has not previously been submitted by me to any other institution of higher education. In addition, I declare that all sources cited have been acknowledged by means of a list of references.

I furthermore cede copyright of the dissertation and its contents in favour of the University of the Free State.

Sbusiso DUMAKUDE

29 November 2023

ACKNOWLEDGEMENTS

I would hereby like to express my sincere gratitude to all who have motivated and helped me in the completion of this dissertation:

- Prof Francois Fourie for supervising and significantly improving this body of work.
- Colleagues in the Amandelbult Geosciences Department for constructive debates and inputs throughout the research. Special Mention Mrs Kesho Tlhagadi, Mr Raymond Makgato and Travis White for always supporting me and having faith in my abilities.
- Mr Magamu Moyo, Ms Nomthi Nxiweni, Mr Owen Chingobo and Mr Philly Mofomme for sharing their insights and experience on water issues in Amandelbult.
- Mr Sasha-Dean Singh, Mrs Julie Loreti and Mr Angus Rowland who entertained my crazy ideas and thoughts on Bushveld Hydrogeology
- Fellow students Libuseng Kulube, Bokang Nkadimeng and Hlengiwe Malatji for support through the coursework and input to my research.
- Last and by no means least, my wife Jennifer and my sons Nhlakanipho and Nhlalo and my mother Busisiwe Ngubane for being an amazing support system.

TABLE OF CONTENTS

LIST OF FIGURES

LIST OF TABLES

LIST OF UNITS, SYMBOLS AND ABBREVIATIONS

^{o}	degree
%	per cent
‰	per mille
^{o}C	degree Celcius
ANCR	anorthosite with chromitite bands
ASG	Advance Strike Gully
BIC	Bushveld Igneous Complex
CRF	Contact Reef
DWAF	Department of Water Affairs and Forestry
DWS	Department of Water and Sanitation
FW	footwall
Ga	Giga annum (one billion years)
ha	hectare
HDD	Haakdoorndrift
HLGE	Haulage
HW	hanging wall
km	kilometer
km^2	square kilometer
L/d	liter per day
L/h	liter per hour
LGS	Lebowa Granite Suite
m^3/d	cubic meter per day
Ma	mega annum (one million years)
mamsl	metre above mean sea level
mbgl	metre below ground level
mbmsl	metre below mean sea level
meq	milliequivalents

MER	Merensky reef
mg/L	milligram per liter
ML	megaliter
ML/d	megaliter per day
mm	millimeter
NMR	Normal Reef
P1	Lower Pseudo Reef
P2	Upper Pseudo Reef
PGEs	platinum group elements
PHR	Pothole Reef
RGS	Rashoop Granophyre Suite
RLS	Rustenburg Layered Suite
RMR	Rock Mass Rating
TRZ	Transition Zone
TML	Thabazimbi Murchison Lineament
UG1	Upper Group 1
UG2	Upper Group 2
UG2FW1	feldspathic pegmatoidal pyroxenite
VRT	Virgin Rock Temperature
Xcut	Cross Cut

CHAPTER 1:
INTRODUCTION

1.1 GENERAL INTRODUCTION

Dishaba Mine is reported to experience approximately 16 ML of groundwater ingress daily. The water ingresses occur across the mine, from off-reef haulages to mostly Merensky reef stopes. The water enters the mine workings through fractures, boreholes, and open mining excavations, and poses a risk in terms of mine safety. However, the water entering the mine also presents an opportunity for the mine to reduce its reliance on potable water and potentially use groundwater to meet day to day water requirements for mining and ore processing.

1.1.1 Location of Study Area

Dishaba Mine is a platinum mine in the southern part of the Limpopo province some 25 km south of Thabazimbi (Figure 1). The mine forms part of the Amandelbult Mining Complex of Anglo-American Platinum.

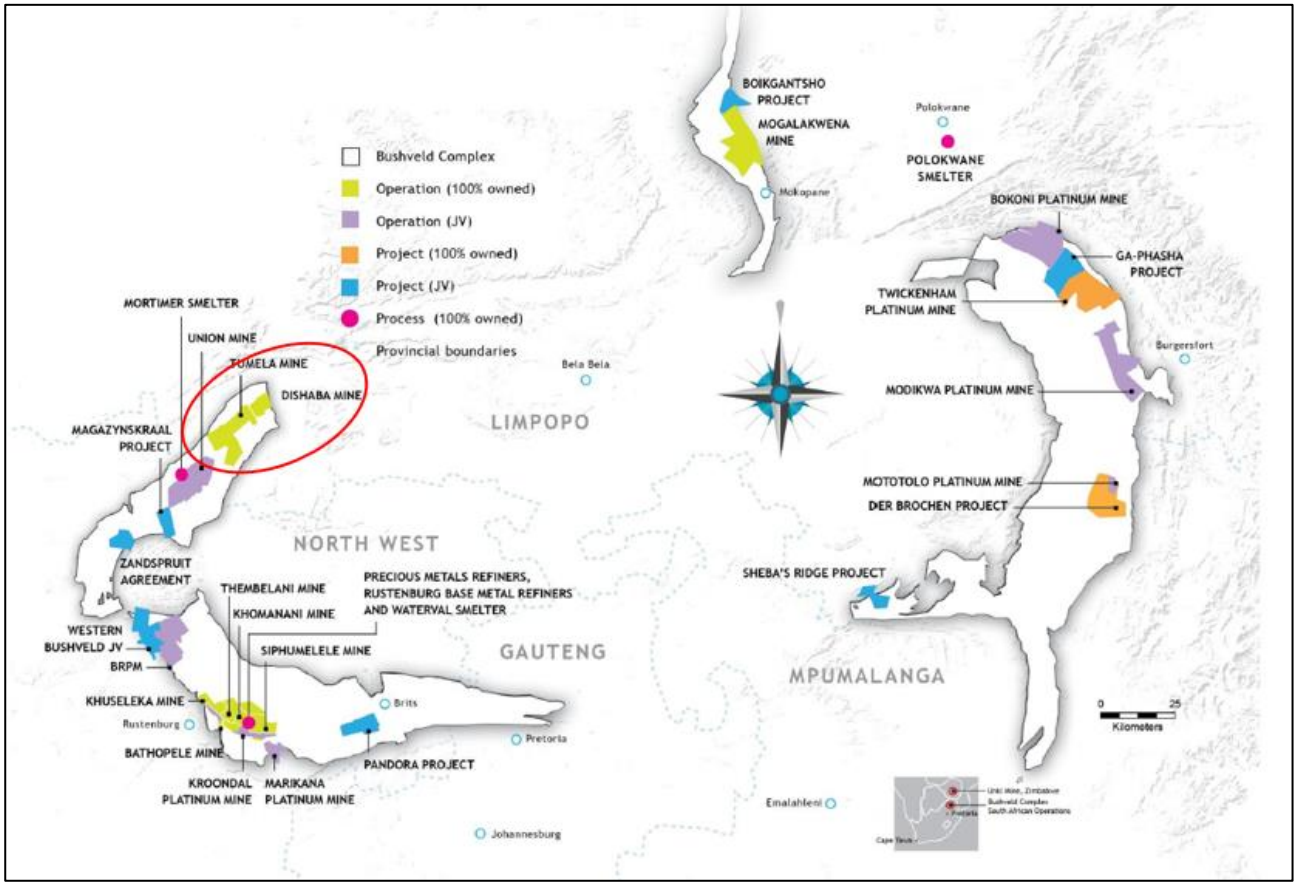

Figure 1: Location of Anglo American Platinum Operations. Note the Amandelbult Complex consisting of the Tumela and Dishaba Mines circled in red (Anglo Platinum, 2009).

The mine lies on the northernmost edge of the western limb of the Bushveld Igneous Complex (BIC). The north-eastern boundary of the mine lease extends along the Bushveld-Transvaal contact (Figure 1). The western boundary sits along the Middellaagte Graben and separates the mine from Tumela Mine lease area. The mine lease area covers an area of approximately 2700 ha across the farms: from west to east, Middellaagte 382 KQ, Elandskuil 378 KQ, Haakdoorndrift 374 KQ, and Grootkuil 376 KQ (Figure 2).

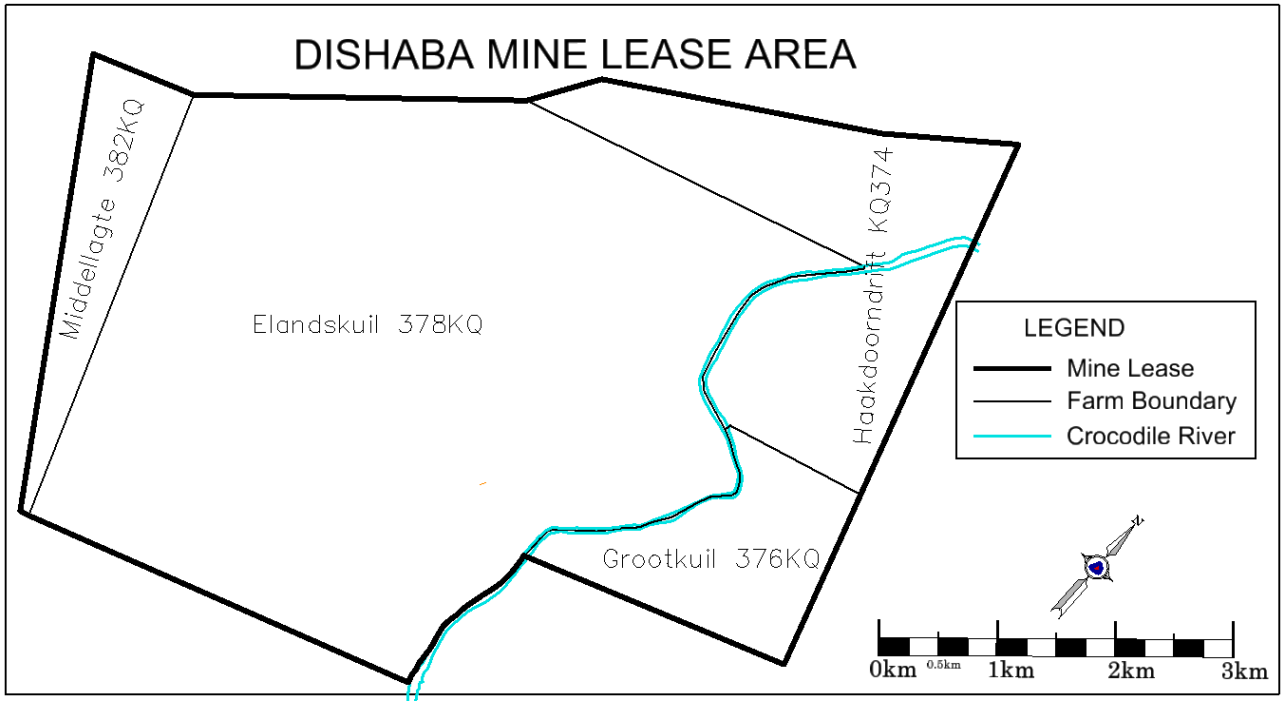

Figure 2: Farm portions covered by the Dishaba Mine lease.

1.1.2 Mining Method and Infrastructure

The UG2 (Upper Group 2) and MER (Merensky) reefs are narrow tabular orebodies (Moxham, 2004) with an average thickness of 1.5 m, dipping in the south-easterly direction between 18° and 25° (Walters *et al.*, 2004). The reefs are extracted from surface via an opencast operation, and through underground operations to depths of over 1 km below surface. Access to the underground portion of the mine is via the Vertical Shaft (#2 Shaft), three decline shafts (#44E, #50E and #62E) and 44E raise-bore (Figure 3).

Due to the inclined nature of the orebodies, the mine gets deeper in the S-E direction with middling of approximately 70 m between levels. Figure 4 shows a typical platinum mine section across a vertical shaft. The decline shafts are located on the outcrop side of the mine and at Dishaba Mine the deepest decline shaft ends on 9 Level, which is approximately 546 m below surface.

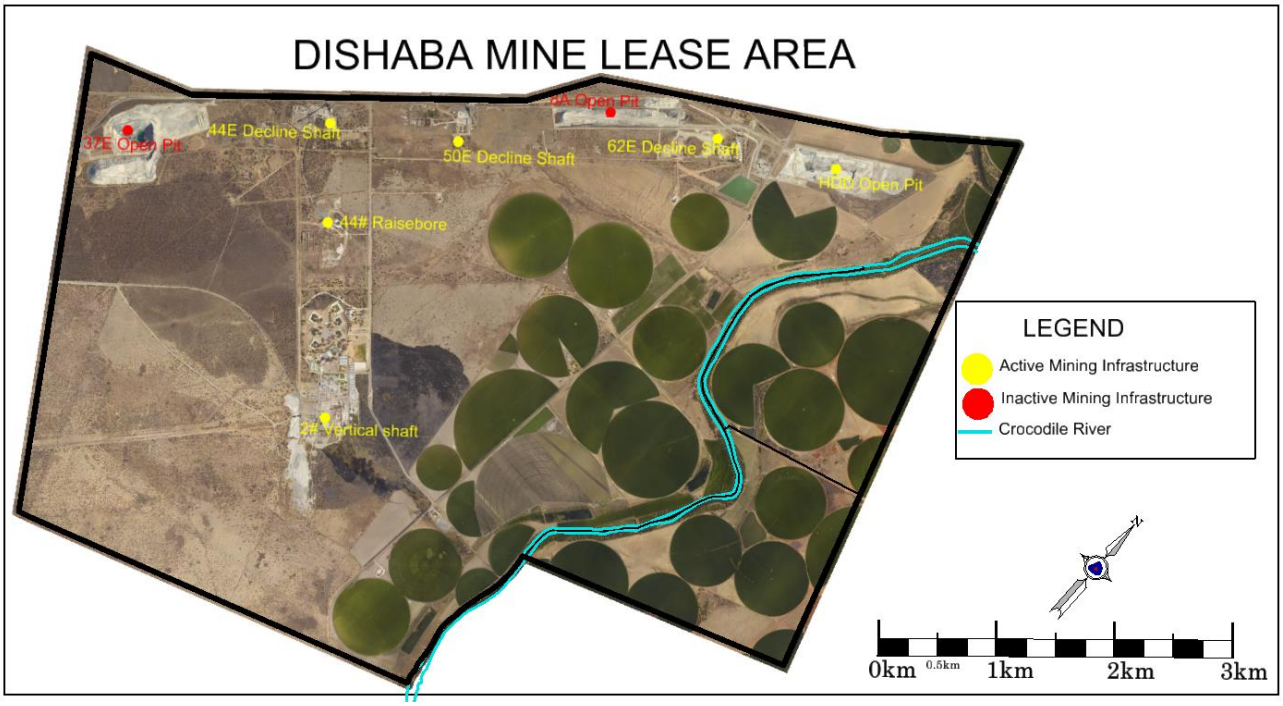

Figure 3: Mining infrastructure within the mine lease area.

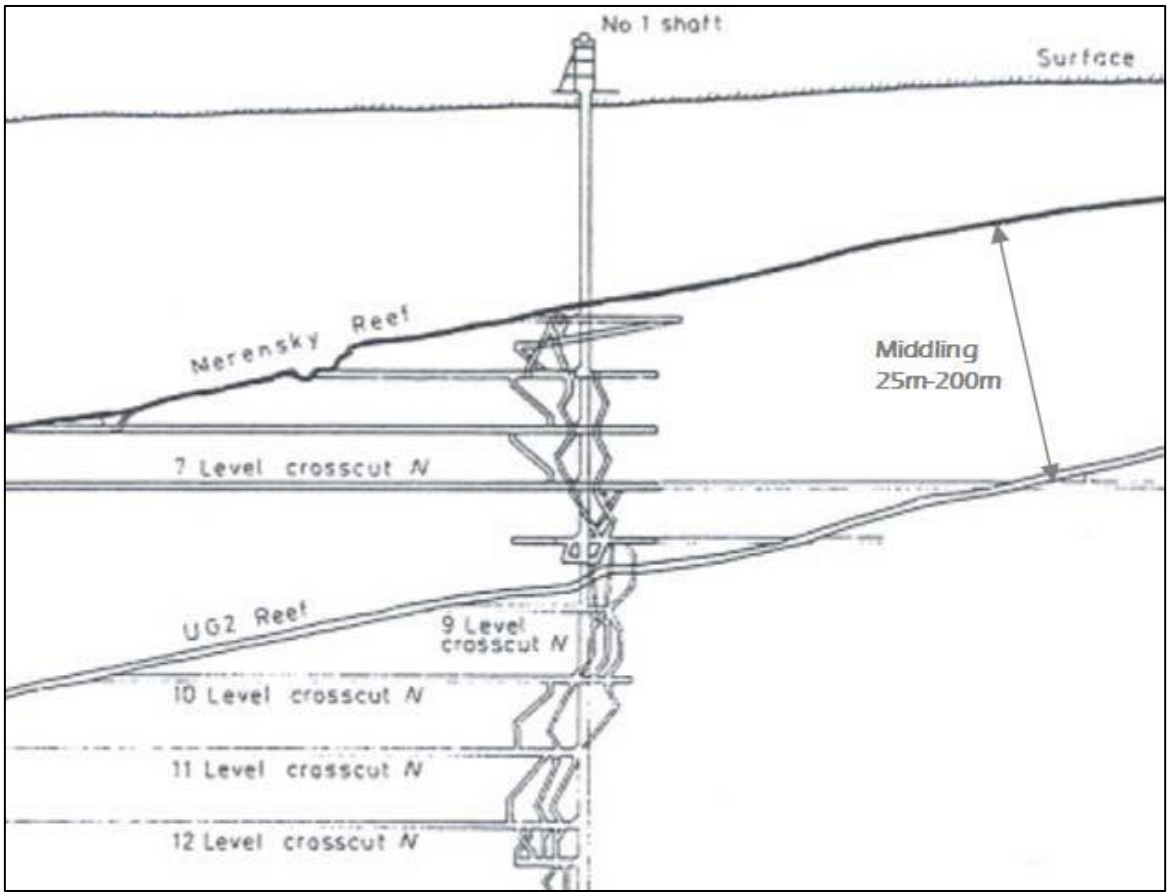

Figure 4: Typical section across a vertical shaft in the BIC. The middling between the UG2 and MER reef at Dishaba Mine is between 40 m and 60 m (adapted from Buchanan, 1987).

Conventional scattered breast mining is used across the underground operations of the mine. The reef is extracted from panels with a stoping width of approximately 1.5 m, then the blasted ore is

scraped into the 2.8-m-high advance strike gullies and raises. The blasted ore goes from the raise into a locomotive via an ore-pass (also called a box) which connects the raise and the crosscut. The locomotive then transports the blasted ore via the crosscut and haulage tunnels which are typical 3 m wide by 3 m high. The ore is then hoisted to surface and transported to the plant via the railway. Figure 5 shows a typical scattered breast mining layout.

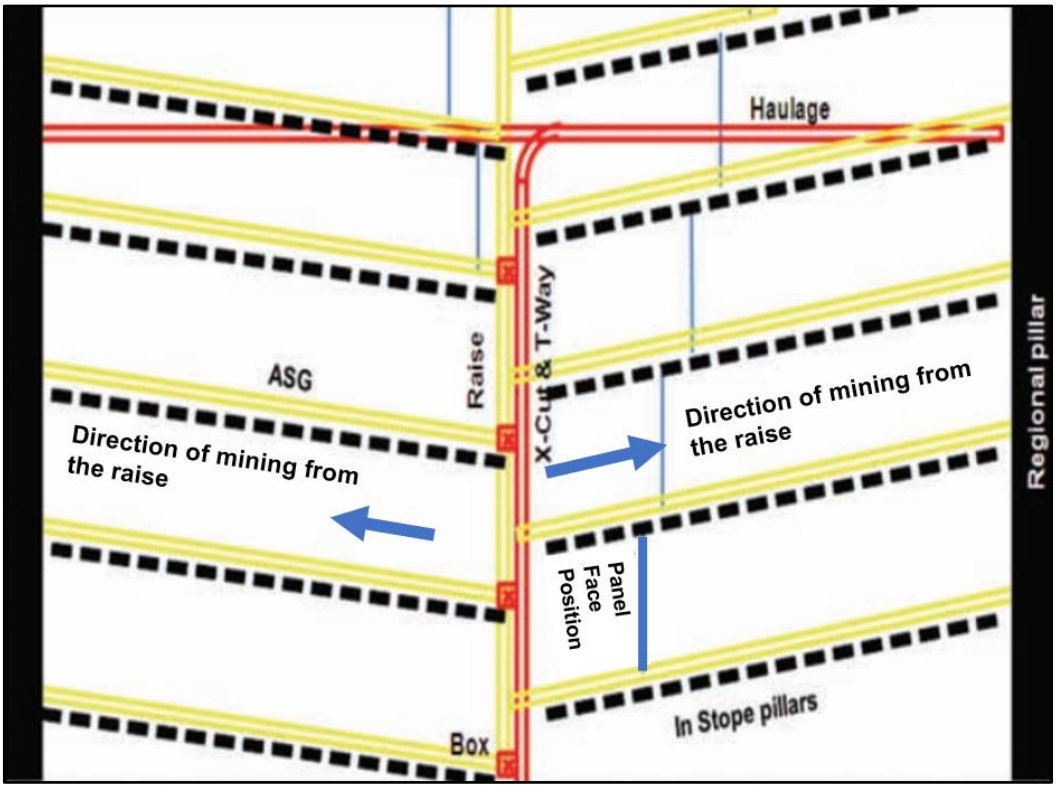

Figure 5: Typical scattered breast mining layout (adapted from Ferreira, 2012).

Figure 6 shows the layout of the mine. Locations in the mine are described using haulages and crosscut/raise lines. The naming is in the order of Level/Crosscut/Panel e.g., 5/55E means "5 Level, 55E Crosscut" while 5/55AE 3W means "5 Level, 55AE raise line, 3W panel". Panels are additionally specified whether they are UG2 or MER panels. A block of reef generally extending to about 100 m on either side of a raise is called a stope and consists of a few panels (typically up to five) on either side of a raise. Haulages are relatively flat (5° inclination) 3 m by 3 m tunnels excavated roughly along the strike direction of the orebody, i.e., along a SW-NE direction. The haulages are numbered as depth levels starting from 3 Level close to surface up to 20 Level at the bottom of the #2 Vertical Shaft. The vertical distance between the haulages is approximately 70 m. Crosscuts are also relatively flat (5° inclination) 3 m by 3 m excavations that are almost perpendicular to the haulages. Raise lines are developed from the crosscuts and share the same numbering as the crosscuts. Raise lines follow the dip of the reef (18° - 23° inclination) and connect multiple levels. A raise line will hence have the same number from 3 Level down to 19 Level. No active mining takes place on 20 Level and this level is used for hoisting.

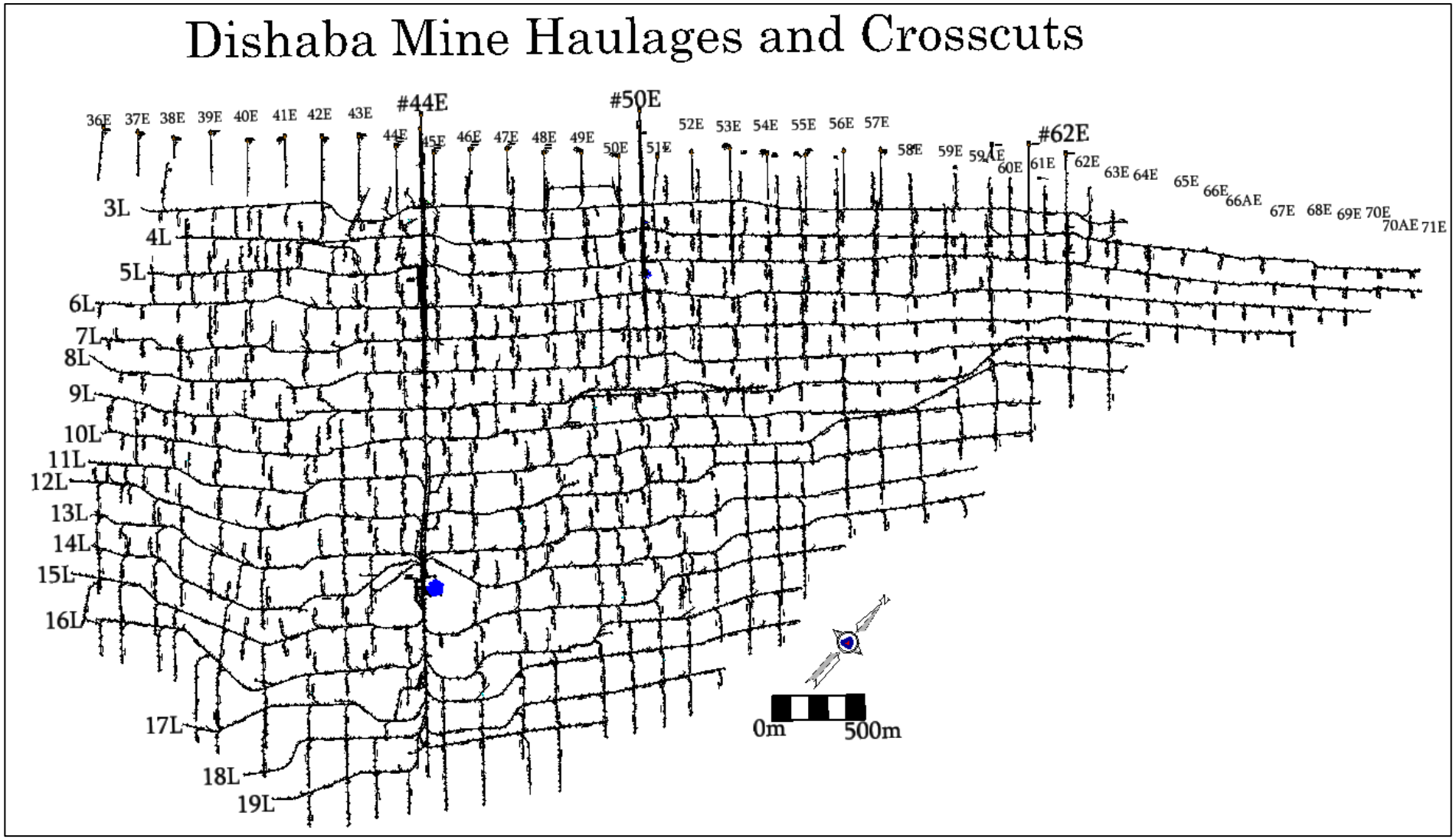

Figure 6: Plan view of the mining haulages and crosscuts at Dishaba Mine. The 2# Vertical Shaft is located on the blue dot along the 44E Line.

The crosscuts/raise lines are numbered laterally from 36E on the western side of the mine to 71E on the far eastern side of the mine. Note that the 0E to 34E lines occur in the neighbouring Tumela Mine, located on the south-western side of Dishaba Mine.

Figure 7 shows a typical raise line cross-section (along AB) while Table 1 shows the average depths of the different levels along the 44E Line and the #2 Vertical Shaft.

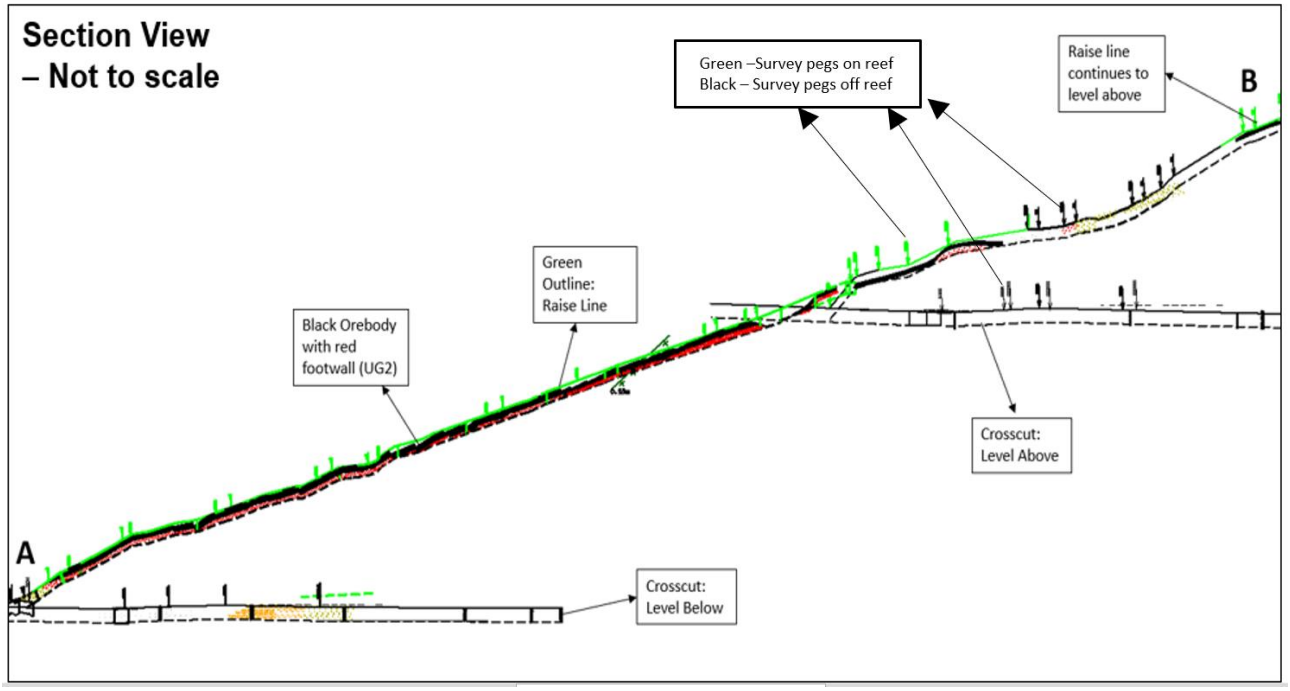

Figure 7: Typical raise line and crosscut configuration at Dishaba Mine.

Table 1: Average depths and elevations of different levels along the 44E line and #2 Vertical Shaft.

Level	Average depth below surface (m)	Elevation (mamsl)
3	150	787
4	211	726
5	277	660
6	344	593
7	410	527
8	477	460
9	546	391
10	610	327
11	681	256
12	752	185
13	823	114
14	894	43
15	964	-27
16	1033	-96
17	1101	-164
18	1169	-232
19	1240	-303

mamsl = meters above mean sea level

1.1.3 Historical Background

Dishaba Mine has been experiencing groundwater ingress into mine workings at various depths for many years (Ngubane *et al*., 2015). The hard lockdown brought about by the COVID pandemic brought mining operations to a complete standstill between March and April 2020. During this time, engineering pumping records (N. Nxiweni, personal communication, 2020) show that approximately 16 ML of groundwater was pumped out of the mine daily, and all water supply from surface was stopped. It can therefore reasonably be assumed that the water pumped from the mine was groundwater.

From where and how the water enters the mine is a subject of debate. Titus *et al.* (2009) proposed that the water enters the mine from surface via fracture networks that either drain the surface weathered aquifer or the nearby Crocodile River. Exploration boreholes (surface and underground) and open mining excavations then intersect these fractures leading to water running into the mining excavations.

Golder (2018) estimated an inflow of 16 ML/d into mine workings and indicated that this large volume of water would require recharge from another source other than the BIC. They then proposed that the water sources lie below and above the mining areas and identified possible source aquifers to be Chuniespoort Group, Magaliesberg quartzite and the Crocodile River alluvial sediments.

In a study into Limpopo thermal springs, Morrow (2015) concluded that the water originated from meteoric water which underwent water-rock interaction. The Piper plots of the analysed water samples revealed a Na-K-HCO_3 water. The geochemistry of the water was found to be largely influenced by the lithology through which the water flows, namely the Rustenburg Layered Suite of the BIC and the Pretoria Group sediments and dolomites of the Transvaal Supergroup. The tritium ages provided water-cycling age of 14.38 years.

Underground observations by Ngubane *et al*. (2015) showed that the water is mostly intersected along the anorthosites of the UG1 (Upper Group 1) footwall and the Merensky hanging wall. The water intersections are largely unpredictable and vary in quantity from 100 L/h to over 10 000 L/h. This water ingress impacts business planning and execution, causes safety concerns and accelerated wear and tear of equipment. However, the water ingress also presents an opportunity for groundwater harvesting and consequently a reduction in the reliance of the mine on fresh water supply from the Magalies Water Board.

The concentrator plant of the mine requires a water volume of approximately 24 ML/d. Currently, 10 ML/d comes from the Dishaba Underground and approximately 13.5 ML/d comes from Magalies Water Board (N. Nxiweni, personal communication, 2020). The groundwater intersections at Dishaba Mine therefore play a critical role in the business sustainability of the Amandelbult Mining Complex. However, a catch-22 situation arises. On the one hand, a dry mining environment is required for underground mining operations to continue safely and profitably. This means that groundwater must be sealed-off from the mine workings. Indeed, problems that arise due to the water ingress are well documented by Ngubane *et al*. (2015). On the other hand, the groundwater ingress is a significant water source for processing (plant) operations.

1.2 PROBLEM STATEMENT

Striking the balance between keeping the mine workings at Dishaba Mine dry and still being able to supply the plant with water remains a challenge. To get this right, a comprehensive groundwater management plan needs to be put in a place. For an appropriate and useful water management plan, it is imperative that water ingress is correctly mapped, the quantity and quality of water is known, and the structures that transmit water are well mapped and analysed.

1.3 AIMS AND OBJECTIVES

The research aims to aid in the development of a groundwater management plan, in updating the existing hydrogeological conceptual model and in assessing whether more groundwater can be

abstracted from underground workings to reduce the reliance of Dishaba Mine on potable water supplied by the Magalies Water Board.

The main objectives of the project are:

- To investigate groundwater ingress into the mine in terms of locations, origins, volumes, and qualities,
- To assess the groundwater harvesting potential of the mine,
- To create a groundwater management plan that will ensure dry mining conditions whilst maintaining a supply of groundwater to surface operations of the mine,
- To contribute data about the fractured aquifer that will improve the conceptual model, and,
- To create an effective mine operating procedure for dealing with groundwater intersections.

1.4 RESEARCH METHODOLOGY

To achieve the objectives stated above, the workflow shown in Figure 8 was carried out. The key actions were:

- Groundwater seepage survey – An assessment of water ingress volumes and locations was undertaken across the mine. The assessment consisted of physical underground mapping and field parameter testing with a handheld multiparameter probe (the Hanna 9811-5 model). The parameters tested were pH, temperature, electrical conductivity (EC) and total dissolved solids (TDS). The lithology and geological structures through which groundwater is flowing was also recorded. An analysis of various records of groundwater intersections and ingress in the mine was also carried out. The records consisted of mine plans and maps, drilling records, geology borehole database and the pumping records of the mine. The aim of this investigation was to establish where, how much and, based on field parameters, what kind of groundwater flows into the mine.
- Hydrochemical sampling was undertaken from underground areas with sustained groundwater ingress across the mine. The sampling covered areas in the upper section (levels closer to surface) and the lower section of the mine, as well as areas in the eastern and western sections of the mine. The aim was to achieve spatial coverage that would be representative of the different areas and geological structures across the mine. The hydrochemical analyses were carried out at the Aquatico laboratories in Pretoria and isotope analyses were done at the iThemba laboratories in Johannesburg. The hydrochemical and isotopic analysis aimed to

establish the groundwater facies across the mine, the possible sources of the groundwater as well as the quality and by extension the possible usability of the groundwater in the mine.

- The collected data were compiled into various tables and graphs. Various plots from the hydrochemical analysis were created such as Piper diagrams to better visualise and interpret the results obtained.

- From the gathered data, the conceptual hydrogeological model for Dishaba Mine was updated to better explain the causes of the observations made across the mine with particular reference to where and how groundwater flows relative to the geology of the mine.

- A water management strategy was developed that would allow for the harvesting and monitoring of groundwater across the mine whilst ensuring dry mining conditions.

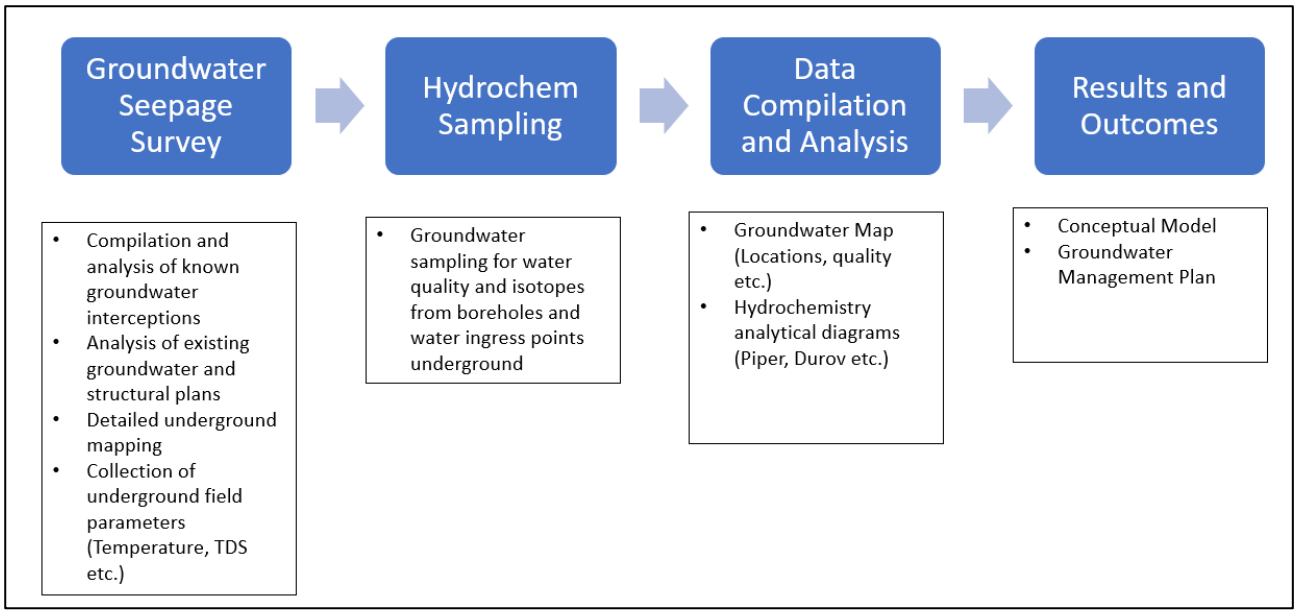

Figure 8: Research project workflow.

1.5 STRUCTURE OF DISSERTATION

The dissertation discusses various aspects of groundwater ingress and geology at Dishaba Mine. The dissertation is structured as follows:

- Chapter 1 gives an introduction and background information on Dishaba mine. It gives an overview and rationale behind the research project.

- Chapter 2 is a review of literature and existing information on the geology and groundwater aspects of the mine.

- Chapter 3 describes the data collection that took place during the research project.

- Chapter 4 presents the findings and results from the work done as described in Chapter 3.
- Chapter 5 discusses the results and gives possible reasons for the results obtained and their influence on the conceptual model.
- Chapter 6 gives recommendations and suggests a way forward for groundwater management and future research work at the mine.

CHAPTER 2:
LITERATURE REVIEW

2.1 GEOLOGY AND REGIONAL SETTING

2.1.1 Overview of the Bushveld Igneous Complex

The Bushveld Igneous Complex (BIC) occupies an area of approximately 65 000 km^2 in the north-eastern part of South Africa (Figure 9). The BIC outcrops in four limbs (Viljoen and Schurman, 1998) named the northern, southern, eastern, and western limbs (Cawthorn and Lee, 1998). The northern limb extends from Mokopane in the south to Villa Nora in the north. The western limb forms a semi-circular arc which stretches from Thabazimbi to Rustenburg and further eastwards to Pretoria. The eastern limb of the BIC lies opposite the western limb, stretches from Burgersfort to Belfast, and is generally similar to the western limb (Cawthorn *et al.*, 1998). The southern limb is found in Belfast in Mpumalanga and is buried under younger sediments (Eales and Cawthorn, 1996).

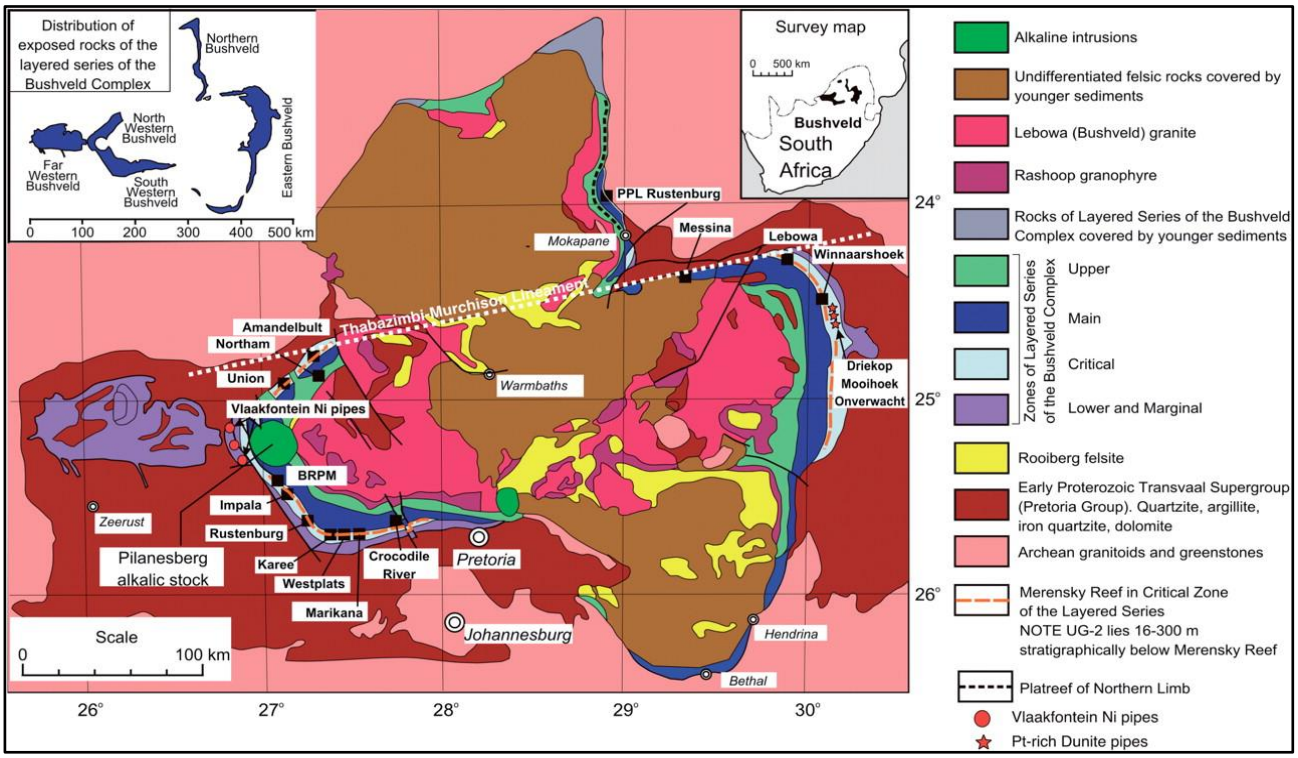

Figure 9: Detailed geology map of the Bushveld Igneous Complex (Naldrett *et al.*, 2009).

The BIC is thought to have been formed by several repeated magma injections into a sub-volcanic, shallow level chamber (Kruger, 2005). These magma injections resulted in the formation of various lithostratigraphic suites, namely the Lebowa Granite Suite (LGS), the Rashoop Granophyre Suite

(RGS) and the Rustenburg Layered Suite (RLS). The approximately 9 km thick RLS is the most economically significant suite as it hosts the platinum deposits. It is divided into the Upper, Main, Critical, and Lower Zones. The Critical Zone is where the most important mining activities take place because of its richness in platinum group elements (PGEs) (Cawthorn, 1999).

The BIC is host to the largest platinum group resources in the world (Cawthorn, 1999). The three main orebodies from which platinum is mined are the Merensky Reef, the Upper Group 2 (UG2) and the Plat Reef. Other notable world class mineral deposits found in the BIC include chromium, vanadium, fluorite and andalusite (Cawthorn *et al*., 2006).

2.1.2 Local Stratigraphy

Dishaba Mine is located in the northernmost part of the western limb of the BIC. The mine also lies in the uppermost part of the Critical Zone from where the Merensky and UG2 Reefs are mined. Several cyclic units are exposed by mining excavations (Kruger, 1990); these are locally termed *marker horizons* or simply *markers*. Underground excavations generally reveal the Upper Group 1 (UG1) to Bastard Reef marker horizons (Figure 10).

Figure 10 shows a detailed local stratigraphic succession of the Amandelbult Complex (refer to Figure 6 for the spatial location of the different crosscuts). The lithological units are sequentially numbered relative to a marker e.g. UG2 FW 1 refers to the first lithology in the FW of the UG2. A brief description of the critical markers and their associated rock types follows below. For detailed descriptions, the reader is referred to Maier and Walters (1994) and Walters *et al*. (2004).

2.1.2.1 The UG1

The Upper Group 1 (UG1) is a chromitite layer, approximately 1 m thick. It is underlain by an anorthosite with chromitite bands (ANCR). The ANCR is about 2 m thick and has a *zebra-stripes* appearance. Below the ANCR are over 100 m of alternating anorthosite-norite layers that lead to the middle group chromitites.

Directly on top of the UG1 chromitite is a strata-parallel shear that is possibly a thrust fault (Friese, 2004). The hanging wall of the UG1 consists of over 10 m of pyroxenite leading up to the UG2 horizon.

2.1.2.2 The UG2

The Upper Group 2 (UG2) is one of the two orebodies currently being exploited for its PGE content. The UG2 is made of two or three chromitite layers; the main band, which is between 0.8 m and 1 m thick, and one or two leader seams, which are 10 cm to 15 cm thick. The main band and the leader seams are separated by approximately 10-cm-thick pyroxenite bands.

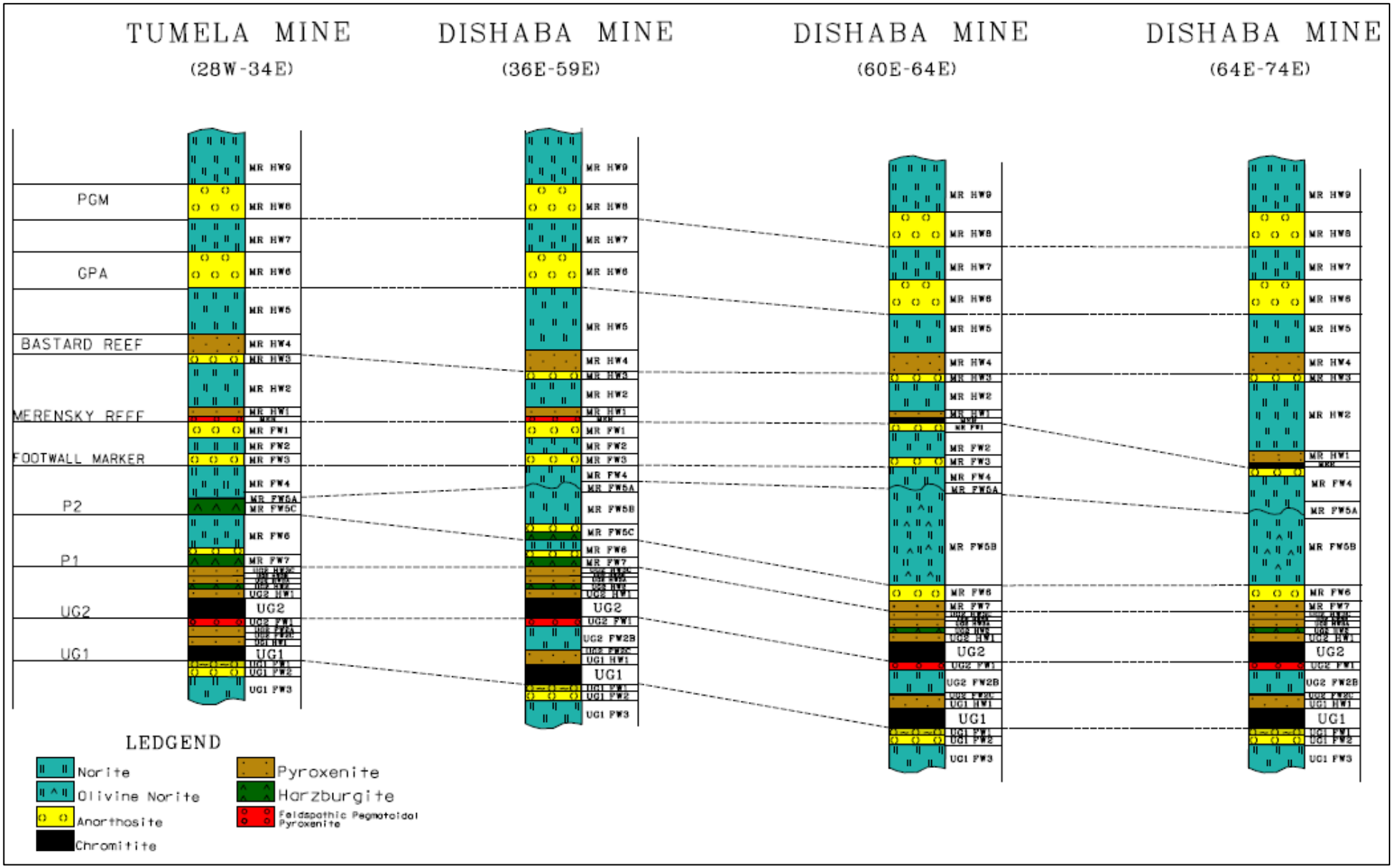

Figure 10: Local stratigraphy from the west to the east of the Amandelbult Complex Area (Sibiya, 2017).

The UG2 usually sits above a 1-m-thick feldspathic pegmatoidal pyroxenite (UG2FW1) with a 1 cm chromitite stringer at its base. The UG2FW1 is underlain by a leuco-norite that is about 5 m thick and also has a chromitite stringer at its base surrounded by pyroxenite. This pyroxenite marks the start of the UG1 hanging wall pyroxenite. The vertical distance between the UG1 and UG2 is about 20 m.

The hanging wall of the UG2 consists of a 10 cm feldspathic pyroxenite followed by an approximately 80-cm-thick olivine-rich pyroxenite or harzburgite which is followed by about 8 m of pyroxenite. The hanging wall marker is a chromitite stringer that sits between 1.0 and 1.2 m above the UG2 and is surrounded by pyroxenite.

2.1.2.3 The P1

The Lower Pseudo Reef (P1) lies approximately 11 m above the UG2 reef. The term pseudo reef implies a resemblance to the Merensky Reef (Viring and Cowell, 1999). The P1 consists of an approximately 0.5- to 1-m-thick feldspathic pegmatoidal pyroxenite or harzburgite capped by a 1 cm chromitite stringer. The P1 has interstitial sulphide mineralisation with low Pt grades (≈1.5 g/t). The footwall of the P1 is the approximately 8-m-thick pyroxenite which extends to the UG2 horizon. In the hanging wall of the P1 is an anorthosite with scattered chromitite or olivine grains. The thickness of the hanging wall anorthosite varies between <10 cm to about 1 m and terminates on the feldspathic harzburgite of the P2.

2.1.2.4 The P2

The Upper Pseudo Reef (P2) is a feldspathic harzburgite with a thickness of 3-5 m. The P2 is not economically mineralised; however, there are traces of sulphide mineralisation above and below the P2 across the north-western limb of the BIC (Mitchell et al, 2019). Directly above the harzburgite is a 20- to 30-cm-thick feldspathic pegmatoidal pyroxenite with minor sulphide mineralisation. From around the 55E Line (refer to Figure 6), the harzburgite disintegrates and scatters olivine into norite in an easterly direction. This results in the formation of a 30 m thick olivine-rich norite in the eastern part of the mine (60E to 74E in Figure 10) (Maier and Walters, 1994).

In some parts of the mine, the P2 sits directly on the P1 with the *normal* footwall anorthosite (hanging wall of the P1) completely absent. The hanging wall of the P2 consists of a norite layer with a small anorthosite and chromitite band, locally named the Lone Chrome Stringer (Walters *et al*., 2004) sitting just above the P2. This is followed by an alternating norite, anorthosite (footwall marker) and norite horizon leading to the footwall of the Merensky Reef.

2.1.2.5 The Merensky Reef

The world-famous Merensky Reef consists of a feldspathic pegmatoidal pyroxenite bound by chromitite stringers and the bottom and the top. The thickness of the Merensky Reef varies from less than 10 cm to just over 1.5 m. The normal Merensky reef sits on a 5- to 6-m-thick poikilitic anorthosite and has significant sulphide mineralisation with over 5 g/t Pt grade. The hanging wall consists of a 1- to 3-m-thick pyroxenite.

Mining at Dishaba Mine takes place through the Swartklip facies of the Merensky Reef (Viljoen, 1999). The Swartklip facies consist of various pothole facies whereby the reef transgresses into the FW lithologies (Figure 10). The Merensky reef at Dishaba Mine can thus be divided into three broad facies, the Normal Reef (NMR), the Transition Zone (TRZ, including the Contact Reef (CRF) and the Pothole Reef (PHR)) and the Haakdoorndrift (HDD) facies (Figure 11). Haakdoorndrift is the name of the farm where this type of Merensky reef in the mine is mainly found (see Figure 2). The presence of various Merensky facies has been described to be the result of regional potholing (Viljoen, 1999) and more recently to be the result of step-and-stair-type of transitions because of intruding sills to successive stratigraphic levels (Mitchell *et al*., 2019).

The transition zone consists of mixed potholed facies whereby the reef is unstable and sits on various footwall lithologies (Viljoen, 1999). In the HDD facies, the reef sits on the footwall marker and has significant footwall mineralisation extending beyond 2 m below the reef. The reef itself is <10 cm thick with large sulphide mineralisation.

The Merensky Reef horizon represents the best depiction of the cyclic units of the BIC (Kruger, 1992) whereby the mafic rocks (pyroxenite) are found at the base with upward grading into acidic rocks (anorthosite) at the top. The total thickness of this unit is about 20 m and terminates on the Bastard Reef.

The middling between the UG2 and the Merensky Reef goes from about 40 m in the western section of the mine (Normal Merensky Reef) to over 60 m in the eastern HDD facies (Mohulatsi, 2022).

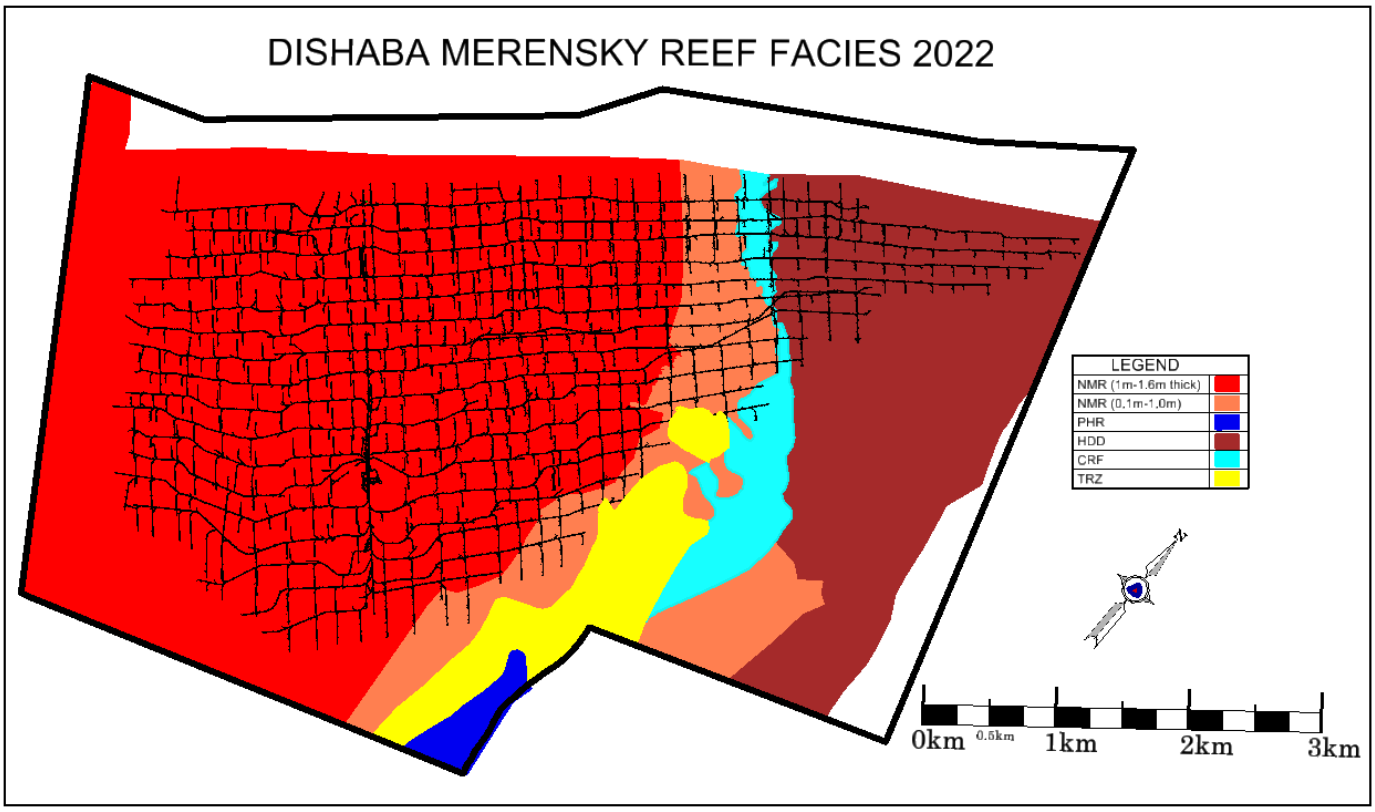

Figure 11: Distribution of Merensky Reef facies across Dishaba Mine (Dumakude *et al*., 2022).

2.1.2.6 The Bastard Reef

The Bastard reef is a 2- to 3-m-thick pyroxenite with about 10 cm of sulphide mineralisation at its base. It is located some 18 to 20 m above the Merensky Reef. The pyroxenite of the Bastard Reef grades upwards into a fine-grained mela-norite, followed by norite and the approximately 10-m-thick giant poikilitic anorthosite (GPA) at 10 to 15 m above the Bastard Reef marks the end of the Critical Zone. The Porphyritic Gabbro Marker (PGM) is found in the lower part of the Main Zone (Mitchell, 1990) and is only exposed by surface exploration drilling as it sits over 500 m above the Merensky Reef. It has no known economic mineralisation.

2.1.3 Structural Setting

Basson (2019) gave detailed effects and properties of the major deformation structural features of the BIC. Dishaba Mine sits between the Crocodile River Fault and the Middellaagte Graben (Figure 12). The Thabazimbi Murchison Lineament (TML) lies immediately north of the mine. The Middellaagte Graben marks the western boundary of the mine and separates it from the neighbouring Tumela Mine. The graben is estimated to have a throw of 500 m on the east and 700 m on the west (Bamisaiye, 2016). Underground observations show that there are several sympathetic faults with relatively smaller throws (Figure 13).

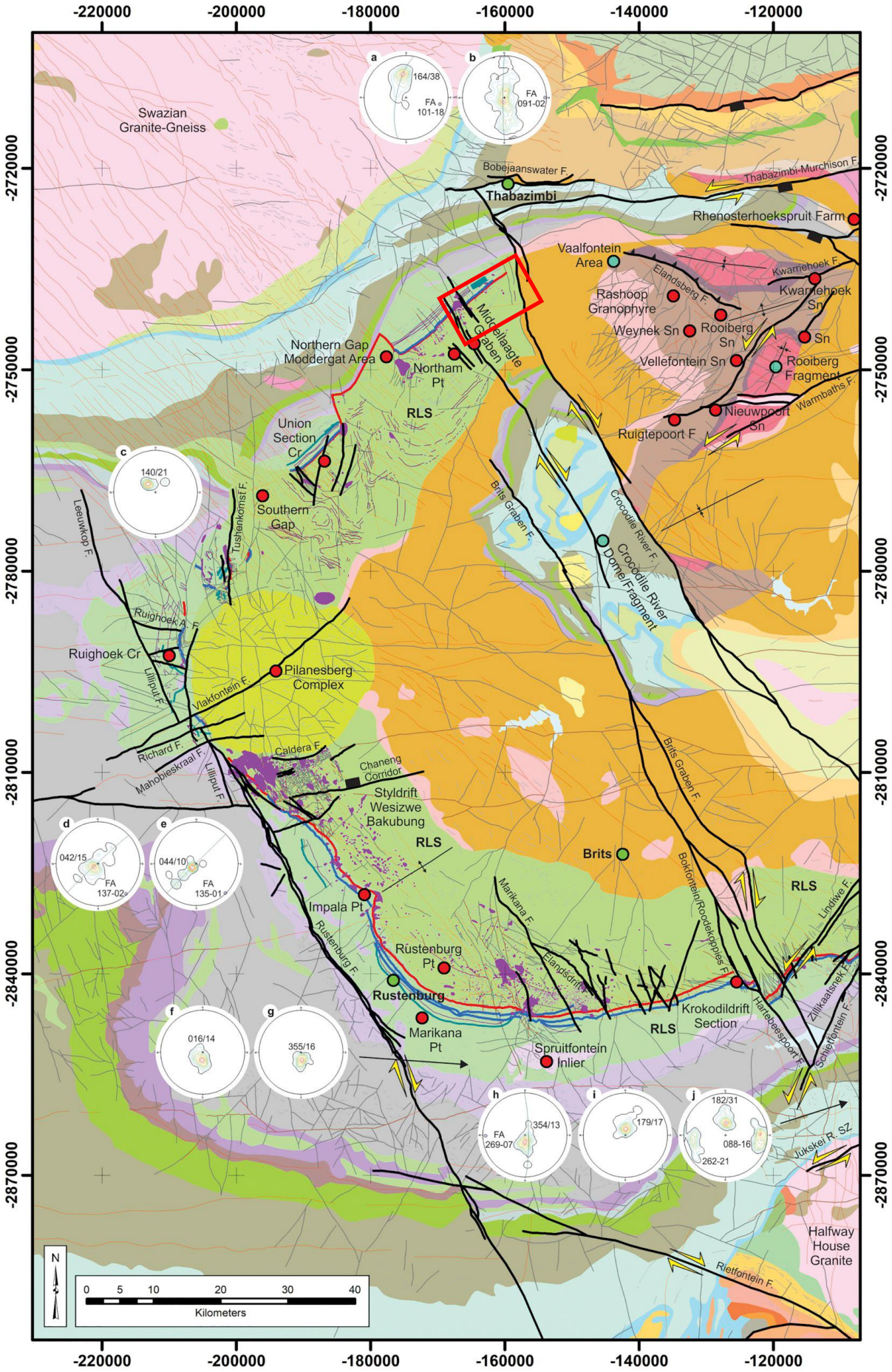

Figure 12: Structural geology map of the western limb of the Bushveld Igneous Complex (Basson, 2019). Dishaba Mine lies inside the red rectangle south of Thabazimbi.

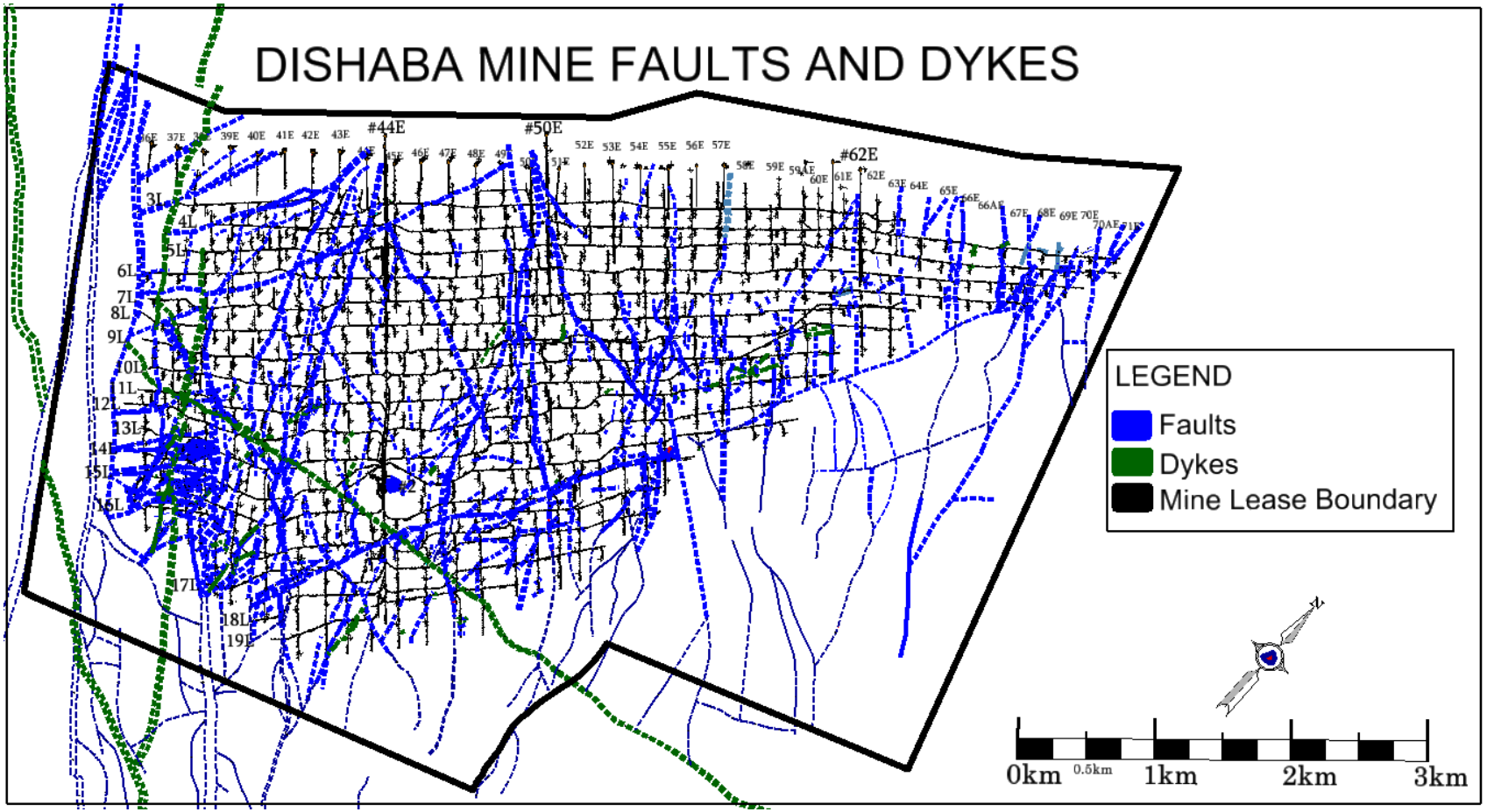

Figure 13: Distribution of faults and dykes across Dishaba Mine on the Merensky Reef horizon.

The Crocodile River Fault lies north-east to the mine (Figure 12). The fault apparently marks the northern end of the western limb of the BIC (Basson, 2019). The TML further north of the mine is associated with thrust faults (Mohlahlana, 2019). Although there is prominent thrust faulting in the north-eastern part of the mine (Maakamedi and Moyo, 2018), no direct correlation has been established between the major thrust fault system in the mine and the TML.

A detailed study of the faults and associated joints in the mine lease area was conducted by Friese (2004) and are briefly described below:

- The Pongola extensional fault zones: These are the oldest structures ~2.07-1.93 Ga. They are moderate-steeply inclined and have a north-west/south-east to north-north-west/south-south-east strike.
- The Ventersdorp extensional fault zones: These are of similar age to the Pongola extensional fault zones, and trend north-east/south-west to north-north-east/south-south-west. They are confined to an approximately 4 km zone across the Dishaba lease area and represent a graben or half graben as part of the Neoarchaean Ventersdorp impactogenal rift system in the basement to the BIC.
- North-west-verging, layer-parallel thrust zones on major litho-stratigraphic boundaries, i.e., on the top contacts most predominantly of UG1, P1, and P2. The thrust zones represent load stress compensation thrusts, which formed during Rustenburg Layered Suite emplacement in Upper Zone time in response to thermal subsidence of the RLS and vertical load stresses induced into the floor rocks and pre-Upper Zone stratigraphy.
- North/south trending, moderate to steeply dipping Kibaran extensional fault zones which formed in response to east/west crustal extension induced by the Kibaran Orogeny at ~1.35 to 1.2 Ga. There are fault zones with relatively smaller net displacements and are low-angled. They developed as interlinking structures that are parallel to and oblique to the Pongola extensional fault zones. These are genetically related to individual phases of sinistral and dextral transtensional reactivation tectonics along these prominent extensional fault zones during the Eburnean (Kheis) and Kibaran orogenies at ~1.83 to 1.73 Ga and ~1.35 to 1.2 Ga, respectively.
- A group of pervasive west-south-west-, west- and west-north-west-trending extensional fracture zones that traverse all other fault zones. These have no significant displacement and are generally the youngest, i.e., post-Karoo extensional fracture systems formed at ~180 to 90 Ma.

Friese (2004) also noted that the Dishaba Mine area has a smaller abundance of dykes relative to the rest of the Amandelbult Mining Complex. He further stated that several generations and petrological types have intruded along the various groups of faults as follows:

- The Pongola extensional fault zones – north-west trending, up to 10m wide diabase dykes,
- The Kibaran fault set – north/south striking, relatively thin (up to 2 m wide) carbonate rich alkaline dykes, and,
- The post-Karoo system – west-south-west- and west-trending, variable thickness dolerite dykes.

Joints in the mine occur randomly and in sets, sometimes parallel to major structures such as faults and dykes. The joints tend to be filled with chlorite, serpentine, and calcite (Gerber, 2022). Two detailed studies were carried out on the characteristics of the joints on the mine (Gerber, 2022). One on the Merensky Reef horizon and another on the UG2 horizon. A total of four and six prominent joint sets were found on the Merensky Reef horizon and the UG2 horizon, respectively. The joints on the Merensky Reef horizon are generally subvertical, dipping at over 80°. One anomaly was a particular set of joints (J4) dipping at below 40° and striking at 094° (Table 2). The joints on the UG2 reef horizon are generally relatively shallower and more varied in dip. They broadly dip between 70° to just over 80° (Table 3).

Table 2: Characteristics of joint sets found on the Merensky Reef horizon (Gerber, 2022).

Set	Orientation				Spacing (m)		
	Dip (°)		Dip Direction (°)		Minimum	Average	Maximum
	Mean	Standard deviation	Mean	Standard deviation			
J1	88	8	62	22	0.10	0.82	5.50
J2	83	7	107	21	0.14	1.32	6.70
J3	88	8	161	23	0.11	0.65	2.30
J4	39	10	94	21	0.12	1.94	6.30

Table 3: Characteristics of joint sets found on the UG2 Reef horizon (Gerber, 2022).

Set	Orientation				Spacing (m)		
	Dip (°)		Dip Direction (°)		Minimum	Average	Maximum
	Mean	Standard deviation	Mean	Standard deviation			
J1	77	8	166	8	0.10	2.00	6.00
J2	82	9	245	13	0.00	2.60	9.00
J3	79	10	103	11	0.40	3.20	6.70
J4	80	9	6	5	4.00	4.00	4.00
J5	74	8	316	15	0.30	2.60	4.80
J6	72	11	205	6	0.10	0.20	0.30

2.2 HYDROGEOLOGICAL SETTING

This section discusses the climate and hydrological setting, groundwater occurrence, groundwater quality, and the groundwater conceptual model based on current understanding of the groundwater regime across the Dishaba Mine.

2.2.1 Climate and Hydrological Setting

The Thabazimbi area receives most of its rainfall in summer from November to April. On average, the area receives an average of 602 mm of rain per year. The winter season has the lowest amount of rainfall with July being the driest month with almost 0 mm while January has the most with 500 mm. In June, the average daytime temperature is 21.8°C, while in January, it is 31.7°C (Meteoblue, 2022). Figure 14 shows the average climate conditions based on 30 years of hourly weather observations.

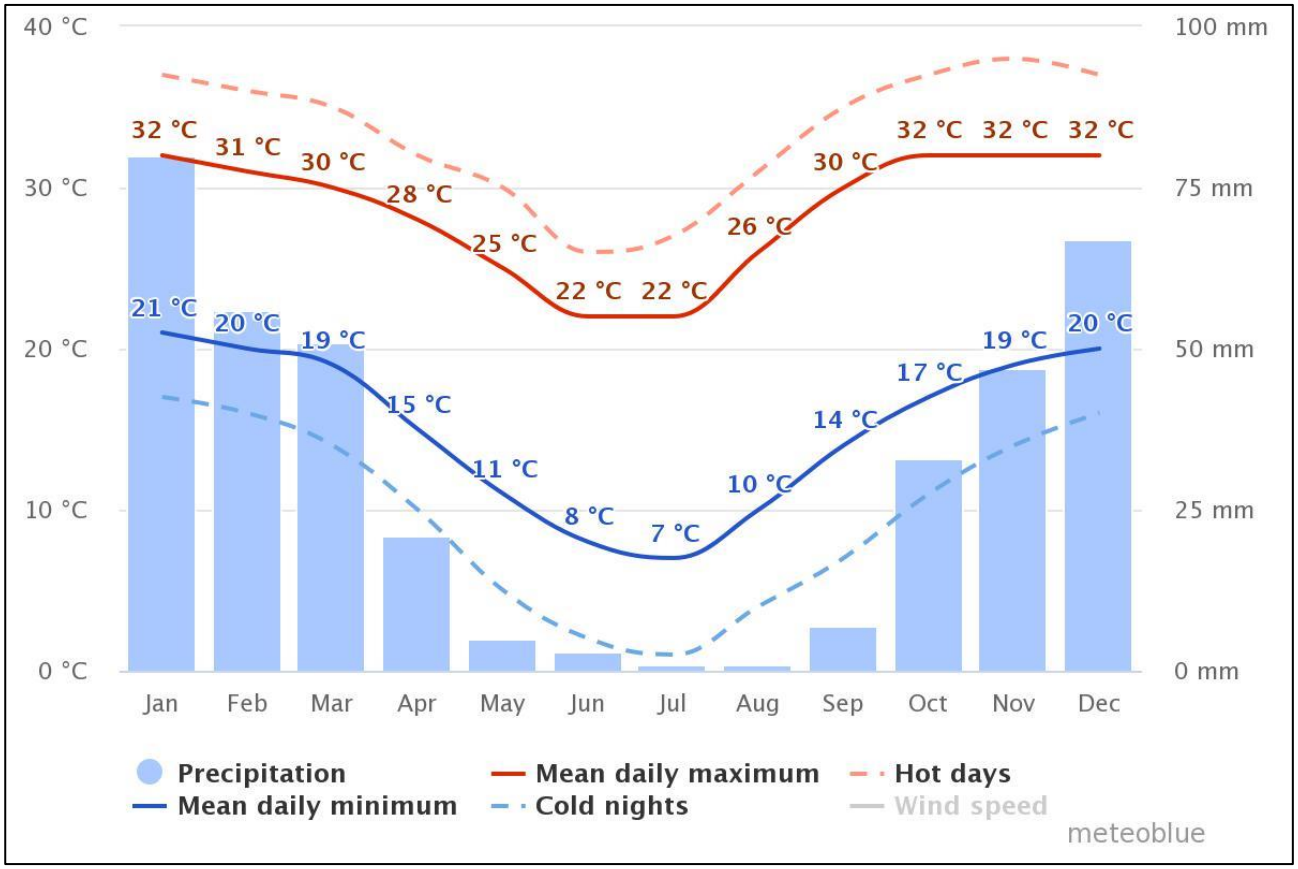

Figure 14: Average weather conditions in the Thabazimbi area (Meteoblue, 2022).

The Dishaba Mine lease area falls within the Crocodile (West) Marico Water Management Area within the quaternary catchments A24F (Bierspruit River) to the west and A24C (Crocodile River) to the east of the #2 Vertical Shaft (Figure 15).

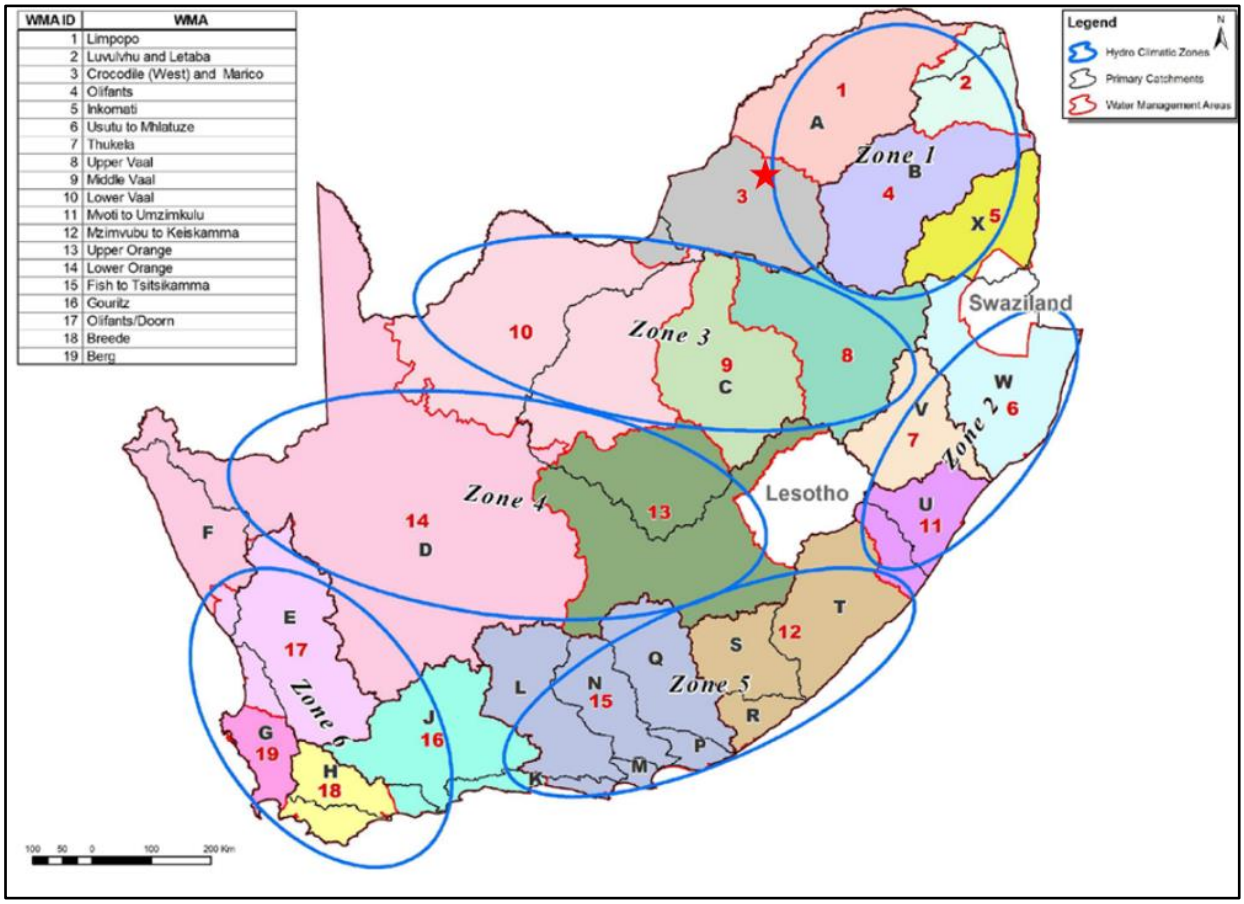

Figure 15: The nineteen Water Management Areas, primary catchments, and the six-general hydro-climatic zones of South Africa (DWA, 2013). Dishaba Mine falls within Water Management Area 3 as indicated with the red star.

The topography of the area surrounding the mine is generally flat and featureless. The most prominent surface features being the agriculturally active farms (the dark green crop circles in Figure 3) and mining related infrastructure. The Transvaal Supergroup mountains occur approximately 10 km north of the mine.

According to Golder (2018), hydrological units found at and below the mine are those belonging to the BIC, the Chuniespoort Group, Magaliesberg quartzite and the Crocodile River alluvial sediments (Figure 22). Aquifers within the BIC can be generally divided into three types: an alluvial aquifer on the banks of rivers and streams; a shallow, weathered bedrock aquifer; and a deep, fractured bedrock aquifer (Gebrekristos and Cheshire, 2012).

2.2.2 Groundwater Occurrence

Groundwater in the Dishaba Mine lease area occurs mainly in the shallow weathered aquifer and the deep fractured aquifer (Titus *et al*., 2009). The weathered aquifer system generally occurs down to a depth of approximately 40 mbgl (meter below ground level) and is connected to the deeper fractured bedrock aquifer system through fractures at specific localities. Groundwater travels

through these interconnected fractures from the weathered aquifer system into the fractured bedrock aquifer system (Figure 16).

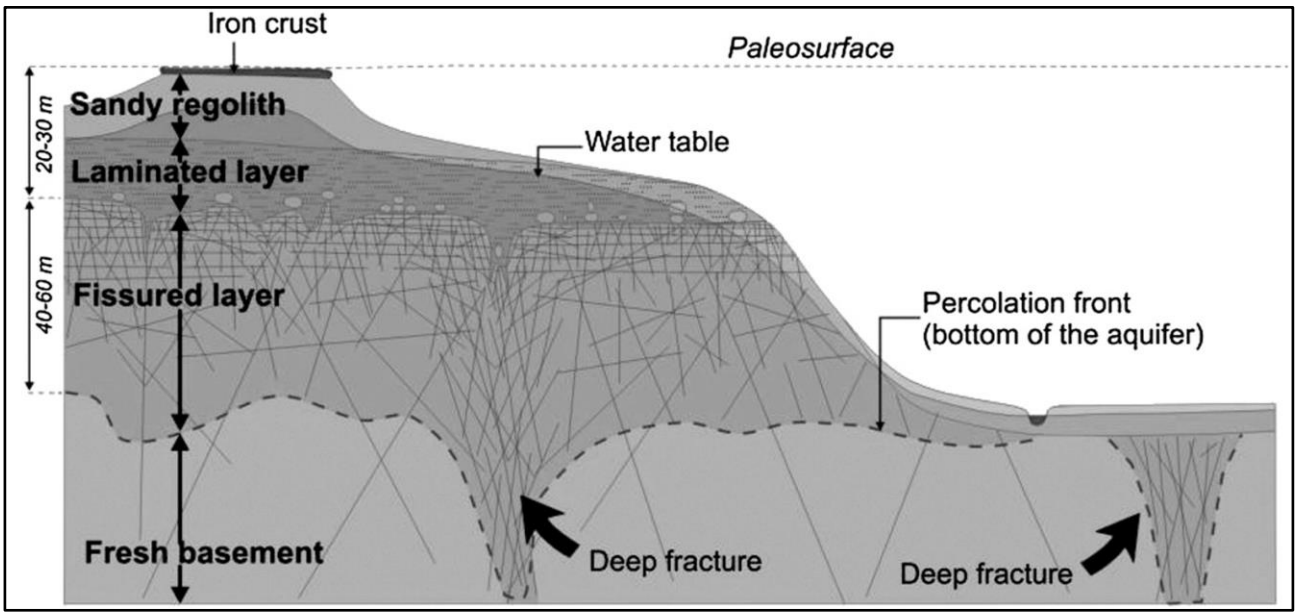

Figure 16: Idealised single-phase weathering palaeo-profile in a hard rock, crosscut by the current topography (from Wyns *et al*., 2004). The laminated layer and fissured layer refer to saprolite and saprock layers defined by Titus *et al*. (2009).

The shallow weathered aquifer is monitored through a number of boreholes (Figure 17) distributed across the Amandelbult Mining Complex with special focus on the tailings storage facility. A far smaller network of vibrating wire piezometers exists underground at depths over 100 mbgl.

2.2.2.1 The shallow weathered aquifer

Titus *et al*. (2009) described the shallow weathered bedrock aquifer system as being composed of the saprolite and saprock zones which are formed due to weathering of the underlying bedrock. These zones are water-bearing due to natural recharge, irrigation return flows, and other surface water sources. Along the river courses, this system is partially or fully replaced by alluvial aquifers.

The alluvial aquifers consist of sand, silt, clay and gravel deposited by the rivers and have a great variety of thickness. Linkages with surface water cause them to have high yields. However, low yields have also been encountered in areas where there is much less clay and silt contents (Gebrekristos and Cheshire, 2012).

Dishaba Mine has an extensive network of groundwater monitoring boreholes (Figure 17) spread across the Amandelbult Mining Complex. These boreholes are mainly used for monitoring the shallow surface aquifer. The groundwater level occurs at average depths of between 1.9 and 19.7 mbgl on the Bierspruit River side and between 2.1 and 51.1 mbgl in the Crocodile River drainage side (Figure 18) (Groundwater Complete, 2021). The shallow groundwater depths in the

vicinity of the tailings dam and its holding dam are presumed to be the result of artificial aquifer recharge in the form of seepage from the dams.

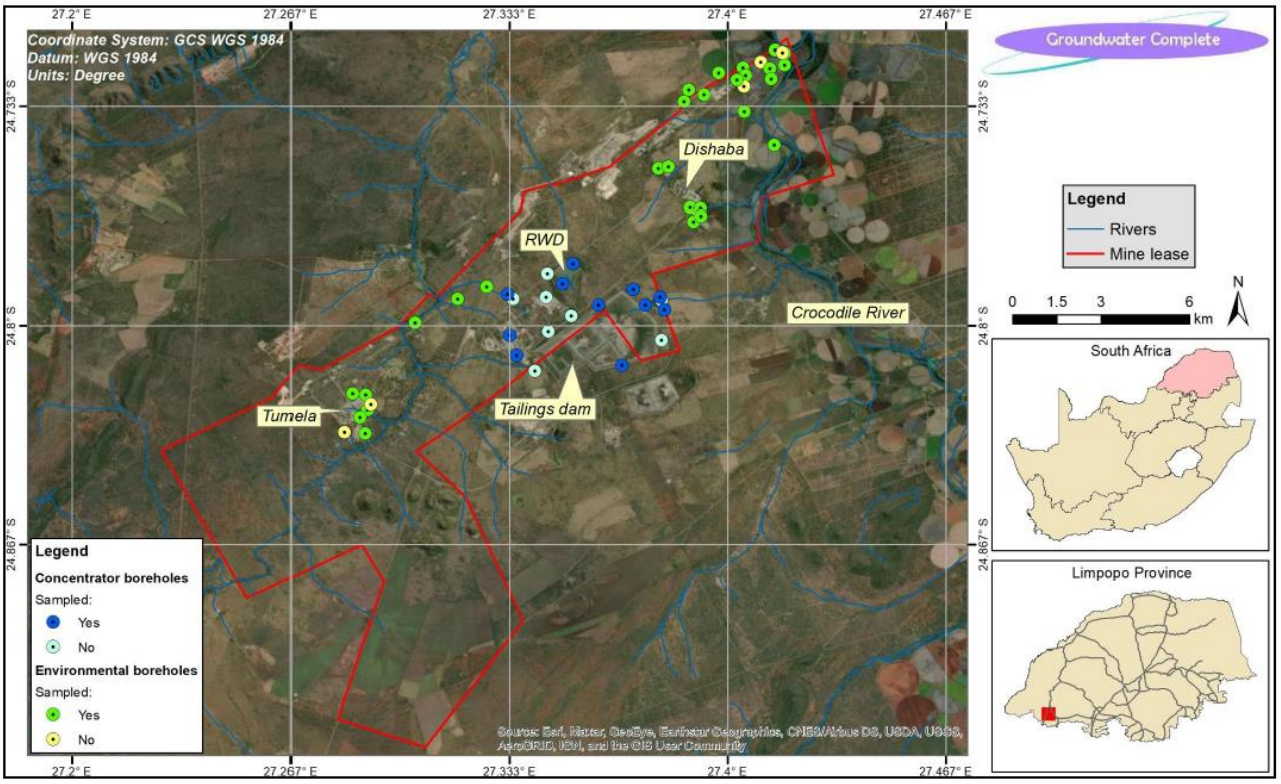

Figure 17: Distribution of groundwater monitoring boreholes across Amandelbult Complex (Groundwater Complete, 2021).

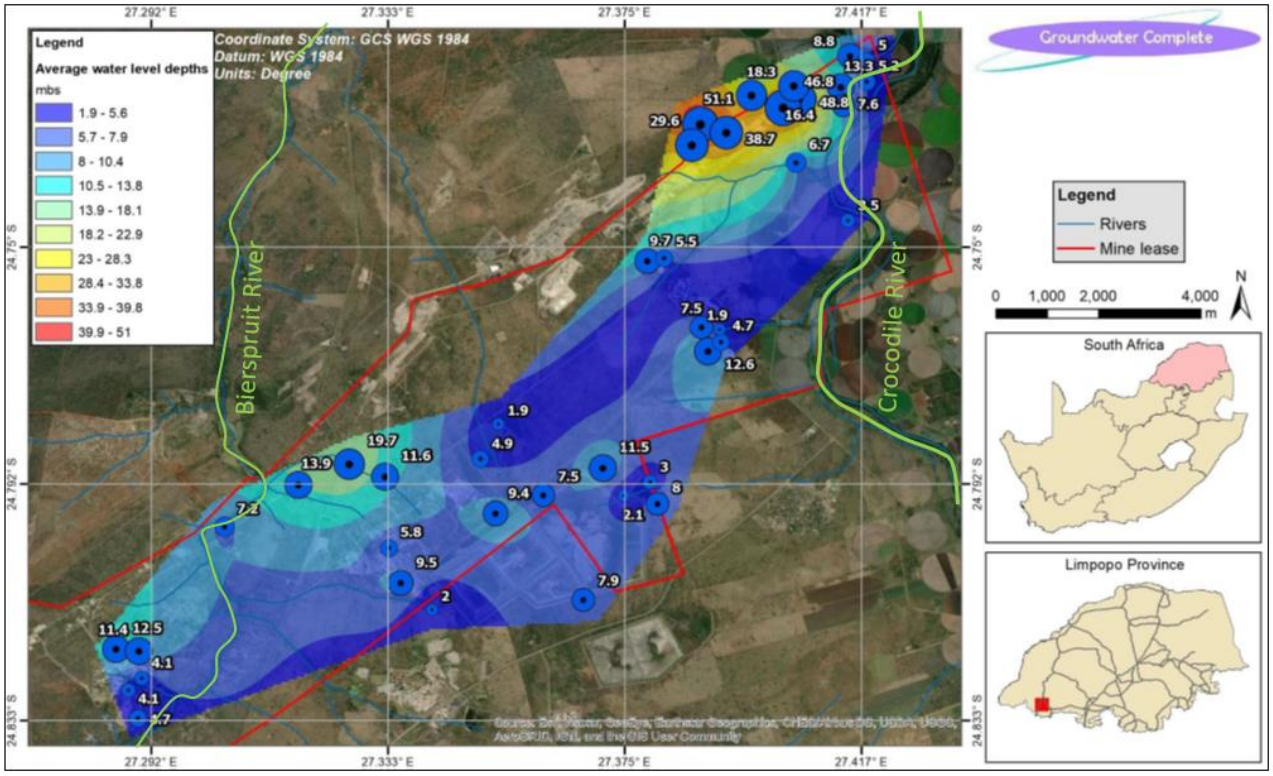

Figure 18: Water level depths across Amandelbult complex as observed in the groundwater monitoring network boreholes (Groundwater Complete, 2021).

The groundwater flow direction is generally towards the Bierspruit River and the Crocodile River i.e., north/northwest towards Bierspruit and north-east towards the Crocodile River. Figure 19 shows the groundwater elevations and flow trends as observed in the year 2020.

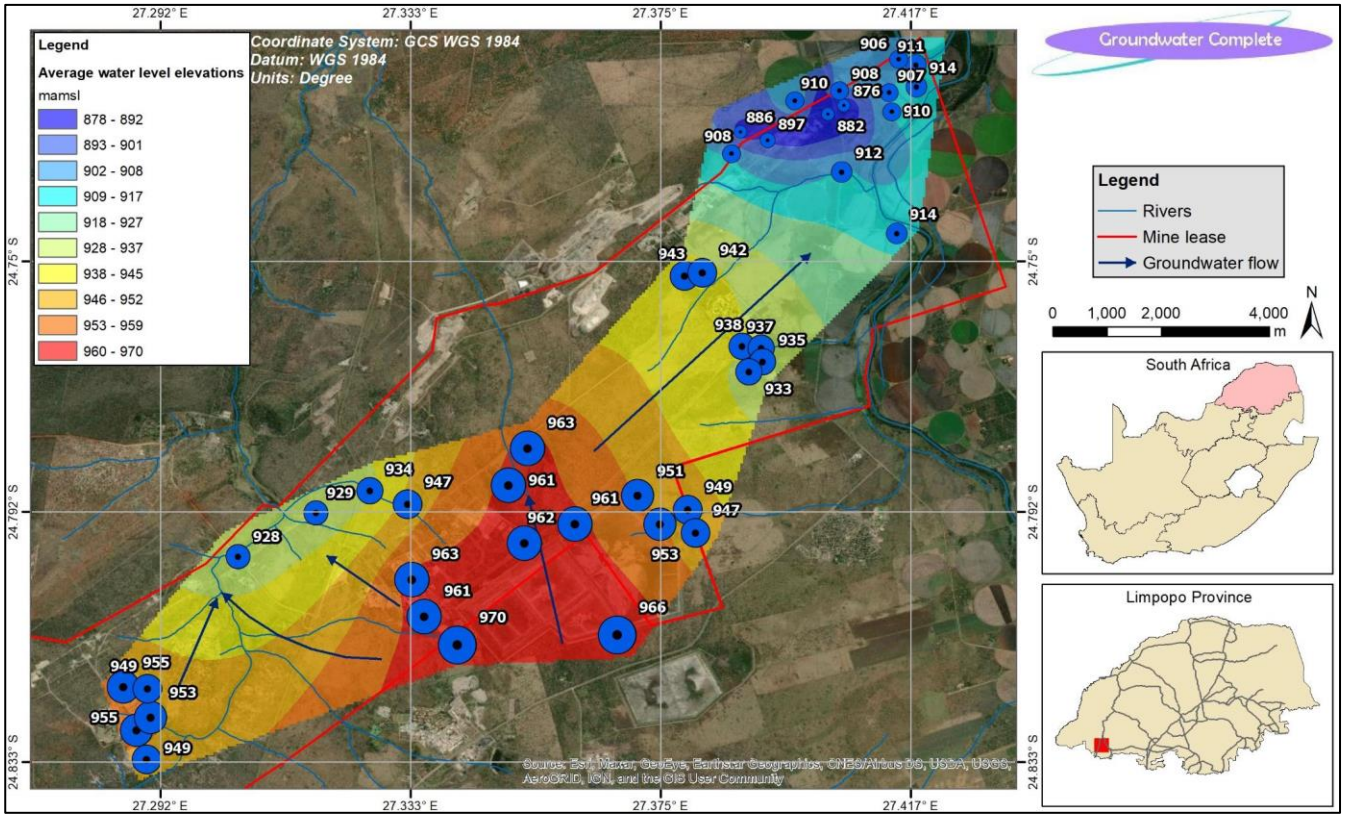

Figure 19: General shallow groundwater flow across Amandelbult Complex. (Groundwater Complete, 2021).

The monitoring boreholes are sampled on a quarterly basis. Groundwater Complete (2021) concluded that the groundwater qualities varied within relatively short distances, and that this could be ascribed to aquifer heterogeneity and compartmentalisation.

2.2.2.2 The deep-seated fractured aquifer

Fractured rock aquifers comprise a network of fractures that cut through a relatively impermeable rock matrix (Cook, 2003). When characterising the fractured rock aquifers, information on the nature of the fractures and the rock matrix is critical. Fractures are planes along which stress has caused a loss of cohesion in the rock and there is hardly any visible displacement parallel to the surface of the fracture. If there is any movement or displacement, then the fracture is classified as a fault.

The following fracture properties have an impact on the nature of groundwater flow (Cook, 2003):

- Dimensions (aperture, length width),
- Location (orientation, spacing, etc.), and,

- The nature of the fracture walls (surface roughness).

Variation in the fracture properties listed above, leads to variation in conductivity of a rock mass. Dykes can also cause fracturing of the country rock, thereby leading to an increase in the yield/hydraulic conductivity of the fractured rock (Sami and Hughes, 1996). Bromley *et al*. (1994) found that dykes that are thicker than 10 m tend to form water barriers while those of smaller width are permeable as they develop cooling joints and fractures.

At Dishaba Mine, groundwater is intersected in the underlying solid and unweathered crystalline rocks (i.e., below the weathered zone). These rocks at depths over 100 mbgl, generally have low porosity, and high hydraulic conductivity along fractures (Titus *et al*., 2009a). The hydraulic properties and conductivity vary within the same rock mass and over short distances. This is evident through the varied yields in underground boreholes, mine excavations and geological fractures over short distances (Ngubane *et al*., 2015). Titus *et al*. (2009) noted that structural features (fractures) are also extremely variable with regards to frequency, spatial extent, aperture, and interconnectedness.

The volume of groundwater and pumped from the #2 Vertical Shaft is estimated to be approximately 16 ML per day (N. Nxiweni, personal communication, 2020). This estimate is derived from a simple calculation of water pumped up, minus water pumped down, and the difference is assumed to be groundwater ingress. The yields of individual groundwater intersections vary from less than 100 L/h to over 10 000 L/h. Figure 20 shows the distribution of known groundwater intersections in the mine excavations. In Figure 20, there appears to be a significant difference in water intersections between levels above 10 Level and those below. 10 Level and below appear to have groundwater intersections across the length of mining excavations from west to east, whereas 9 Level and above appear to have sporadic intersections and hardly any intersections in the middle (i.e., between 38E and 62E raise lines).

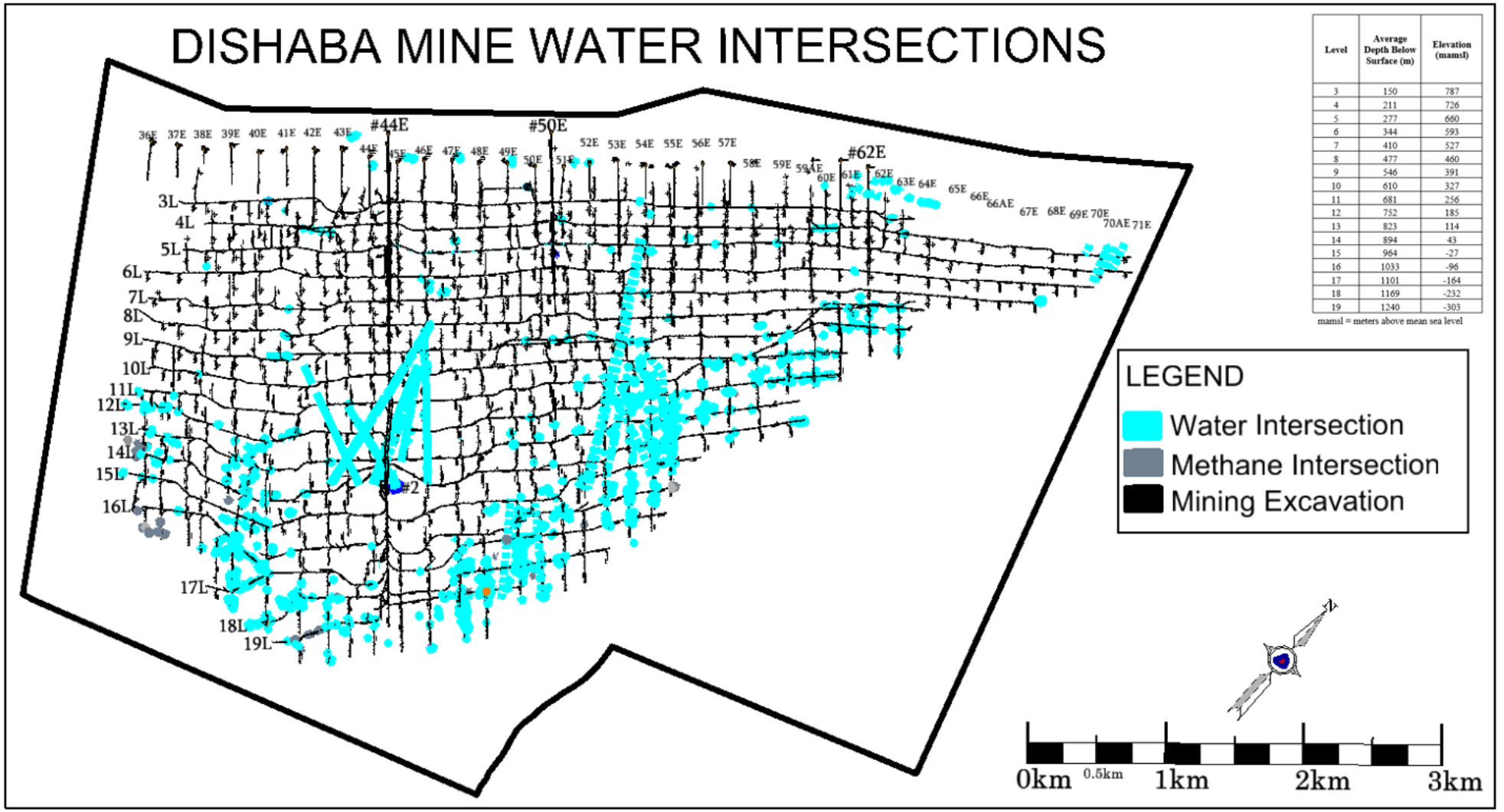

Level	Average Depth Below Surface (m)	Elevation (mamsl)
3	150	787
4	211	726
5	277	660
6	344	593
7	410	527
8	477	460
9	546	391
10	610	327
11	681	256
12	752	185
13	823	114
14	894	43
15	964	-27
16	1033	-96
17	1101	-164
18	1169	-232
19	1240	-303

mamsl = meters above mean sea level

Figure 20: Plan view showing the spatial distribution of known water intersections in underground mine excavations across Dishaba Mine.

2.2.2.3 Conceptual models

Titus *et al*. (2009) conducted a groundwater modelling exercise at Dishaba Mine. In their conceptual model, they proposed a two-layer aquifer system consisting of the shallow weathered aquifer and the deep fractured aquifer. The surface water inflows into the mine workings were estimated at a third (~8 ML/d) of the total mine fissure inflows, regional groundwater inflows at 46% (~11 ML/d) and direct recharge from rainfall at approximately 20% (~5 ML/d) (Figure 21). No direct link was found between the Crocodile River and the mine workings. It was suggested that the regional groundwater flow could be recharging from outside the A24C catchment.

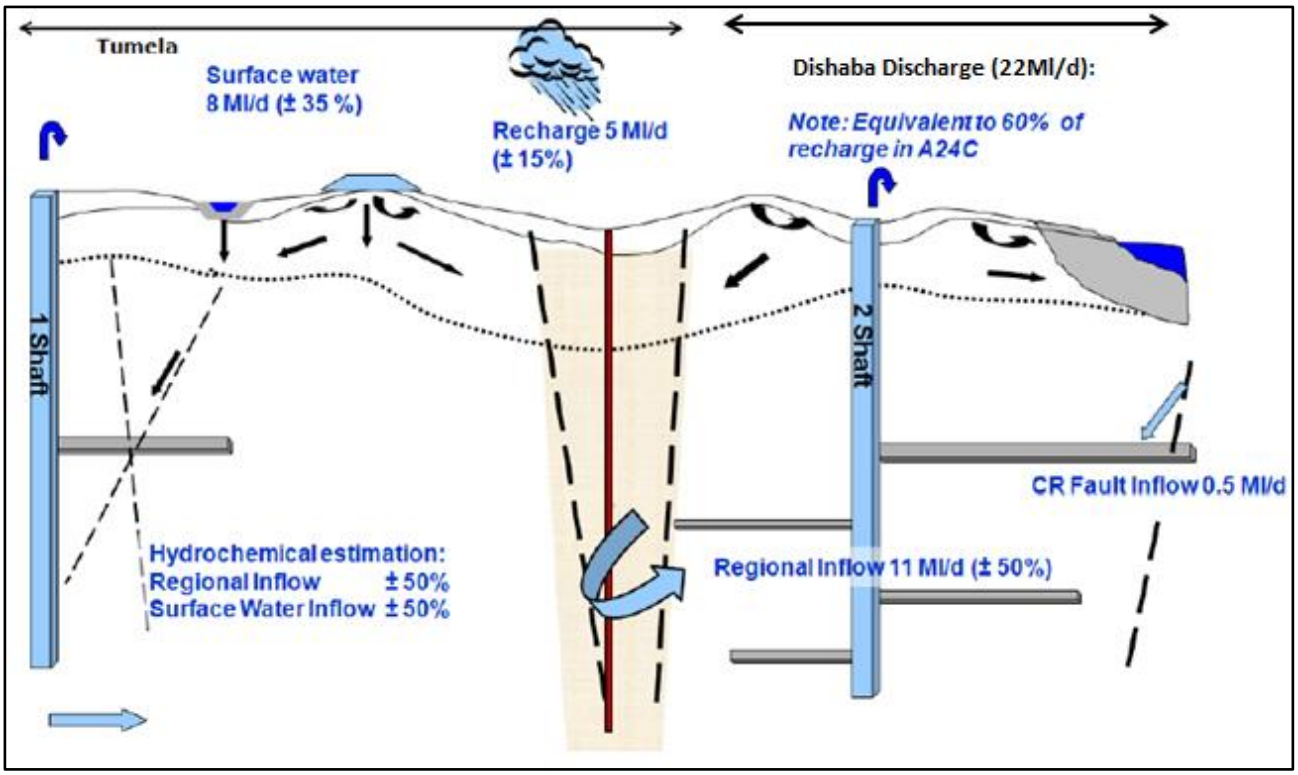

Figure 21: Hydrogeological conceptual model of Amandelbult Complex (Titus *et al*., 2009).

In a more recent update of the conceptual model (Figure 22 and Figure 23), Golder (2018) proposed that the regional groundwater flow is from sources above and below the mining areas, and recharge occurs further afield from the BIC. The main identified aquifers are those belonging to (1) the BIC, (2) the Transvaal Supergroup (specifically the Chuniespoort Group and the Magaliesberg quartzite), and (3) the Crocodile River alluvial sediments. The conceptual model also suggested that since faulting is assumed to be continuous between the Transvaal Supergroup and the BIC, groundwater exchange between the two formations is possible. The Crocodile River Fault and the Middellaagte Graben were identified as the key fault structures that allow for groundwater exchange between the various aquifers and the mine voids.

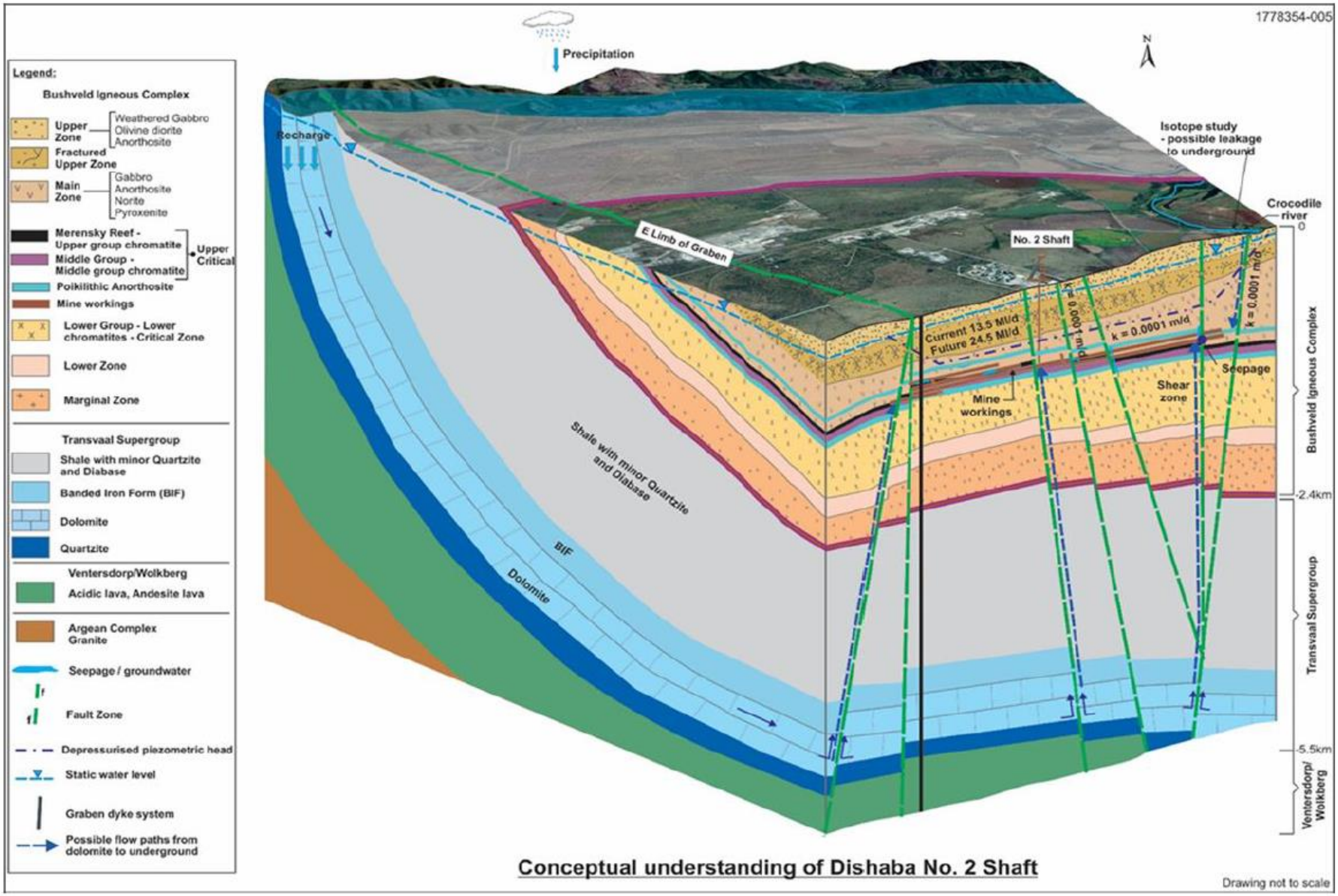

Figure 22: Hydrogeological conceptual model for Dishaba Mine proposed by Golder (2018).

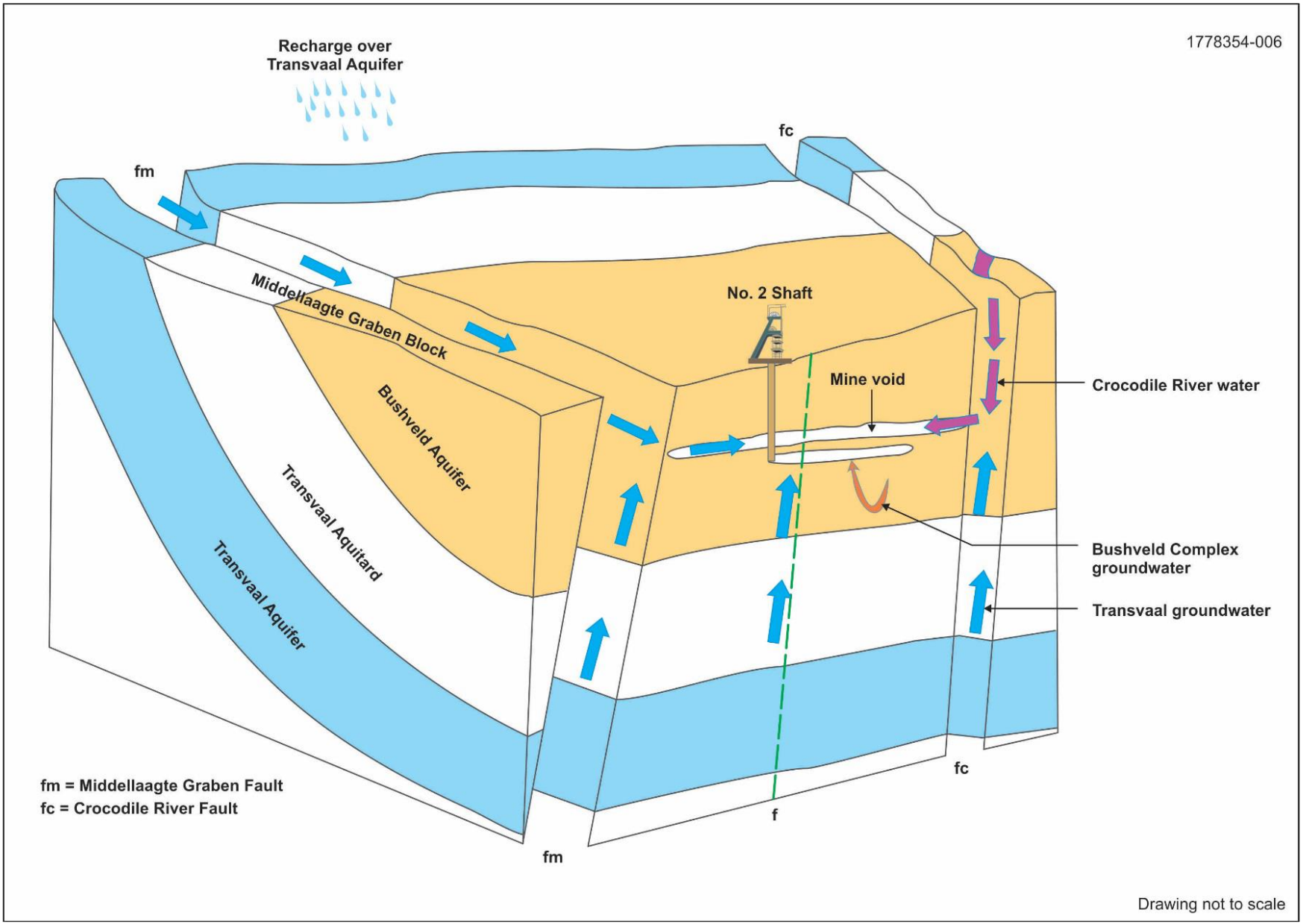

Figure 23: Regional groundwater flow around in Dishaba Mine following the conceptual model by Golder (2018).

2.3 GROUNDWATER QUALITY

Over the years, various sampling and chemical analysis campaigns have been undertaken at Dishaba Mine to understand the groundwater quality on surface and at deeper levels within the mine.

2.3.1 Shallow Groundwater

A quarterly groundwater sampling survey is undertaken on the monitoring boreholes across the Amandelbult Complex (Figure 17). As of 2021, a total of 58 monitoring boreholes across Amandelbult were incorporated in the survey. The survey focuses mainly on groundwater level and quality trends across the Amandelbult Complex (Groundwater Complete, 2021). One of the reasons the environmental boreholes are sampled regularly is to ensure the mine remains compliant to the water use license as granted by the Department of Water and Sanitation (DWS) (P. Mofomme, personal communication, 2021).

The monitoring boreholes provide an easy way to build a continuous database and perform trend analysis that describe water in the shallow weathered aquifer. A total of 20 boreholes within the Dishaba Mine lease area were sampled in 2020 (Figure 24). The values highlighted in red are major ion concentrations that exceed the prescribed levels of the water use licence; these could be impacted by farming and open cast mining operations (Groundwater Complete, 2021).

Sulphate and nitrate were identified as the most dominant contaminants. This is possibly due to mining and farming activities. The Expanded Durov Diagram compiled for the water samples (Figure 25) showed high heterogeneity in terms of the hydrochemistry of the sampled sites. The groundwater quality changed over short distances, which could be caused by contamination from the various source areas, aquifer heterogeneity and compartmentalisation.

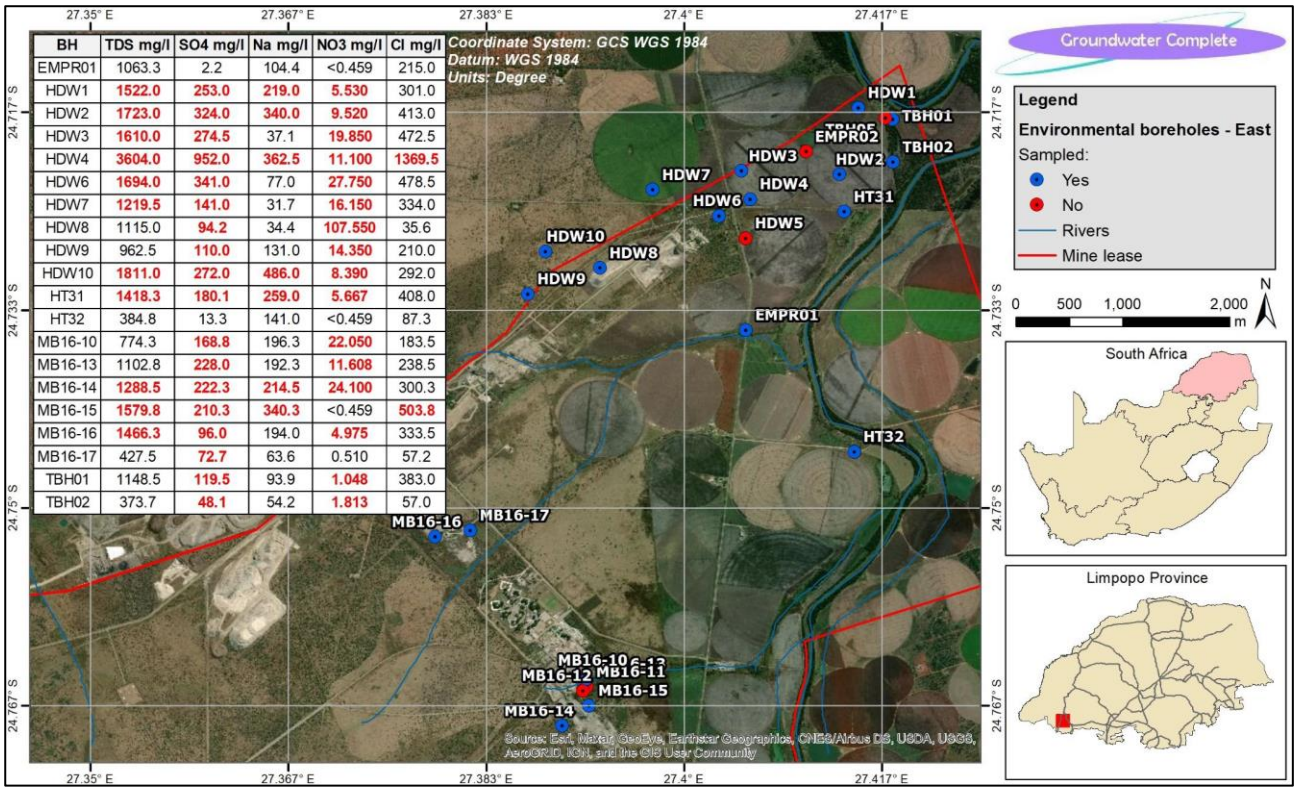

BH	TDS mg/l	SO4 mg/l	Na mg/l	NO3 mg/l	Cl mg/l
EMPR01	1063.3	2.2	104.4	<0.459	215.0
HDW1	1522.0	253.0	219.0	5.530	301.0
HDW2	1723.0	324.0	340.0	9.520	413.0
HDW3	1610.0	274.5	37.1	19.850	472.5
HDW4	3604.0	952.0	362.5	11.100	1369.5
HDW6	1694.0	341.0	77.0	27.750	478.5
HDW7	1219.5	141.0	31.7	16.150	334.0
HDW8	1115.0	94.2	34.4	107.550	35.6
HDW9	962.5	110.0	131.0	14.350	210.0
HDW10	1811.0	272.0	486.0	8.390	292.0
HT31	1418.3	180.1	259.0	5.667	408.0
HT32	384.8	13.3	141.0	<0.459	87.3
MB16-10	774.3	168.8	196.3	22.050	183.5
MB16-13	1102.8	228.0	192.3	11.608	238.5
MB16-14	1288.5	222.3	214.5	24.100	300.3
MB16-15	1579.8	210.3	340.3	<0.459	503.8
MB16-16	1466.3	96.0	194.0	4.975	333.5
MB16-17	427.5	72.7	63.6	0.510	57.2
TBH01	1148.5	119.5	93.9	1.048	383.0
TBH02	373.7	48.1	54.2	1.813	57.0

Figure 24: Sampled boreholes on the Dishaba Mine lease area with their results in 2020 (Groundwater Complete, 2021).

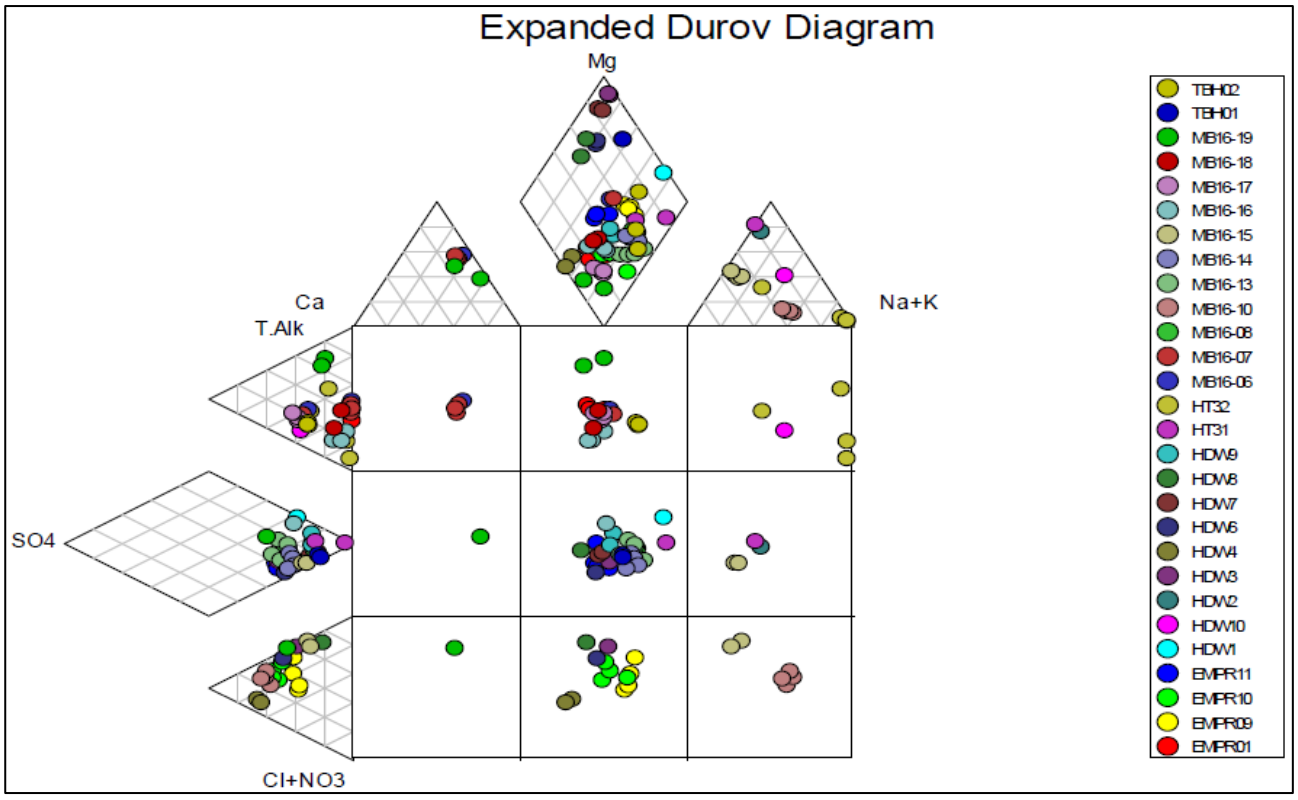

Figure 25: Expanded Durov diagram from data collected in 2020 from the monitoring boreholes in the Dishaba Mine lease area (Groundwater Complete, 2021).

The plot positions of monitoring boreholes in the first two fields of the Expanded Durov diagram represent relatively clean, fresh groundwater dominated by calcium/magnesium cations and

bicarbonate alkalinity on the anion side. On the other hand, plot positions lower down on the Expanded Durov diagram may be indicative of mine induced impacts on the groundwater quality conditions.

To better understand trends and spatial variation in the Expanded Durov diagram, the boreholes have been grouped by where they are located in the Amandelbult Complex, i.e., Tumela Mine, Dishaba Mine, HDD Open Pit and the Concentrator Plant (Table 4). The samples mostly plot within three categories on the Expanded Durov Diagram, i.e., fresh young water with limited ion exchange, a mix of different waters with sulphate contamination and a mixed type with nitrate contamination.

The Dishaba Mine samples show relatively more variety, with young water with both sulphate and nitrate contamination. This trend extends to the HDD Open Pit samples. The nitrate contamination appears to be more pronounced in the HDD, possibly due to the mining activities. The Tumela Mine samples are generally mixed type with sulphate contamination which is possibly due to leakages from the tailings dam.

Table 4: Grouping of groundwater monitoring holes according to their location across the Amandelbult Complex.

Monitoring holes per section of the Amandelbult Complex			
Concentrator	**Tumela Mine**	**HDD Open Pit**	**Dishaba Mine**
EMPR 05	EMPR 01	HDW1	EMPR 09
EMPR 07	EMPR 02	HDW10	EMPR 10
EMPR 08	HT 31	HDW2	EMPR 11
EMPR 15	HT 32	HDW3	MB16-06
EMPR 19	MB16-10	HDW4	MB16-07
EMPR 20	MB16-11	HDW5	MB16-08
EMPR 22	MB16-12	HDW6	MB16-09
EMPR 23	MB16-13	HDW7	MB16-18
WB 01	MB16-14	HDW8	MB16-19
WM 04	MB16-15	HDW9	MB16-20
WM 05	MB16-16		MB16-21
WM 07	MB16-17		
WM 08	TBH01		
MB16-01	TBH02		
MB16-02	TBH05		
MB16-03			
MB16-04			
MB16-05			

2.3.2 Deep Groundwater

The following water facies are commonly found in the vicinity of the mine lease area with the associated geology (Titus *et al*., 2009):

- BIC: Ca-Na-Mg-HCO_3 water type,

- Dolomites: Ca-Mg-HCO_3 water type, and
- Crocodile River Valley: Mg-Na-HCO_3-Cl water type.

Following a sampling program carried out by Titus *et al*. (2009), three clusters of water chemistry were identified from the samples taken in Amandelbult (Figure 26):

- Cluster 1 and 2: typical BIC,
- Cluster 2: dolomitic water, and,
- Cluster 3: Mine water inflows (fissure water), generally associated with high Na-Cl concentrations.

Compared to the shallow aquifer water, the deep mine inflows were found to be relatively uniform in chemical character, dominated by the NaCl water type.

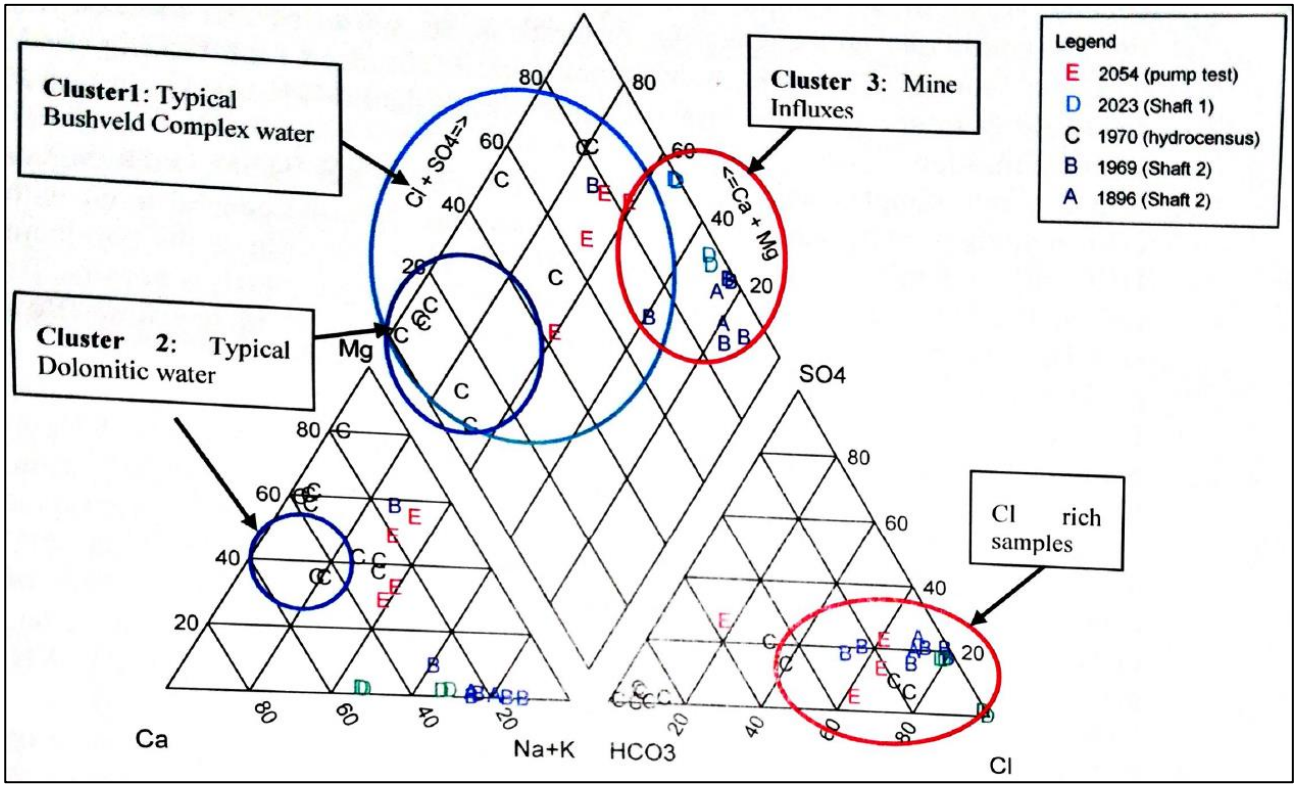

Figure 26: Groundwater quality in Tumela Mine (Shaft 1) and Dishaba Mine (Shaft 2) (from Titus *et al*., 2009).

In 2016, 16 samples from the underground mine workings (Figure 27) were submitted for hydrochemical and environmental stable isotope assessment (Golder, 2016). All these water samples grouped together in the NaCl quadrant of the central diamond of the Piper diagram (Figure 28).

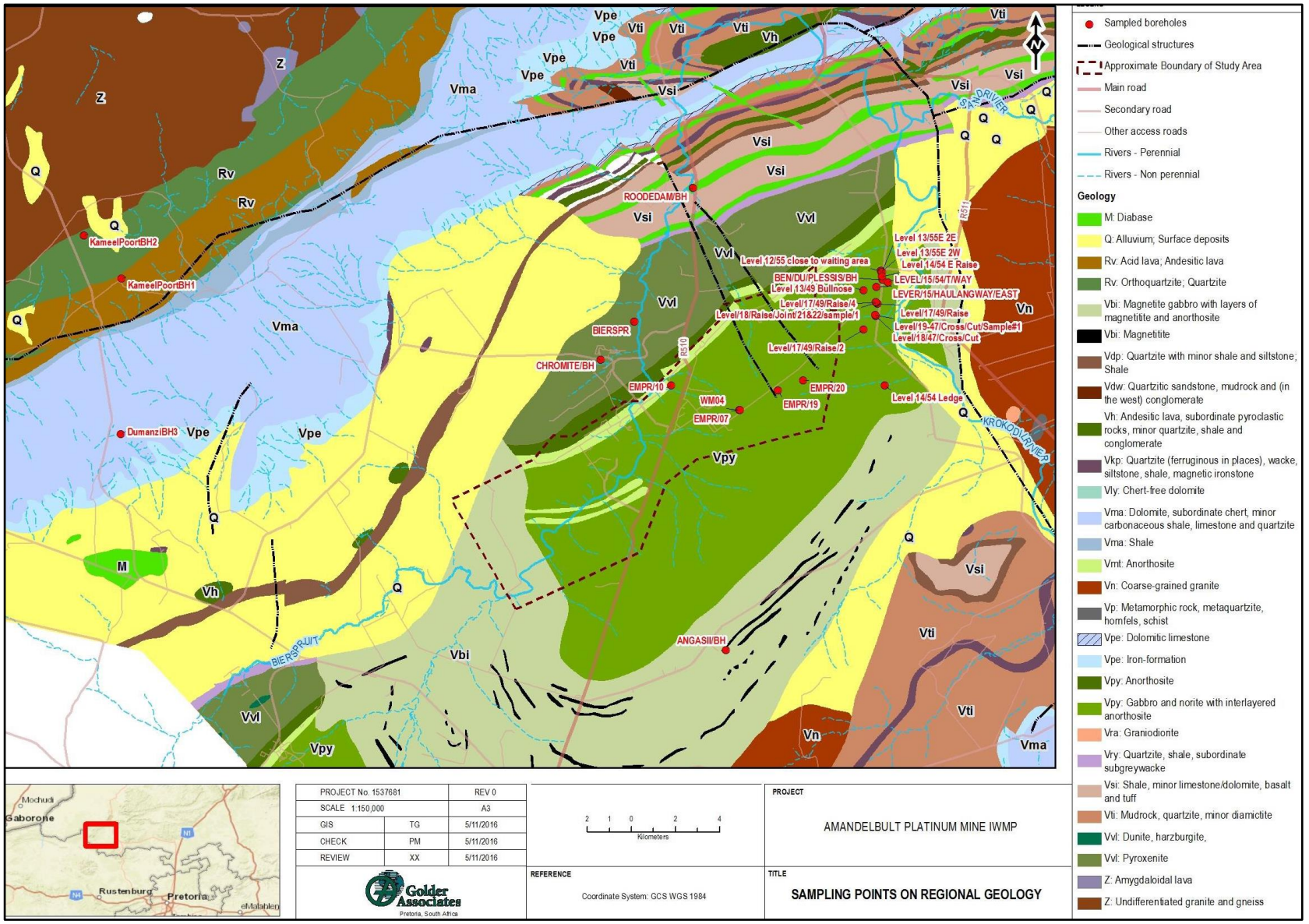

Figure 27: Geology and spatial distribution of samples taken in the 2016 sampling program by Golder (2016).

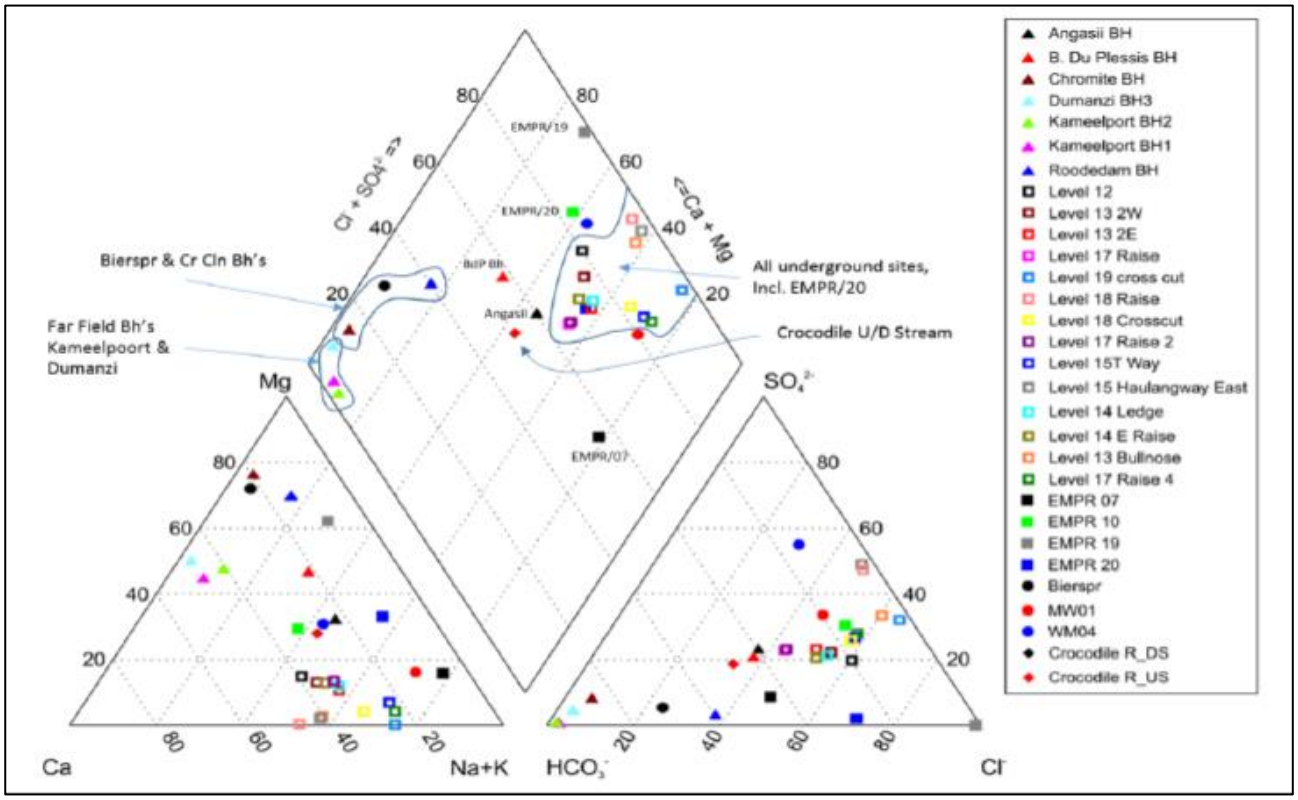

Figure 28: Piper diagram for the water samples from the 2016 sampling programme by Golder and Associates (Golder, 2016).

In a 2017 hydrochemical survey (Golder, 2018a), five underground water samples were taken from the following working areas:

- 5/41AE Crosscut
- 5/55AE Crosscut
- 14/55E 5W Merensky Reef Panel
- 16/40E Haulage
- 17/49E Crosscut

The samples were found to have a varied chemical composition (Figure 29). From these samples, it was concluded that there are two main sources of groundwater ingress into the mine, the Chuniespoort Dolomite (Ca/Mg–HCO_3 signature) and the Crocodile River (Na/Mg-Cl/SO_4 signature). It was suggested that the Crocodile River water with its strong evaporation signature forms part of the mine water cycle.

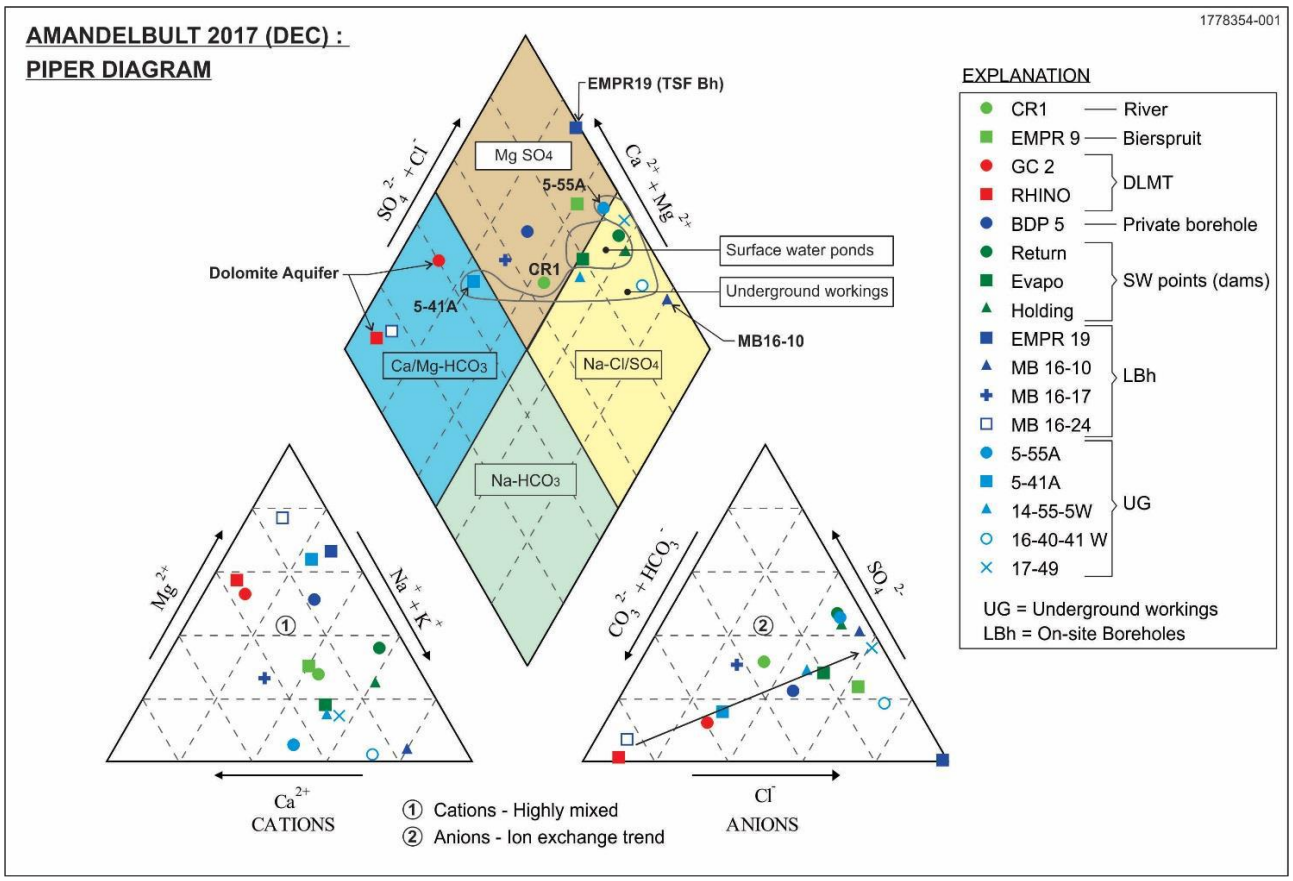

Figure 29: Piper diagram for the water samples from the 2017 sampling run (Golder 2018a).

2.4 GROUNDWATER MANAGEMENT

The presence of groundwater in a mine has a negative effect on production, ground control, ventilation, and safety (Ngubane *et al.*, 2015; Straskraba and Effner, 1998). The DWAF (2008) further lists the following negative effects of groundwater ingress into mine workings:

- Reduction in the ability of affected surface/groundwater resource to provide other water users with water,
- Water quality deterioration due to contact between water and ores with sulphide minerals, cyanide from backfill operations, explosives and other chemicals used in mining operations,
- Flooding of the underground mine,
- Closed mines may decant contaminated water into the surrounding aquifers or surface water resources, and,
- Inter-mine flow may occur where water from adjacent mine flows into and becomes part of the water balance of the receiving mine.

Failure to adequately plan for and mitigate against any adverse groundwater impacts is perilous for any mining operation. The fundamental principle that applies to water management in underground

mines according to DWAF (2008) is: *Plan, design, operate and close the underground mining operations in a manner that reduces the ingress of clean water into the mine, minimizes the volume of water used in mining operations, maximizes water reuse, minimizes the water quality deterioration within the mine and minimizes the impacts on the water resource.*

The groundwater management strategy of Dishaba Mine is continuously being revised as new information becomes available. The excess water that is pumped from the underground is used in processing operations, for sanitation, and is also recycled to obtain water of high-quality drinking standard (N. Nxiweni, personal communication, 2020).

Groundwater control in underground mining usually takes the form of grouting or dewatering (Straskraba and Effner, 1998). The two methods can be applied simultaneously depending on a number of factors, such as the hydrogeological characteristics of the mine, the depth of the mine and the mining method. At Dishaba Mine, the function of groundwater control lies within the Geology Department. Groundwater control is guided mainly by the standard operating procedure titled “Cover drilling and water / flammable gas intersections underground”.

According to the mine standard procedure, cover holes are drilled ahead of mining at an inclination of between 0° and 5° and almost parallel to or along haulages and crosscuts. The holes are 120 m long. The primary purpose of the cover holes is to intersect water and flammable gasses ahead of mining. On water intersection, the holes are either grouted or allowed to drain freely (dewater) depending on the volume of water intersected.

A staggered single or double cover pattern is used, depending on the groundwater risk classification of the area (Figure 30). The single cover pattern requires that the holes have an overlap of 15 m on either side of the mining excavation. The double cover requires an overlap of 60 m. Currently the underground hydrogeological risk areas are divided into two: the low risk - single cover areas (3-14 Level) and the higher risk - double cover areas (15-19 Level). Figure 31 shows the cover drilling layer of the mine water plan with the groundwater risk classification.

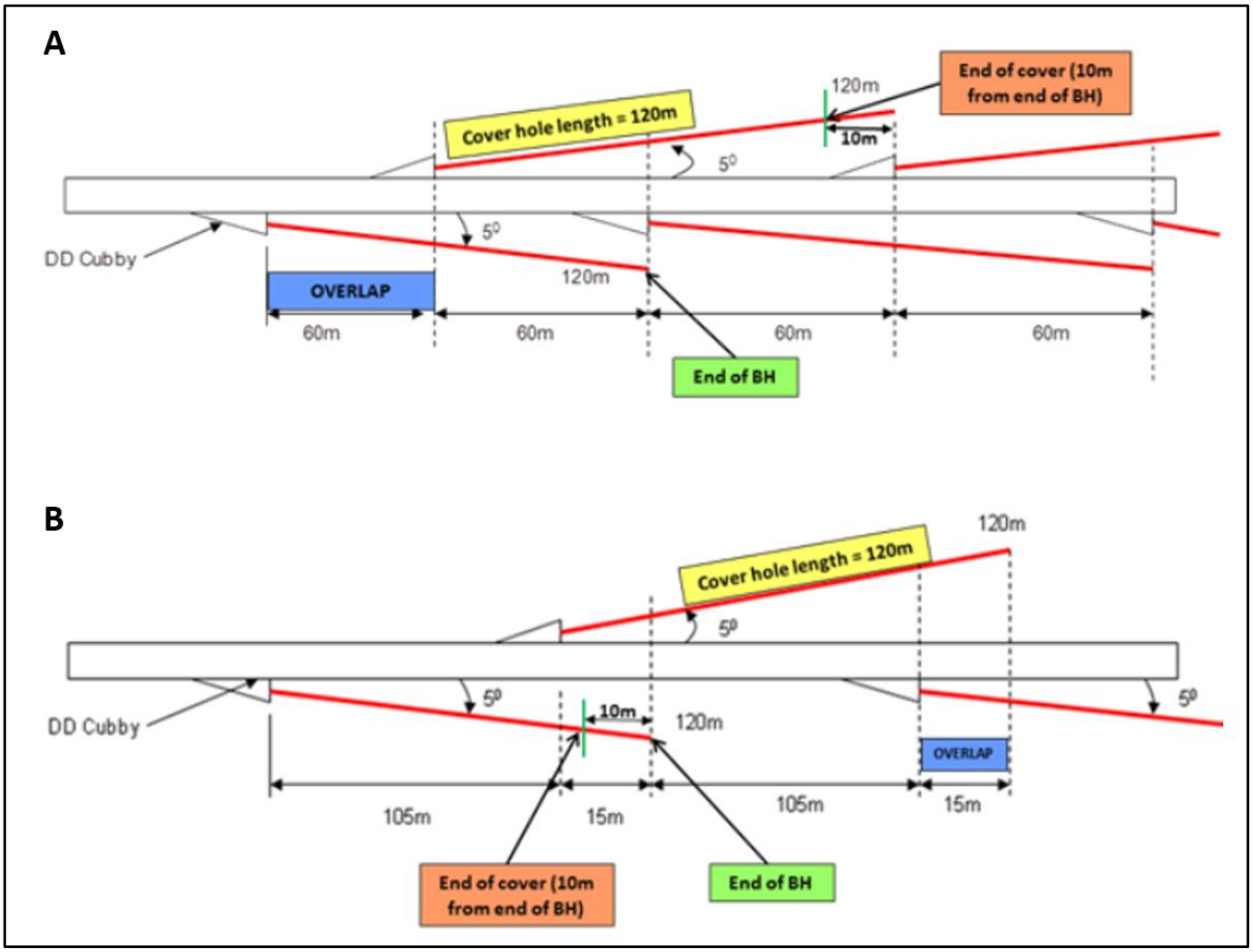

Figure 30: (A) Double cover drilling pattern and (B) single cover drilling pattern.

When groundwater is intersected by a haulage or crosscut, mining is stopped i.e. all mining activities are stopped and the mining crew is withdrawn from that specific mining excavation that has intersected water. A diamond drilling crew moves in and starts ring cover drilling (i.e., flat holes drilled on the face of the excavation in a ring-like configuration) and the ring cover holes are then grouted with cement. Due to cost implications, grouting is done using normal portland cement. "Water sealing chemicals" tend to be far more expensive and less effective in preventing groundwater ingress into mine workings (M. Moyo, personal communication, 2022). Depending on the amount of water intersected, grouting takes anything from three production shifts to well over a month's worth of production shifts lost.

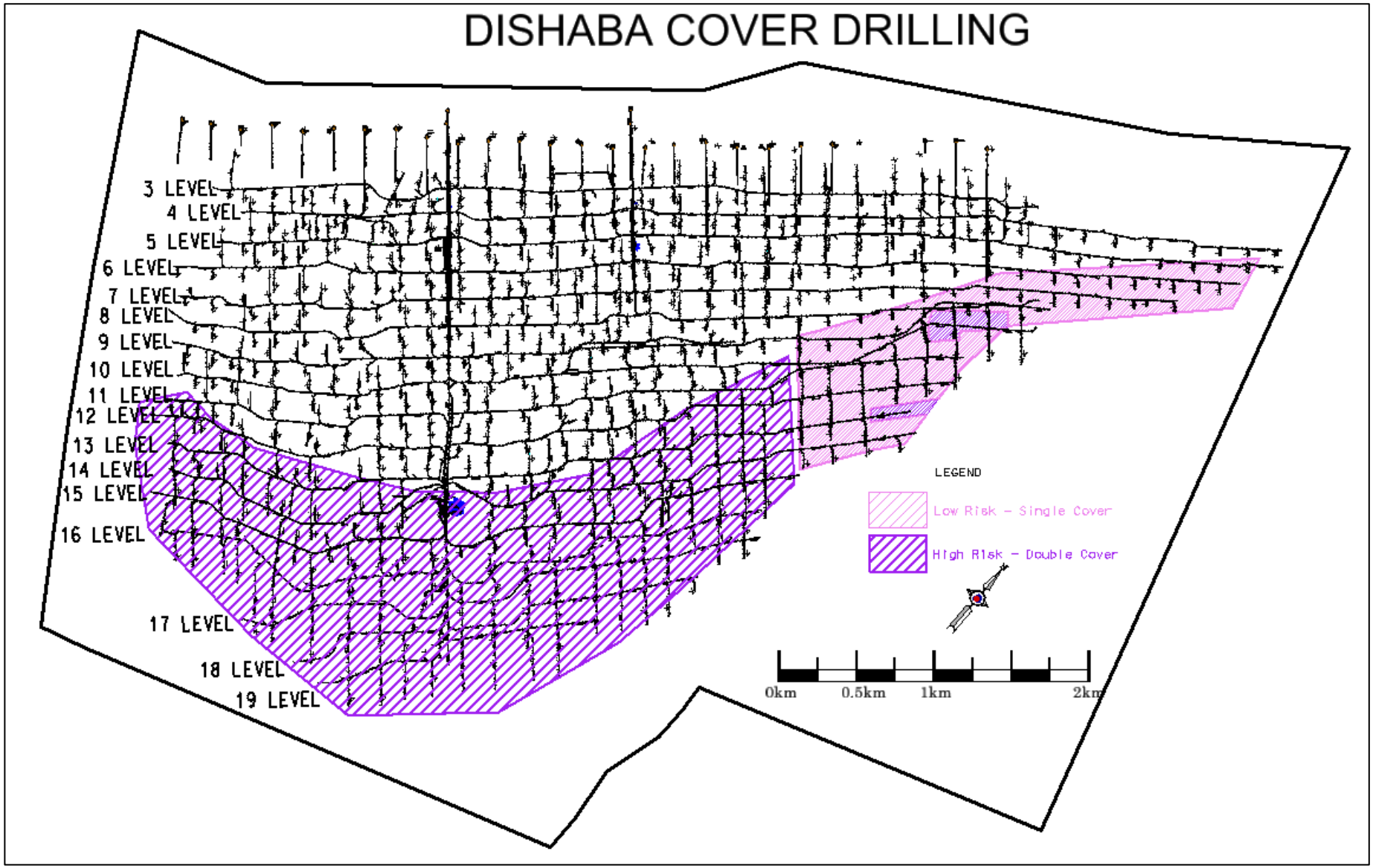

Figure 31: Cover drilling layer of the mine water plan, showing the different groundwater risk classifications and associated cover drilling requirements.

CHAPTER 3:
DATA COLLECTION

3.1 INTRODUCTION

Data collection for this research project was carried out through a seepage survey which included a desktop study, seepage survey and underground mapping, analysis of the existing borehole database, groundwater sampling, and hydrogeochemical analysis through the Aquatico and iThemba laboratories. This chapter details the processes followed and equipment used in the data collection, processing, and interpretation for this project.

3.2 GROUNDWATER SEEPAGE SURVEY

The seepage survey started with a review of existing data and was followed by underground mapping and recording of field parameters (temperature, pH, EC and TDS). The existing data and information consist of the water plan, the borehole database, the geology plan and flow meter data.

3.2.1 The Water Plan

The water plan (or map) is a multi-layered digital plan depicting all the development (tunnel) excavations at the mine with water-related information. The plan shows groundwater intersections, groundwater properties, the cover drilling plan, gas intersections (especially methane) and the virgin rock temperatures.

The mine is divided into two zones based on the geology and historic hydrogeological information which define the risk of disruptive groundwater intersections (Figure 31). The two zones are the single cover, and the double cover zones. The single cover zone starts at 3 Level (approximately 150 mbgl) and ends at 14 Level (approximately 900 mbgl). Extensive mining has taken place across this zone and as a result the classification applies mainly to the eastern edge of the mine. The western and central part was mined out in the 1980s-1990s and most of the historical water intersections have been grouted (M. Moyo, personal communication, 2022). Some of the cover drilling data were not recorded even though water was intersected. There are five water-prone zones demarcated on the plan, particularly at the centre of the mine, but no details are given.

The double cover zone starts at 15 Level (approximately 970 mbgl) and extends to the bottom of the mine at 20 Level, approximately 1300 mbgl. In this zone, relatively recent expansion of the mine into virgin ground has taken place. A better record of groundwater intersections is also found in this

zone. Water intersections are generally found in cover holes across the haulage excavations. They tend to be associated with calcite-rich joints and leucocratic rocks in the footwall of the UG1.

Another important component of the water plan is the virgin rock temperature (VRT) plan (Figure 32). As would be expected with a normal geothermal gradient, the VRT increases with depth. The VRT closer to surface on 3 Level is 26°C and steadily increases to over 46°C at shaft bottom on 20 Level. Recorded water temperatures vary between about 21°C close to surface and 45°C on 19 Level. This implies a direct relationship between VRT and groundwater temperature.

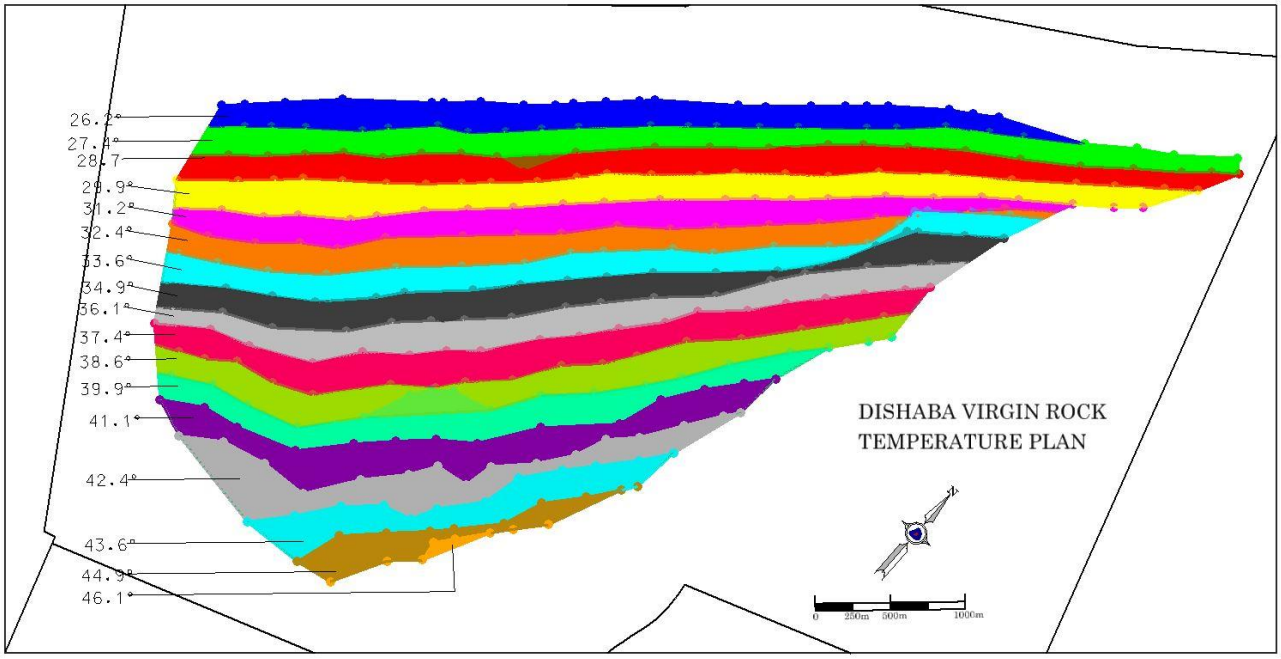

Figure 32: The Virgin Rock Temperature layer of the water plan.

In terms of spatial distribution, the most prominent water intersections are recorded on 18-19 Level east haulage, 53E to 55E Merensky stopes across all levels, and the western haulages approaching the Show-Stopper Fault and Middellaagte Graben (Figure 20 and Figure 33). A prominent anomalous area is the 17/49E Merensky stope. The stope is not connected to any known water-prone geological structure, but a surface borehole is continuously bringing water into the stope. Other notable mining excavations with water ingress are:

- 17/40E Merensky Stope,
- 41E Line Across all levels (in the vicinity of the Show-Stopper Fault),
- 19/45E UG2 Stope, and,
- 17W Haulage.

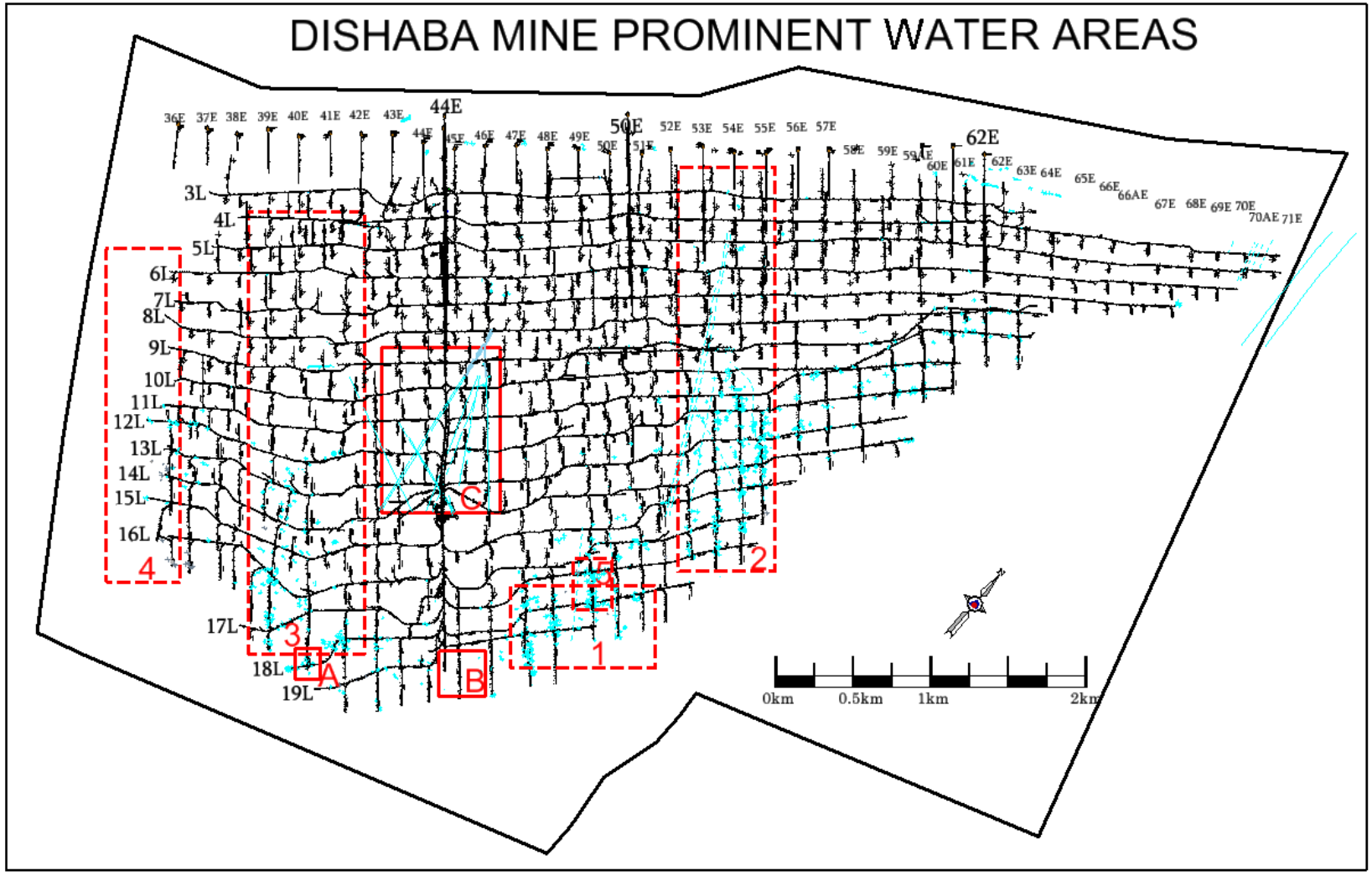

Figure 33: Areas with recorded prominent groundwater intersections: (1) 18E and 19E Haulages, (2) 53E-55E Lines, (3) Show-Stopper Fault area, (4) Western haulages approaching Middellaagte Graben, and (5) 17/49E MER stope. Other notable areas: (A) 17/40E MER Stope, (B) 19/45E UG2 Stope, and (C) Historic intersections in the middle of the mine.

The water plan is revised annually with new intersections added from the mining and drilling activities of the previous year. For the year 2020-2021, the following water intersections were recorded:

- 15/41A Xcut North: Warm water dripping from the hanging wall in the vicinity of the Show-Stopper Fault,
- 15/41EA diamond drilling into the Show-Stopper Fault,
- 15/51E Bullnose: Water dripping from the haulage hanging wall,
- 19/45E 4W UG2 Panel: Water dripping from the hanging wall, and,
- 17/40E 3E and 5E Merensky Panel: Water dripping from the hanging wall.

No new prominent, flowing intersections were recorded; however, all these new intersections fall within the prominent areas described above. The lack of new prominent intersections due to mining could be ascribed to the fact that mining occurred only in the UG2 under the mined-out Merensky stopes. No “virgin ground” mining or development took place during the 2021-2022 production year.

3.2.2 The Borehole Database

The borehole database at Dishaba Mine consists of approximately 5000 boreholes. The most notable groundwater intersections from boreholes are located within the prominent areas described above i.e., on 19 Level Haulage, 54E Line and 41E Line. On 19 Level, the most intersections are through the ring cover and cover holes. These are boreholes drilled relatively flat along the HLGE and crosscuts. The intersections are largely along the footwall of the UG1.

Numerous prospect holes were drilled specifically to dewater the 54E Line. These extend from 10-16 Level. Figure 34 shows an example of ring cover holes drilled into the hanging wall of 13/54E Crosscut. The three holes in the example were drilled along the direction of mining, towards the south-easterly direction as well as in the south-westerly direction.

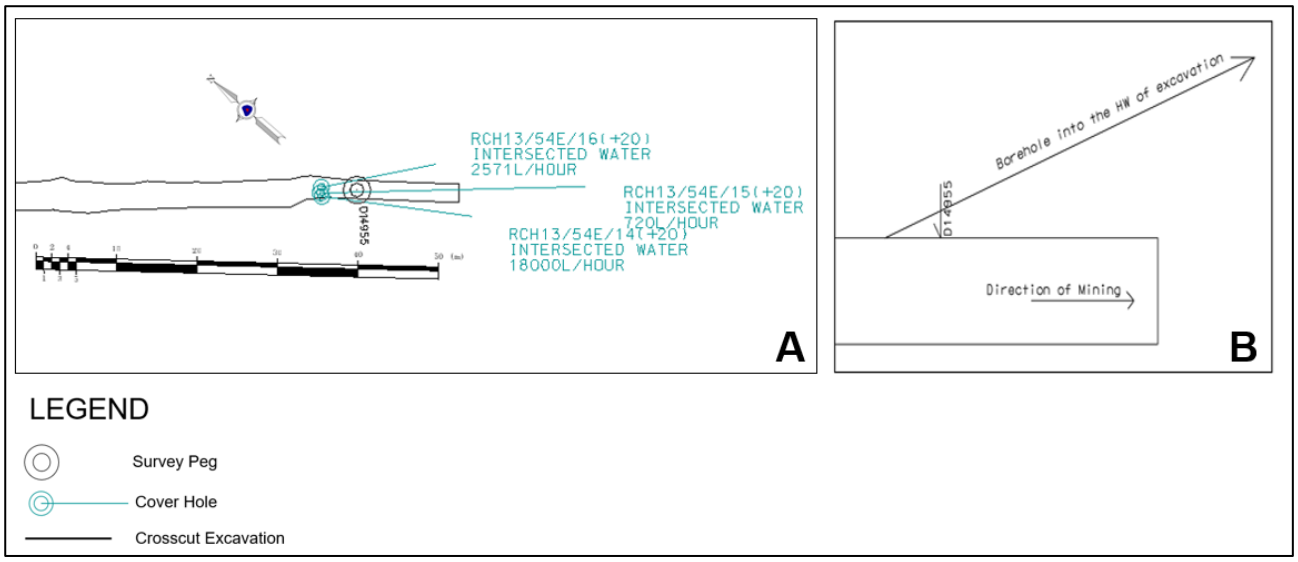

Figure 34: An example of ring cover drilling. (A) Plan view and (B) a representative section of the same area (not to scale).

Boreholes drilled from surface (surface holes) make up approximately a quarter of the overall borehole database. These holes are drilled across the mine lease area in active and inactive farming areas above the mining excavations. The surface holes are generally drilled ahead of mining for resource classification and delineation of geological structures. Mining excavations expose historic surface holes. These exposures are known to have water ingress as water builds up inside the holes.

Historically, only the top 50 m of surface holes were plugged with cement. This was mainly to cover the weathered zone. With the continued exposure of surface holes with water running into mine workings, it became obvious that surface holes act as conduits for groundwater from the weathered zone, rain or even possibly irrigation, to reach the deep mine workings. A decision was taken to fully grout the entire length of any surface borehole to minimise groundwater ingress into the mine workings (M. Moyo, personal communication, 2020). Figure 35 shows the locations of the surface holes drilled across Dishaba Mine and their sealing status as at the end of 2021.

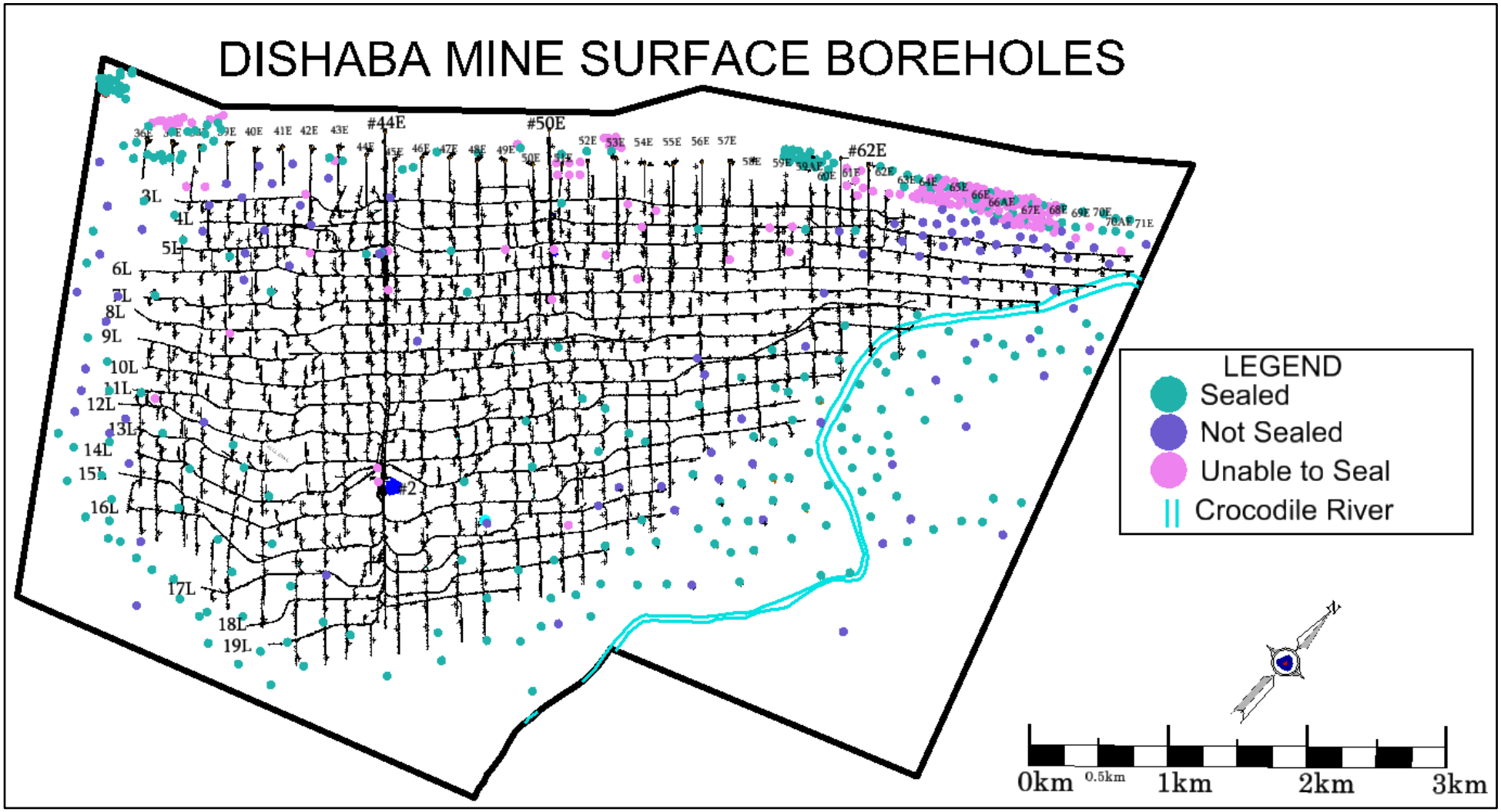

Figure 35: Sealing status of surface boreholes across Dishaba Mine.

3.2.3 The Geology Plan

The geology of the mine is recorded in two digital plans, one for the Merensky Reef horizon and the other for the UG2 Reef horizon. Off-reef excavations (e.g., haulages and crosscuts) are shared for the mining of either reef type, and therefore share the same geological information. The Merensky Reef at Dishaba Mine has been mined since the late 1970s while mining of the UG2 only started in the early 2000s. In 2020 the mine moved to a 100% UG2 mining underground and a far smaller amount of the Merensky Reef (just over 30 000 m^2) was mined in the open pit.

As a result of relatively more mining of the Merensky, there is far more information on the Merensky Reef horizon than on the UG2 Reef horizon. The Merensky Reef horizon plan does, however, have a shortage of geological data in areas mined prior to say 2003. This is possibly due to a shortage of resident mine geologists in the mining industry at the time (M. Moyo, personal communication, 2022).

Figure 13 shows the distribution of major faults and dykes on the Merensky reef horizon. Various linear structures (joints, shears, veins, dykes, and faults), reef disturbances (potholes, slumps, and reef rolls), lithological units and drilled boreholes are all recorded on the geology plan.

In addition to geological features, water intersections are also recorded in the geology plan. Figure 36 shows an example of groundwater information recorded on the geology plan. The individual or small-scale water records build up to a water plan and the water intersections can be extracted on their own without geology information (Figure 20), this allows for simpler spatial analysis of groundwater intersections.

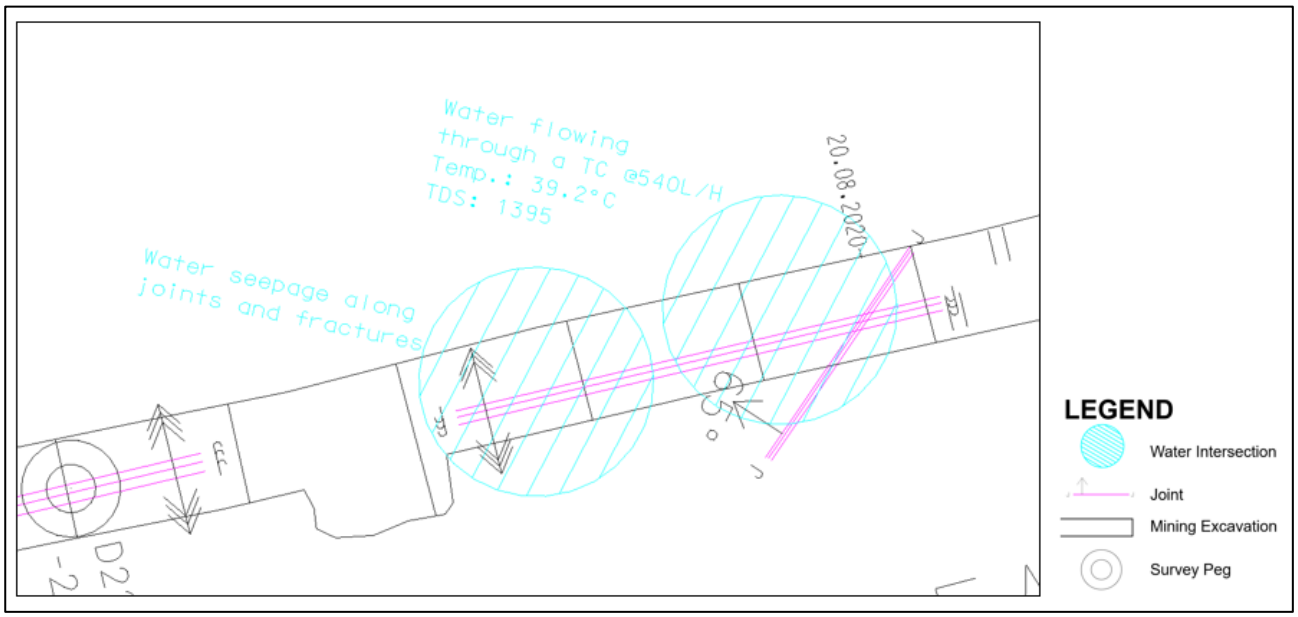

Figure 36: An example of water information recorded on the geology plan.

3.2.4 Flow Meter Data

Several flow meters are installed at the mine, mainly along the different decline shafts and the Vertical Shaft. These flowmeters monitor water sent down to underground workings and water pumped out from the underground. The difference between the volumes of water sent down and water pumped out is assumed to be due to groundwater ingress. For this project, the focus is on the #2 Vertical Shaft data because this is the deepest shaft and accesses the deepest fractured aquifer.

Figure 37 shows the flowmeters data recorded in the #2 Vertical Shaft between January 2017 and September 2022 by the Water Resources Engineer of Dishaba Mine. “Column A and B” is the total water pumped from the shaft, “Water Down Shaft” is the amount of service water sent down the shaft and “Ingress” is the estimated groundwater ingress into the mine. Figure 37 shows that the estimated groundwater ingress varies between 15 500 to 19 000 m^3/d. A detailed analysis of the data was carried out with the results presented in the following chapter.

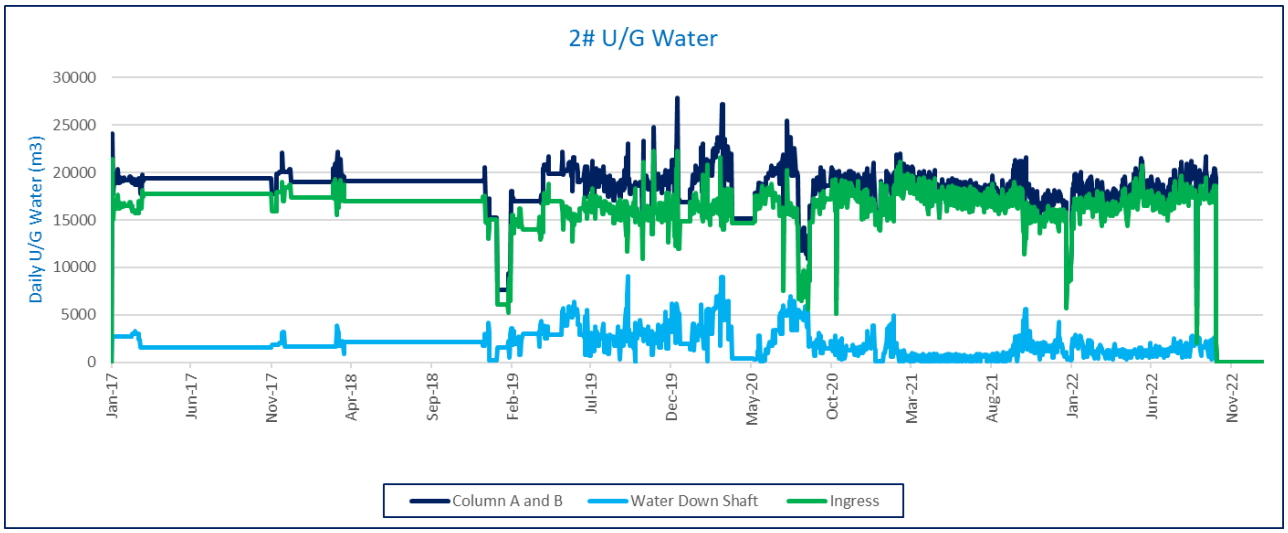

Figure 37: A plot of flow meter data from #2 Vertical Shaft.

3.2.5 Underground Mapping

Underground visits were carried out to identify areas with groundwater inflows, to obtain field measurements pertaining to groundwater intersections, and to sample the water. Most of the water intersections indicated on the geology maps and water plan in Figure 20 have been sealed-off for ventilation control or grouted to allow for dry mining conditions. The areas described below (shown in Figure 48) were found to have significant groundwater flows.

3.2.5.1 3/62E Haulage

3 Level 62E Haulage is located in the upper eastern section of the mine at approximately 148 mbgl at an elevation of 789 mamsl (Figure 38). There is water flowing from behind a ventilation wall. Using a V-notch (Figure 39), the flow rate was found to be about 3312 L/h.

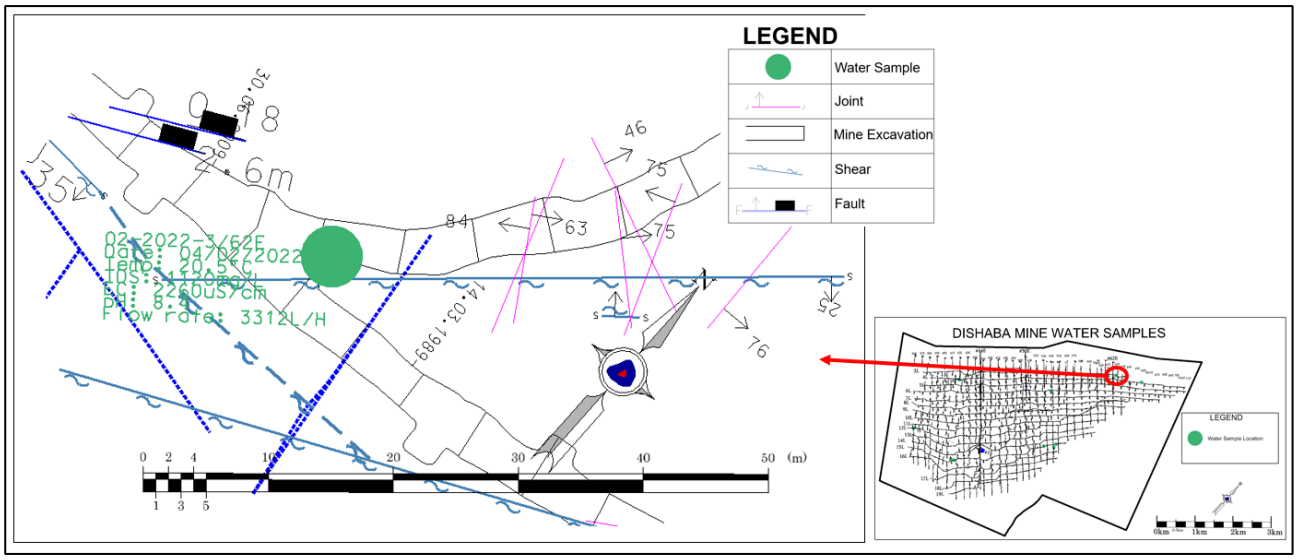

Figure 38: Plan view of the location of the 3/62E sample.

Figure 39: Photographs showing V-notch placement (left) and measuring (right) at 3/62E. The ventilation control wall made of bricks can be seen in the background on the right.

3.2.5.2 4/66E Refuge Bay

The 4 Level 66E Refuge Bay (Figure 48) is located at 195 mbgl at an elevation of 742 mamsl. There is water coming from an annex hole drilled into the hanging wall of the excavation. The depth of the annex hole is unknown. The water has a brownish appearance and using a bucket and watch the flow rate was estimated to be approximately 15 000 L/h.

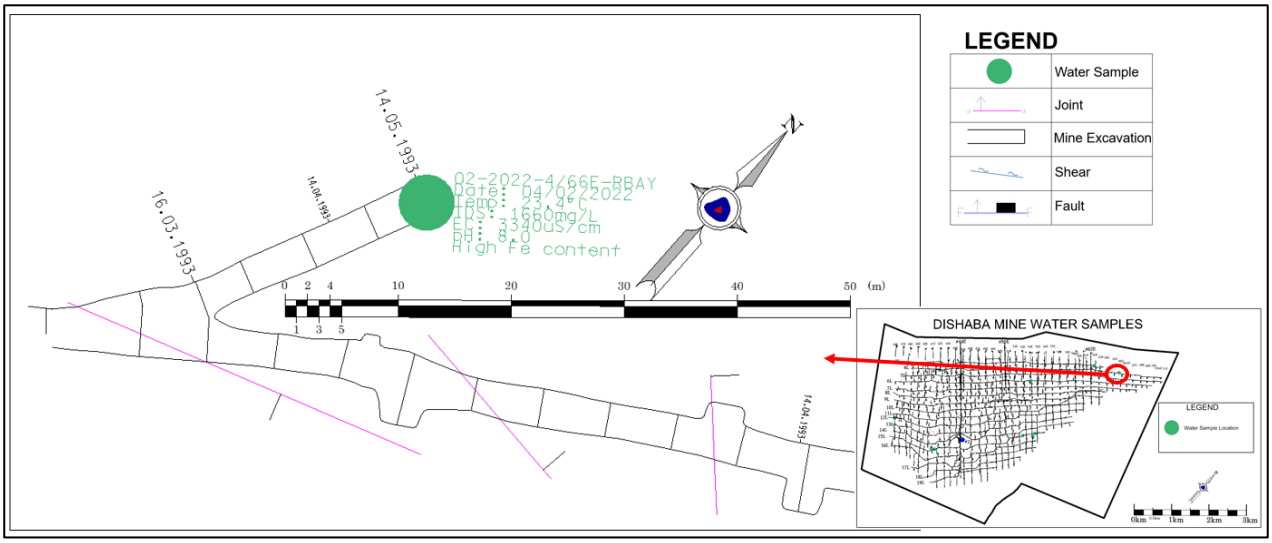

Figure 40: Plan view showing the location of the 4/66E Refuge Bay sample.

3.2.5.3 6/54E Line

A large area extending over a 30 m span at 6 Level East (Figure 41) along the 54E line has abnormally high volumes of dripping water from the hanging wall of the haulage, a workshop and a refuge bay. The 6 Level is at 339 mbgl at an elevation of 598 mamsl. The water appears to be *raining* from the hanging wall of the above-mentioned excavations which are below the Merensky Reef. Historical mine maps show significant water intersections in the past of about 4000 L/h on the Merensky Reef horizon. In recent times, some minor water drips were also reported on the UG2 Reef horizon. These water drips on the UG2 Reef horizon were, however, found to be insignificant and posed no threat to mining continuity.

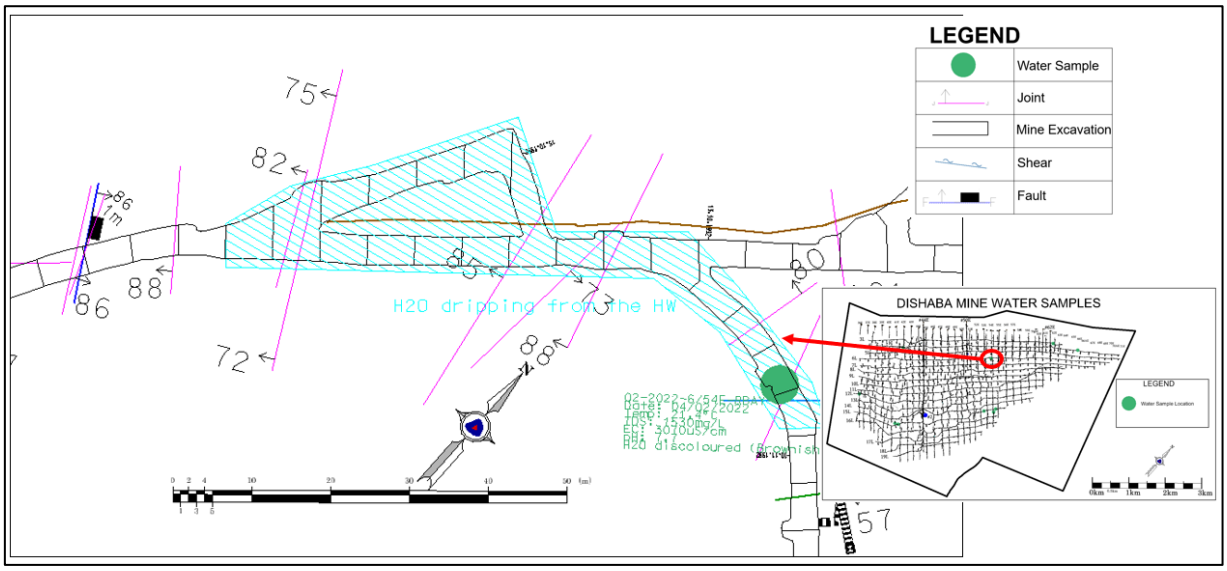

Figure 41: Plan view of 6/54E Battery Bay and Crosscut that has been converted into a Refuge Bay.

3.2.5.4 5/42E HLGE

The 5 Level West Haulage mined through the Show-Stopper Fault (Figure 42). There is an estimated 7200 L/h of water flowing out of the fault in the haulage. The inflow into the haulage is most prominently coming from a southerly direction. The 5 Level is located at 274 mbgl at an elevation of 663 mamsl. The area through which the haulage passes the fault is supported with steel sets. Corrosion on the steel sets and the service pipes through the area was observed. Significant calcite precipitation from the groundwater in the area was also observed.

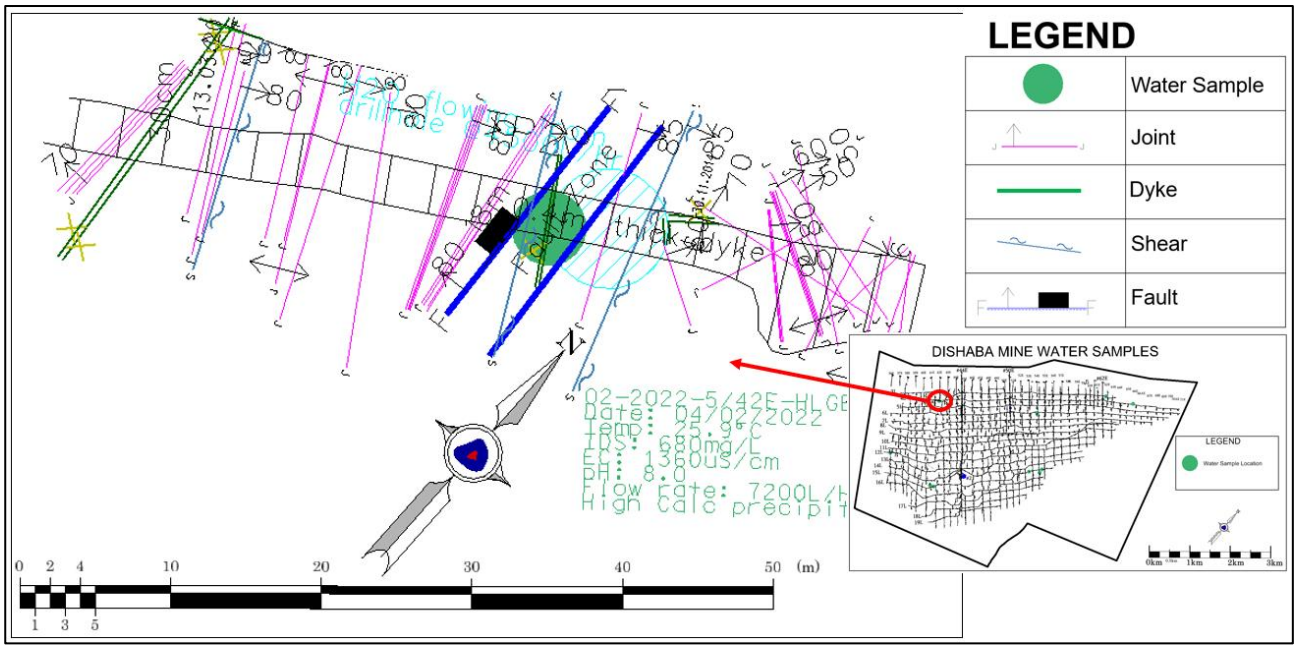

Figure 42: Plan view of the 5/42E Haulage.

Figure 43: Photograph showing water flowing through steel sets supporting the Show-Stopper Fault. Note the white calcite precipitate covering the pipes and on the steel support.

3.2.5.5 12/36E HLGE

The 12/36E HLGE haulage was mined up to approximately 220 m before reaching the major graben fault. Two cover holes were drilled towards the graben and these holes intersected groundwater. There is water flowing from these cover holes and, due to ventilation constraints, the end of the haulage could not be reached. The groundwater ingress was therefore assessed from under a ventilation control wall just past the 36E Crosscut (Figure 44). The water is flowing at an estimated rate of 15000 L/h. The haulage was last mined in 2007 and multiple fault and water intersections are thought to be the reason mining was stopped. In essence, water has been flowing for about 15 years in this area. The geology of the area is mainly anorthosite in the UG1 footwall. There are multiple near-vertical joints with calcite infill. Diamond drilling in the area intersected faults of various scales; these faults are sympathetic to the Middellaagte Graben.

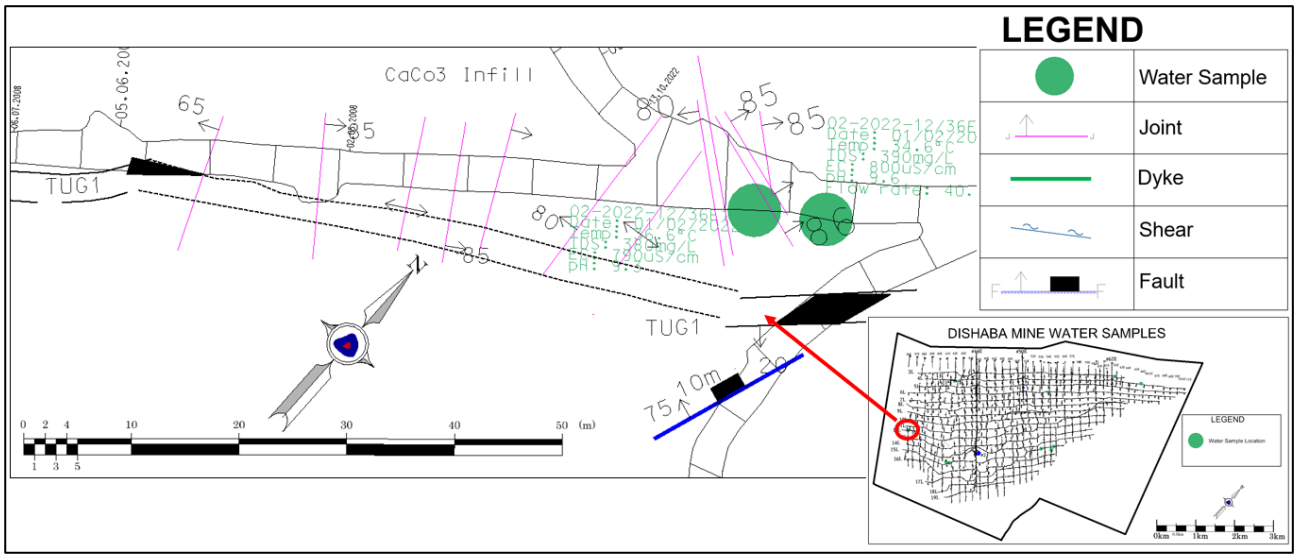

Figure 44: Plan view of the location of the 12/36E samples.

3.2.5.6 15/41E HLGE and Crosscut

In the haulage, there is water flowing at a rate of 26.5 L/h from an historic borehole: 15/42E/6 (Figure 45). The borehole was drilled in February 2004 and intersected the Show-Stopper Fault. The water is thought to be coming from the Show-Stopper Fault. In the relatively newly developed (in 2021) 41AE Crosscut North, there is an area of approximately 150 m^2 with warm water dripping. The water is dripping from the hanging wall through multiple joints and shears. The prominent fractures with water dripping have a general dip of 60° south-westwards and strike at 273° direction. The haulage and crosscut are below the UG1 within norite. These excavations are located at 960 mbgl and 23 mbmsl (meter below mean sea level).

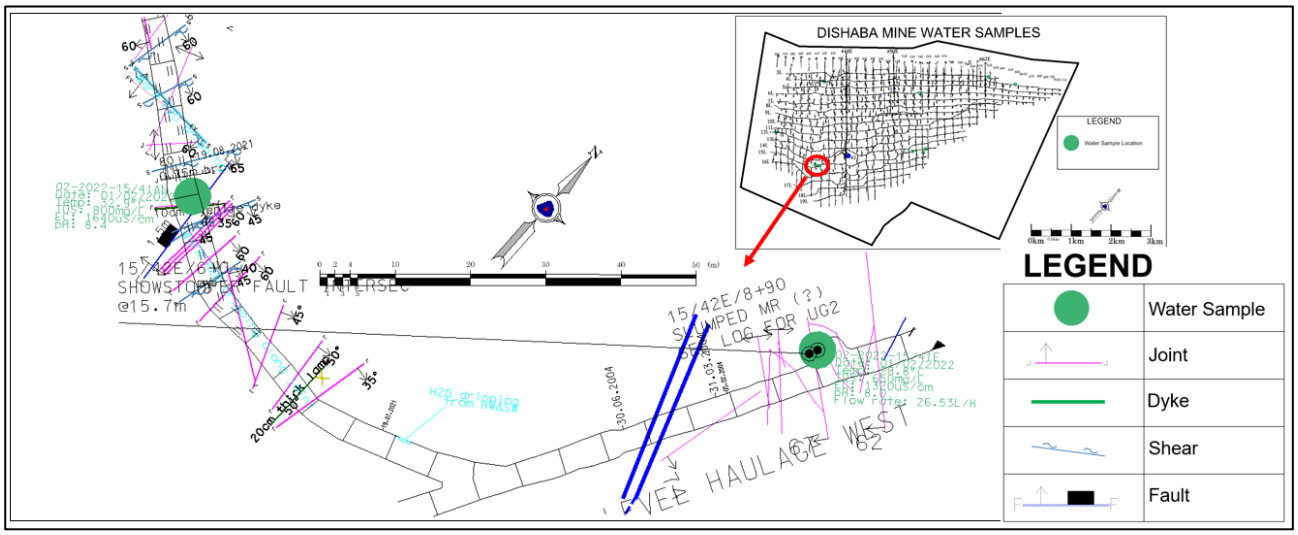

Figure 45: Plan view of the 15/41E Haulage and Crosscut. Note the black dots on the haulage sample mark the collar positions of diamond drilling holes; 15/42E/6 is marked by the line running towards the crosscuts.

3.2.5.7 15/53A to 55E HLGE

On the eastern side of 15E Haulage between the 53A and 55E Lines, there are multiple water intersections. Most of the historic water intersections have been grouted; however, some of the intersections that are still flowing are mainly through boreholes. This area forms part of the 54E Line water pillar. During the seepage survey there were three areas that could be easily accessed (Figure 46):

- 15/53EA HLGE – Water flowing at 134 L/h through a borehole (15/53E/8). The exact lithology or structure from which the water is flowing could not be established. However, the borehole was drilled to a depth of 83.62 m with norite above the Merensky Reef at the end of the hole. The hole was drilled from 955 mbgl at an elevation of 18 mbmsl. Drilling of the hole was completed in the year 2010.
- 15/54E Crosscut – The 54E line is known to have high yielding intersections (over 1000 L/h) and generally warm water, especially on the Merensky Reef horizon. Mining was stopped in 2016 following the intersection of 3600 L/h through a fault. The fault was exposed at 931 mbgl at an elevation of 6 mamsl. The fault is a normal fault and displaces the Merensky Reef by 1 m. It has a dip of 60° eastwards and is striking at 159°. The area is no longer accessible; however, there is water flowing from under the ventilation control wall at a rate of over 15 000 L/h. There is high calcite precipitate observed from the groundwater.
- 15/55E HLGE. There is water flowing from a joint at a rate of 165 L/h. The water has a slimy precipitate (possibly $Mn(OH)_2$). The joint was exposed at 18 mbmsl at a depth of 955 mbgl. The HLGE is in anorthosite in the footwall of the UG1.

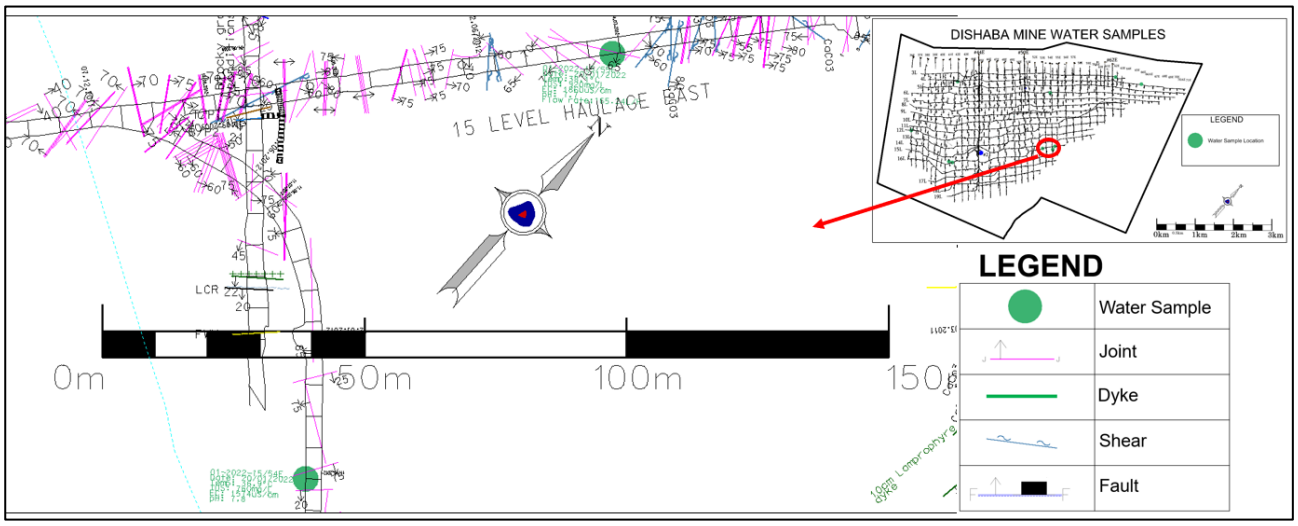

Figure 46: Plan view of the 15/54E Crosscut and 15/55E Haulage samples.

3.2.5.8 19E LEVEL

The 19 Level is located some 1200 mbgl at an elevation of 299 mbmsl. Historical mapping shows numerous water intersections (Figure 47). Most of the intersections have been grouted to allow for safe and dry mining conditions (Ngubane *et al*., 2015). A new water intersection was recorded at 19/48E Crosscut during the course of the study. The water was intersected through a borehole (borehole ID: 19/48E/8) in the anorthosite directly below the Merensky Reef. A calcite-filled joint was found to be the main conduit. The initial flow rate was recorded as 6000 L/h, but within a week it had reduced significantly. Minor water drips in the HLGE and the 48E Crosscut were also observed. The drips are coming from the hanging wall also through calcite-filled joints. Mining on this level has been stopped. The haulage is in the norite below the UG1.

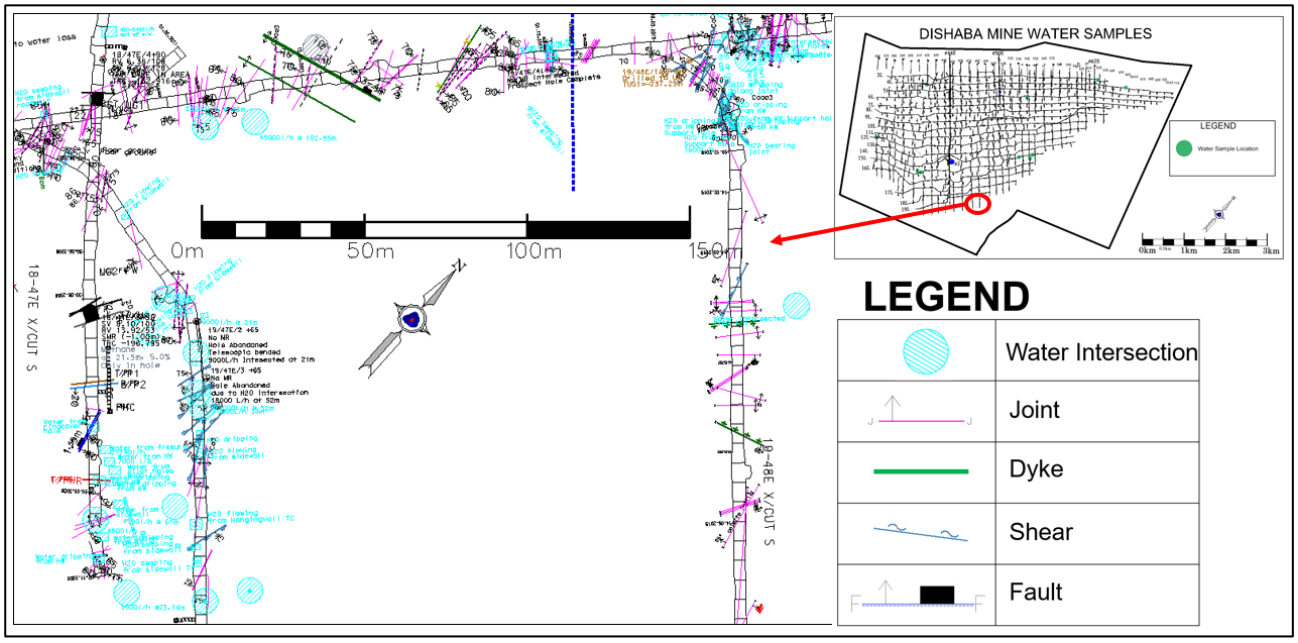

Figure 47: Plan view between the 19/47E and 19/48E Crosscuts.

3.3 GROUNDWATER SAMPLING

Groundwater samples were collected from all sites described in Section 3.2.5, except for the 19 Level. The locations of the groundwater samples are shown in (Figure 48), while the field properties of the water are listed in Table 5. For coordinates, the mine uses the Hartebeeshoesk94 (WGS84) datum and the Gauss Conform projection. The coordinates listed are therefore in line with the mine's coordinate system. Several trends can be seen from the field properties:

- Temperature – Generally increases with depth from 20.5°C on 3 Level to over 38°C on 15 Level. The western side of the mine has relatively lower temperature with 28.8 at 15/41AE compared to 38.8 at 15/55E. 12/36E is oddly higher than 15/41AE, this is possibly due to poor ventilation in the area as no active mining activity was taking place at the time the sample was taken, the rock mass surrounding the mine excavation was therefore not cooled.
- The EC increases in the easterly direction, with the eastern-most samples (4/66E) having the highest EC value. The trend can be seen with 15 level samples where EC increases from 1340 µS/cm at 53AE to 1860 µS/cm at 55E. No clear trend is observed relative to depth.
- The TDS is a calculated value in the instrument from the values of the EC. The TDS therefore shows similar trends to the EC
- The general range is 7.7 to 8.4. The pH is largely similar for samples from the same levels. The outliers were the highest which was found at 12/36E (9.6) and the lowest which was found at 15/53A (7.3).

Two 500 ml samples were collected from each site. One sample was sent to the Environmental Isotope Laboratory of iThemba Labs in Johannesburg for D/H ($^{2}H/^{1}H$) and $^{18}O/^{16}O$ stable isotope analysis. The other sample was sent to Aquatico Labs in Centurion for hydrogeochemical analyses.

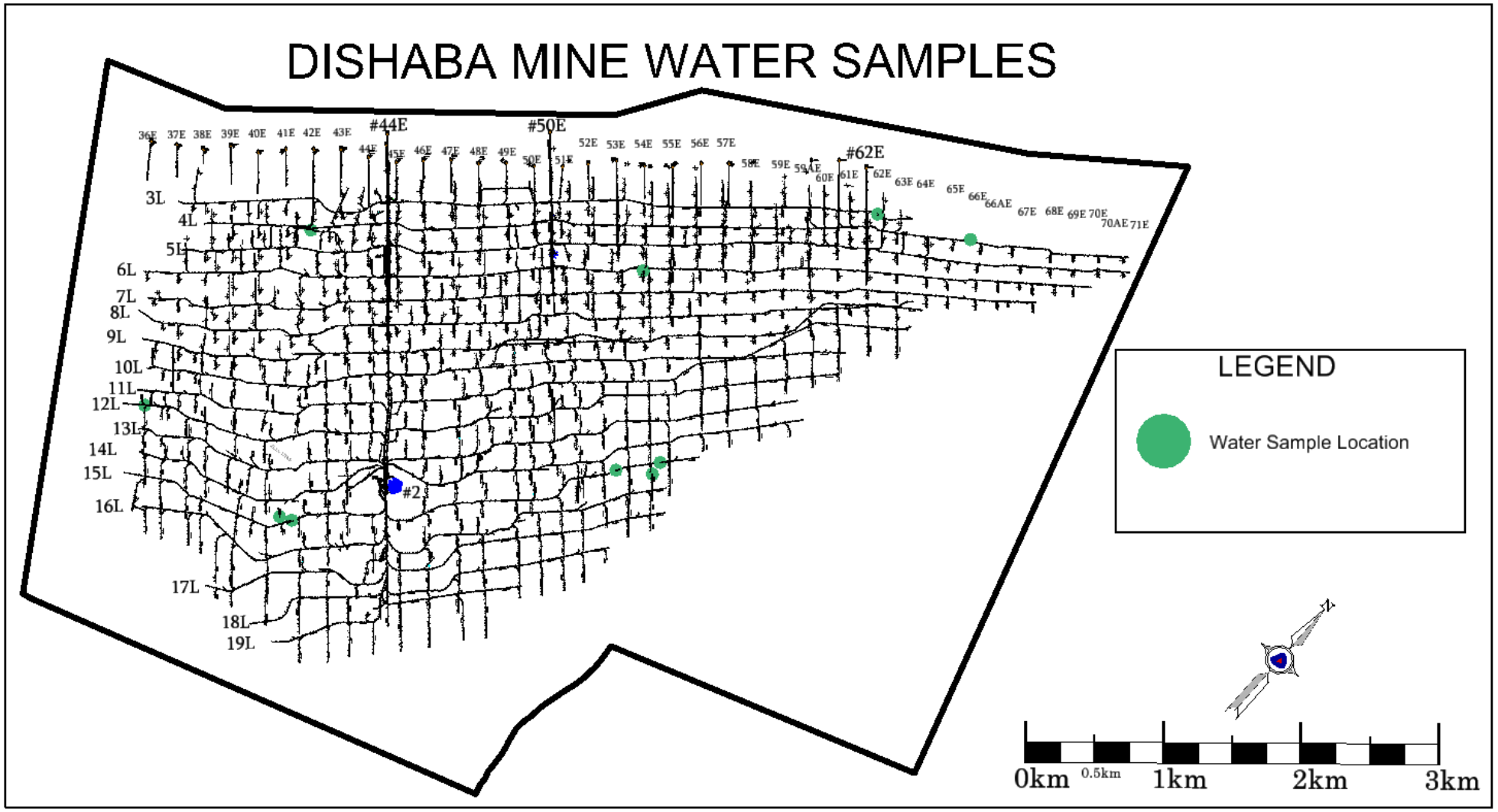

Figure 48: Locations of underground water samples.

Table 5: Field properties of groundwater samples.

2022 Groundwater sampling programme										
Sample ID	Working Place	Sample Coordinates			Field Parameters				Date Sampled	Description
		X	Y	Z	Temperature (°C)	TDS (mg/L)	EC (µS/cm)	pH		
01-2022-15/54E	15/54E XCUT (Drain)	40947.702	-38252.79	-18.936	36.9	760	1540	7.8	2022/01/20	Sample from the Xcut drain Noted high Calc. precipitate Main source: Fault in the MER raise
01-2022-15/55E	15/55E HLGE (Survey peg D07917 - 14.3m)	40937.714	-38153.308	-17.625	38.1	920	1860	7.7	2022/01/20	Sample from southern sidewall of the HLGE Flow rate: 165.24 L/H Slimy precipitate (Possibly $Mn(OH)_2$)
01-2022-15/53AE	15/53AE HLGE (Survey Peg D00995 + 3.0m)	40735.242	-38403.25	-17.61	36.1	640	1340	7.3	2022/01/20	Sample from Borehole 15/53E/8 Exact source lithology not established Flow rate: 134.28 L/H
02-2022-12/36E1	12/36E HLGE (Drain)	37863.264	-40320.738	190.86	36.6	380	790	9.3	2022/02/01	Sample from water flowing from Far Western HLGE under a ventilation control wall Noted possible wood pieces floating in the water Water from the Middellaagte Graben
02-2022-12/36E2	12/36E HLGE (Historical Cover Hole going West on the Southern Sidewall)	37868.802	-40316.955	192.312	34.6	390	800	9.6	2022/02/01	Sample from a historic cover hole drilled on the southern sidewall going westwards Flow rate: 40.32 L/H No known records of the coverhole, possibly drilled in Dec. 2007 Area with a known history of methane exposures
02-2022-15/41E	15/41E HLGE (From diamond drilling hole 15/42E/6)	39209.2	-40238.3	-23.7	28.8	650	1320	8	2022/02/01	Water from the Show-Stopper Fault Flow rate: 26.532 L/H
02-2022-15/41AN	15/41A XCUT North (Survey peg D27652 + 1.4m)	39133.519	-40278.13	-23.103	32.9	810	1640	8.4	2022/02/01	Water dripping from multiple closely spaced joints in the vicinity of the Show-Stopper Fault
02-2022-3/62E	3/62E XCUT (Survey peg H01294 - 10.8m, Drain)	40920.892	-35755.605	788.988	20.5	1120	2260	8.4	2022/02/04	Water running under a vent wall, V-notch flow rate: 3312 L/H
02-2022-4/66E-RBAY	4/66E Refuge Bay	41551.278	-35442.254	741.842	23.4	1660	3340	8	2022/02/04	High flow rate from a pipe drilled into the HW of the Refuge Bay. High Fe content
02-2022-6/54E-RBAY	6/54E Refuge Bay (Survey peg H02319 + 3.2m)	39918.966	-37192.615	598.259	21.4	1530	3070	7.7	2022/02/04	Slightly brownish colour
02-2022-5/42E HLGE	5/42E HLGE (Survey peg D09811 - 5.3m)	37919.509	-38571.216	663.237	25.9	680	1360	8	2022/02/04	Flow rate: 7200 L/H High calcite precipitate Along Show-Stopper Fault

3.3.1 Sampling for Hydrogeochemical Analyses

Following the guidelines of Weaver *et al*. (2007), 500 ml water samples and 100 ml filtered samples were collected per site. Both samples were put into plastic bottles specially supplied by the Aquatico laboratories. Prior to sample collection, the plastic bottles were soaked in filtered water overnight. The samples were kept in the refrigerator and transported to the laboratory within 48 hours of collection.

For each site, field parameters were recorded using a multi-parameter probe. The field parameters are listed in Table 5. Figure 49 is a photograph of the multi-parameter probe being used in a *drain stream* for groundwater in the mine.

Figure 49: Multi-parameter probe collecting field parameters in a drain stream underground.

3.3.2 Sampling for Stable Isotope Analyses

Water samples were collected for stable isotope analyses and submitted to the Environmental Isotope Laboratory of iThemba in Johannesburg for D/H ($^{2}H/^{1}H$) and $^{18}O/^{16}O$ ratio analyses. The analyses were done using a Los Gatos Research (LGR) Liquid Water Isotope analyser. For quality control, laboratory standards were analysed along with each batch of groundwater samples. The

laboratory standards are calibrated against international reference materials; in this case, the standard mean ocean water (SMOW) standard was used.

CHAPTER 4:
RESULTS

4.1 INTRODUCTION

This chapter discusses the results and findings of the investigations carried out in Chapter 3. The results are grouped into three categories, namely the underground mapping and seepage survey, the flow meter data, and the hydrogeochemistry and isotope results.

4.2 UNDERGROUND MAPPING AND SEEPAGE SURVEY

The underground mapping and seepage survey revealed the tendency of groundwater intersections to be largely associated with leucocratic rocks (mainly anorthosite and norite). These rock types are largely found in the footwall of the UG1, and the footwall and hanging wall of the Merensky Reef which is below the Bastard Reef (refer to Figure 10 for the stratigraphy of the mine). This observation corroborates previous observations by Ngubane *et al*. (2015).

In the middle of the mine, in historically mined areas, there is groundwater intersections recorded but the areas are no longer accessible due to ventilation control. There is, however, notable groundwater flow through the old ore-passes and from under the ventilation control walls. This shows that there is still water flowing from the Merensky Reef panels in these areas. Based on observations at 13/54E Merensky stope, the water is likely coming from the hanging wall of the Merensky Reef.

No significant groundwater intersections were observed on the UG2 horizon, except for those associated with surface boreholes that have been exposed by mining. These intersections generally dry up relatively quickly and do not require any sealing or piping for mining to continue. At 6/54E, there are scattered minor drips from the hanging wall of the UG2. These drips are not associated with any surface boreholes.

Calcite-filled joints within the leucocratic rocks appear to play a significant role in groundwater transmission. The calcite was most likely precipitated from fluids that flowed through the joints. In the 54E Line, Show-Stopper Fault and the Middellaagte Graben, significant calcite precipitation from actively flowing groundwater intersections was observed.

Complex fracture networks associated with major dykes have been observed and recorded in the geological maps of the mine. These networks result in the formation of unfavourable ground conditions for mining. However, dykes across the mine are generally dry. During the current

investigations, no groundwater intersections were observed along dykes or in close proximity to any dykes.

An analysis of faults in water prone areas, mainly the 54E and 40E line on the Merensky, shows that the most favourable faults for groundwater intersections are those striking NNW-SSE. This trend is almost parallel to the dip of the reef and the entire Critical Zone formation. Sympathetic joints to these faults also have a higher chance of water intersections and tend to have significant calcite infill, possibly indicating historical water flow. Large faults with displacements of over 2 m striking NE-SW (i.e., parallel to the general strike of the strata) were found to be dry with no significant water intersections recorded. This trend is, however, less prominent with increasing depth, possibly because the number of strike-parallel faults exposed by mining appears to decrease with depth.

The most significant groundwater-fault associations were found along the Show-Stopper Fault, the Middellaagte Graben, and not so prominently on the Bongani Fault. The Show-Stopper Fault has a displacement of between 25 m and 50 m, a dip of 60° eastwards and strikes NNE-SSW. The Middellaagte Graben on the side of Dishaba Mine has a displacement of 250 m to 350 m and also strikes NNE-SSW. The Bongani Fault has a displacement of between 10 m and 15 m and dips at 70° to 80° eastwards. Unlike the other prominent faults, the Bongani Fault strikes NW-SE in a direction towards the Crocodile River. Interestingly, the most eastern part of the Bongani Fault (towards the river) does not have any water flowing through it.

4.3 FLOW METER DATA

Figure 50 shows the estimated groundwater ingress trends from the year 2017 up to October 2022. The data for the years 2017 to 2020 were largely recorded manually. As a result, the data for these years are dominated by what appears to be “default” values rather than actual readings. Standout spikes or outliers are most noticeably found within these years as well.

The year 2020 has highly erratic data and generally does not tie up with the rest of the years. It shows very high ingress close to 20 000 m^3/d, whereas the other years show ingress of between 5000 m^3/d and 10 000 m^3/d. On further investigation, it was established that the automated flowmeters only started properly functioning in 2021. As a result, the data analysis for this research will only focus on the years 2021 and 2022. Figure 51 shows a graphical representation of the 2020-2022 data.

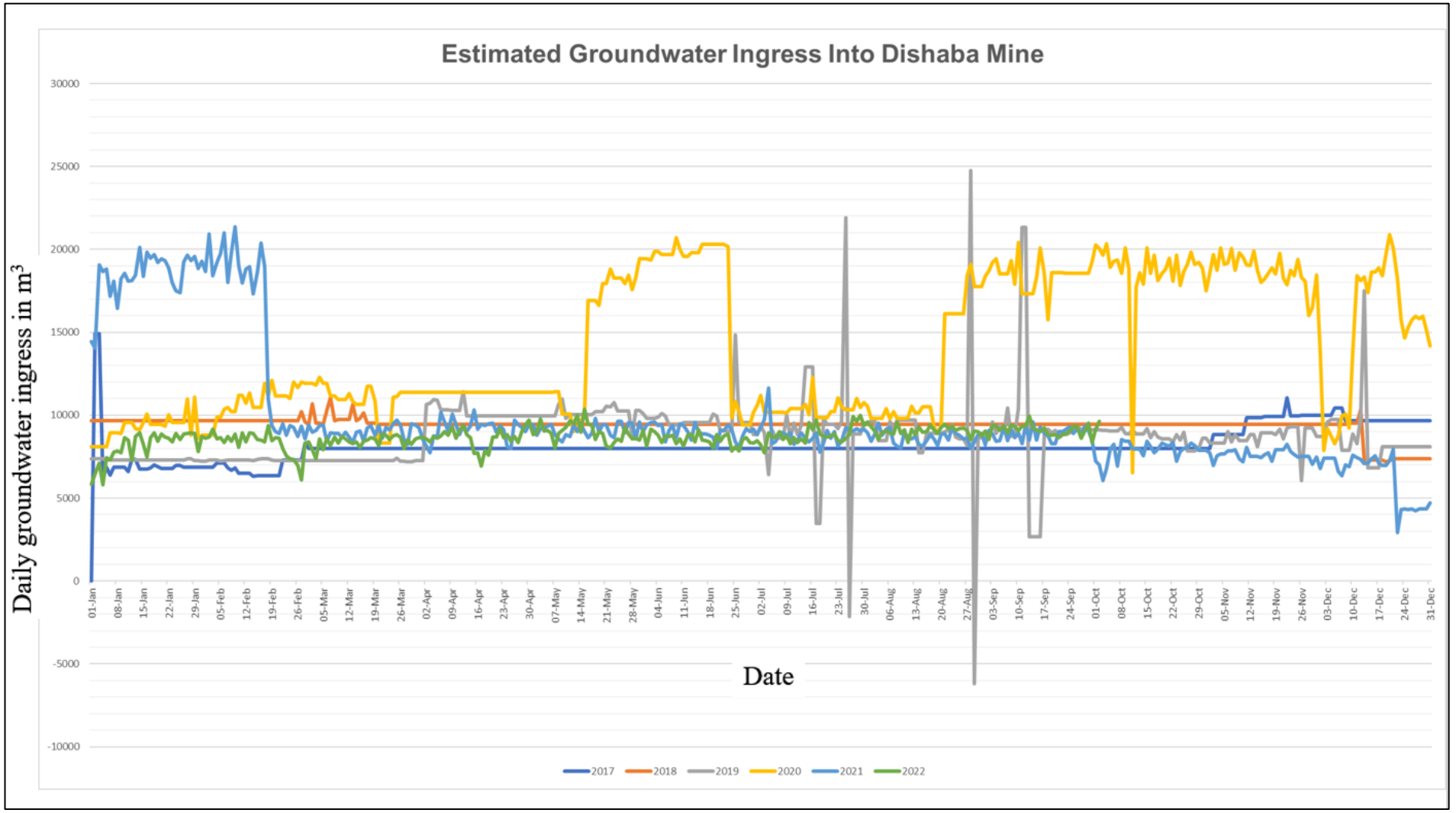

Figure 50: Estimated groundwater ingress into Dishaba Mine between 2017 and 2022.

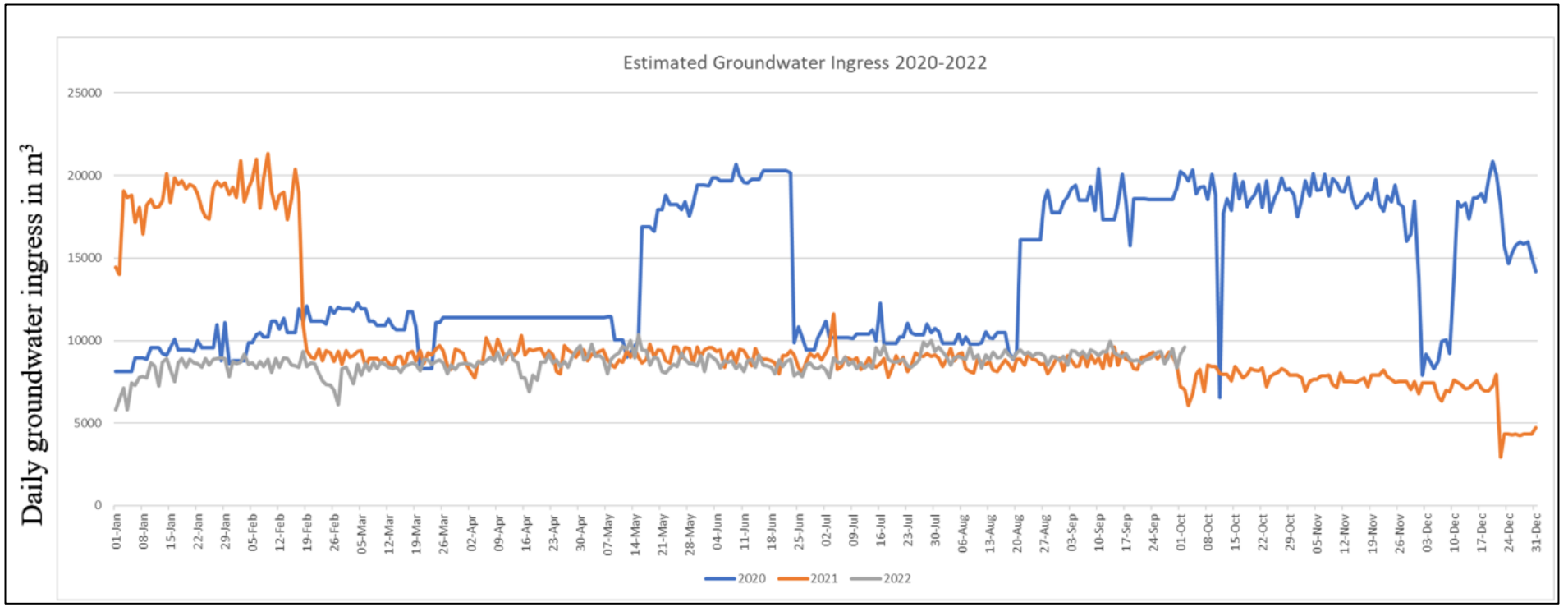

Figure 51: Estimated groundwater ingress into Dishaba Mine between 2020 and 2022.

On average, there was 9791 m^3/d estimated groundwater ingress in 2021. This volume drops significantly to 4221 m^3/d between 22 December and 31 December. During this period the mine is closed for the festive season. This trend of a significant drop in estimated groundwater ingress late in the year is observed in all the years for which this data are supplied (Figure 50). A steady increase from just over 5800 m^3/d on 1 January 2022 (no active mining, still within the festive break) to about 8900 m^3/d by 15 January 2022 is observed, as production increases towards stabilisation after the festive break.

The trends described above could possibly suggest a direct link between the estimated groundwater ingress and mining activity. During active mining there could be leakages that end up deep underground and are therefore counted as groundwater ingress. Two areas where this could be occurring are: leakages from the opencast operations, and water from the upper section of the mine running down to the #2 Vertical Shaft at depth.

4.4 CHEMISTRY AND ISOTOPES

4.4.1 Groundwater Quality

Table 6 shows the results of selected chemical and physical parameters plotted against the SANS 241: 2015 and WRC (1998) standards for drinking water. These particular standards were selected for this project because water of drinking quality would likely meet the needs of machinery, domestic and processing uses around the mine. The different water classes and their use are briefly defined as follows from WRC, (1998):

- Class 0 – Blue – This is ideal water quality, suitable for use without any reservations and is considered safe for everyone.
- Class I – Green – This is good water quality, suitable for all users, may have rare sub-clinical effects.
- Class II – Yellow - This is marginal water quality, generally safe but may have an effect on sensitive users.
- Class III – Red – This is poor water quality, may pose a risk of chronic health effect and should not be used over a long term.
- Class IV – Purple – This is unacceptable water quality, may cause severe acute health effects.

The results in Table 6 are colour-coded according to the upper limit ranges of Class 0, Class I and Class II. All the results that exceed Class II upper limit are highlighted in red. For the purpose of

this project, Class III and Class IV water is not desirable as it would require treatment for long-term use. The full set of results for all parameters that were tested is shown in Table 7.

Samples from the deep levels (12 Level and 15 Level) generally fall within Class II mainly due to chloride content. The 12 Level samples have relatively high pH whilst the 15 Level samples have high conductivity. An outlier is the 15/41AN sample which has high sodium and nitrate which exceed the Class II upper limit; this is possibly due to active mining taking place during the time when the sample was taken. The 15/55E sample also shows high sodium content compared to the other deep level samples, but is still within the Class II upper limit.

The samples from the shallower levels (from 3, 4, and 5 Levels) all exceed the Class II upper limits for magnesium and nitrate content. The 6/54E R-Bay sample has high calcium and sulphate content exceeding Class II upper limits. In terms of usability as described above, the deeper level groundwater (12 and 15 Level) appears to be more readily useable than the shallow level groundwater which would require treatment to be within Class II or lower.

All the samples have some elements which exceed the SANS 241 limits except for 15/54E, 12/36E and 15/41E. The 12/36E samples show a pH on the higher end of the SANS 241 range, one of the samples exceeds the upper limit slightly with a pH of 9.73. The 6/54E samples has the most undesirable quality with as much as 6 elements exceeding the SANS 241 upper limit.

Table 6: Groundwater quality results plotted against SANS 241: 2015 and WRC (1998).

Constituent	Unit	Water Classification			SANS241	Sample ID									
		Class 0	Class I	Class II		01-2022-15/54E	01-2022-15/55E	02-2022-12/36E1	02-2022-12/36E2	02-2022-15/41E	02-2022-15/41AN	02-2022-3/62E	02-2022-4/66E-RBAY	02-2022-6/54E-RBAY	02-2022-5/42E HLGE
pH	[-] @25ºC	6.0 – 9.0	5.0 – 6.0 9.0 – 9.5	4.0 – 5.0 9.5 – 10.0	≥5 to ≤9.7	7.90	8.07	9.54	**9.73**	8.24	8.39	8.59	8.45	8.09	8.4
Conductivity	mS/m @25ºC	70	150	370	≤170	155	**190**	84.9	84	108	139	**245**	**356**	**328**	140
Calcium	mg/L	80	150	300	≤150	90.8	80.4	23.4	24	57.8	63.2	65	105	**378**	58.9
Magnesium	mg/L	30	70	100	≤70	29.6	5.39	0.118	-0.1	4.57	2.31	**276**	**334**	57.9	**130**
Sodium	mg/L	100	200	400	≤200	190	**296**	168	166.0	189	**246**	91.9	158	**335**	79.1
Potassium	mg/L	25	50	100	≤50	2.3	1.85	0.788	0.8	1.47	1.77	1.74	2.59	3.54	1.46
Manganese	mg/l	0.05	0.10	1.00	≤0.4	-0.001	-0.001	-0.001	0.00	-0.001	-0.001	-0.001	0.016	0.009	-0.001
Iron	mg/L	0.10	0.20	2	≤2	-0.004	-0.004	-0.004	0.0	-0.004	-0.004	-0.004	0.162	-0.004	-0.004
Total alkalinity	mg/L $CaCO_3$					240	67.8	37.9	24	46.9	16	244	246	63.6	495
Chloride	mg/L	100	200	600	≤300	251	**337**	208	209.0	221	240	**427**	**476**	**610**	97
Sulphate	mg/L	200	400	600	≤500	208	350	63.3	60	124	208	363	466	**756**	75.4
Nitrate_N	mg/L	6.0	10.0	20	≤12	5.14	6.03	1.88	1.08	11.9	**26.6**	**42.7**	**135**	**16.9**	**31.4**
Fluoride	mg/L	0.7	1.0	1.5	≤1.5	-0.263	-0.263	-0.263	-0.26	-0.263	-0.263	-0.263	-0.263	-0.263	-0.263

Exceeds the limits of Class II

Exceeds SANS241

Table 7: Groundwater chemistry results.

Parameter	Unit	Sample ID									
		01-2022-15/54E	01-2022-15/55E	02-2022-12/36E1	02-2022-12/36E2	02-2022-15/41E	02-2022-15/41AN	02-2022-3/62E	02-2022-4/66E-RBAY	02-2022-6/54E-RBAY	02-2022-5/42E HLGE
pH	pH	7.9	8.07	9.54	9.73	8.24	8.39	8.59	8.45	8.09	8.4
EC	mS/m	155	190	84.9	83.7	108	139	245	356	328	140
TDS	mg/L	999	1176	526	512	712	918	1657	2374	2299	945
Alkalinity	mg $CaCO_3$/L	240	67.8	37.9	24.4	46.9	16	244	246	63.6	495
Cl	mg/L	251	337	208	209	221	240	427	476	610	97
SO_4	mg/L	208	350	63.3	60	124	208	363	466	756	75.4
NO_3	mg/L	5.14	6.03	1.88	1.08	11.9	26.6	42.7	135	16.9	31.4
NH_4	mg/L	0.123	0.037	0.074	0.051	0.07	0.112	0.996	0.47	0.119	0.13
PO_4	mg/L	0.012	0.014	<0.005	<0.005	<0.005	<0.005	<0.005	<0.005	<0.005	<0.005
F	mg/L	<0.263	<0.263	<0.263	<0.263	<0.263	<0.263	<0.263	<0.263	<0.263	<0.263
Ca	mg/L	90.8	80.4	23.4	23.5	57.8	63.2	65	105	378	58.9
Mg	mg/L	29.6	5.39	0.118	<0.077	4.57	2.31	276	334	57.9	130
Na	mg/L	190	296	168	166	189	246	91.9	158	335	79.1
K	mg/L	2.3	1.85	0.788	0.771	1.47	1.77	1.74	2.59	3.54	1.46
Alkalinity	mg/L	<0.002	<0.002	0.031	0.012	<0.002	<0.002	<0.002	<0.002	<0.002	<0.002
Fe	mg/L	<0.004	<0.004	<0.004	<0.004	<0.004	<0.004	<0.004	0.162	<0.004	<0.004
Mn	mg/L	<0.001	<0.001	<0.001	<0.001	<0.001	<0.001	<0.001	0.016	0.009	<0.001
Cr	mg/L	<0.003	<0.003	<0.003	<0.003	<0.003	<0.003	0.009	0.023	<0.003	0.003
Cu	mg/L	0.013	<0.002	<0.002	<0.002	0.002	<0.002	0.03	0.062	0.028	0.025
Ni	mg/L	<0.002	<0.002	<0.002	<0.002	<0.002	<0.002	<0.002	0.022	<0.002	<0.002
Zn	mg/L	<0.002	<0.002	<0.002	<0.002	<0.002	<0.002	<0.002	<0.002	0.192	<0.002
Co	mg/L	<0.003	<0.003	<0.003	<0.003	<0.003	<0.003	<0.003	0.106	<0.003	<0.003
Cd	mg/L	<0.002	<0.002	<0.002	<0.002	<0.002	<0.002	<0.002	<0.002	<0.002	<0.002
Pb	mg/L	<0.004	<0.004	<0.004	<0.004	<0.004	<0.004	<0.004	<0.004	<0.004	<0.004
Total hardness	mg $CaCO_3$/L	348	223	59	59	163	167	1297	1635	1183	683
SAR	SAR	4.42	8.62	9.51	9.43	6.45	8.28	1.11	1.7	4.24	1.32
COD	mg/L	33.9	56.3	13.4	11	14.7	19.1	25.5	38.7	43.3	22
Si	mg/L	21.1	13.9	11.3	12	12	10.6	34.8	31.9	16.1	23.1
Ba	mg/L	<0.002	<0.002	<0.002	<0.002	<0.002	<0.002	0.069	0.133	0.024	0.006
Sr	mg/L	0.172	0.02	0.035	0.023	0.118	0.111	0.426	0.8	0.591	0.453
SiO_2	mg/L	45.2	29.7	24.1	25.8	25.8	22.8	74.5	68.2	34.4	49.5
TON	mg/L	5.14	6.03	1.88	1.08	11.9	26.6	42.7	135	16.9	31.4
Acidity	mg $CaCO_3$/L	30.4	28.9	<0.001	<0.001	7.42	<0.001	<0.001	<0.001	8.29	<0.001
Si (total)	mg/L	11.9	12.4	9.08	10.2	9.66	8.75	7.42	4.32	6.41	9.91

4.4.2 Groundwater Type

Analytical diagrams (Piper, Expanded Durov, Stiff and Schoeller diagrams) assist in interpreting the water type at a sampling point through the assessment of the plot position of a sample in the diagrams. In this section, the analytical results are displayed on different diagrams to allow the water types at Dishaba Mine to be identified, and to relate the various water types to their possible origins. The plots were constructed using the Windows Interpretation System for the Hydrogeologist 3 (WISH version 3.02.189).

A Piper diagram is an effective graphic procedure to segregate relevant analytical data to understand the sources of the dissolved constituents in water (Piper, 1944). A Piper diagram is a representation of the dominant cation and anion concentrations in the lower triangles with the hydrochemical facies shown in the upper diamond (Figure 52).

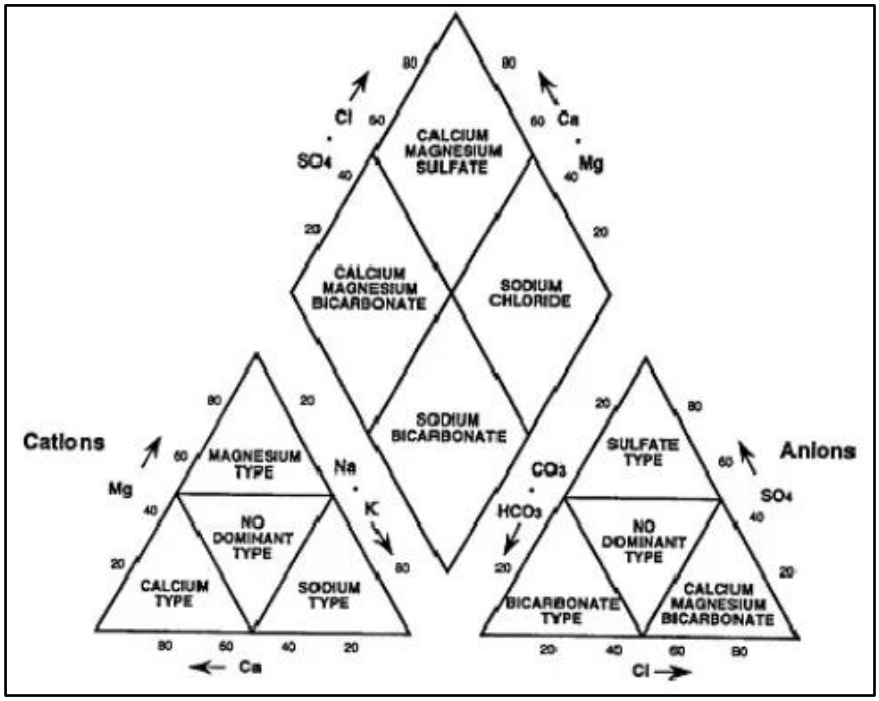

Figure 52: Piper diagram showing cations and anions in the bottom triangles and Water facies in the upper diamond (Lonergan and Cange, 1994).

The results of the analyses performed on groundwater samples from Dishaba Mine are shown in the Piper diagram in Figure 53. In the lower triangles of the Piper diagram, the cations results show the 3/62E, 4/66E and the 5/42E samples to be of the magnesium type, while the 15/41E, 15/55E and the 12/36E samples are the sodium type. The 6/54E and 15/54E samples show no dominant cation type. The anions triangle shows nearly all the samples to be predominantly calcium-magnesium-bicarbonate type. The 5/42E sample (bicarbonate type) and the 15/54E sample (no dominant type) are the exceptions in the anion triangle.

In the upper diamond of the Piper diagram the 3/62E, 4/66E and 6/54E samples show calcium-magnesium-sulphate facies, while the 5/42E sample stands out as the only calcium-magnesium-bicarbonate facies. The rest of the samples (15/41E, 15/55E, 12/36E and 15/54E) show a sodium-chloride facie.

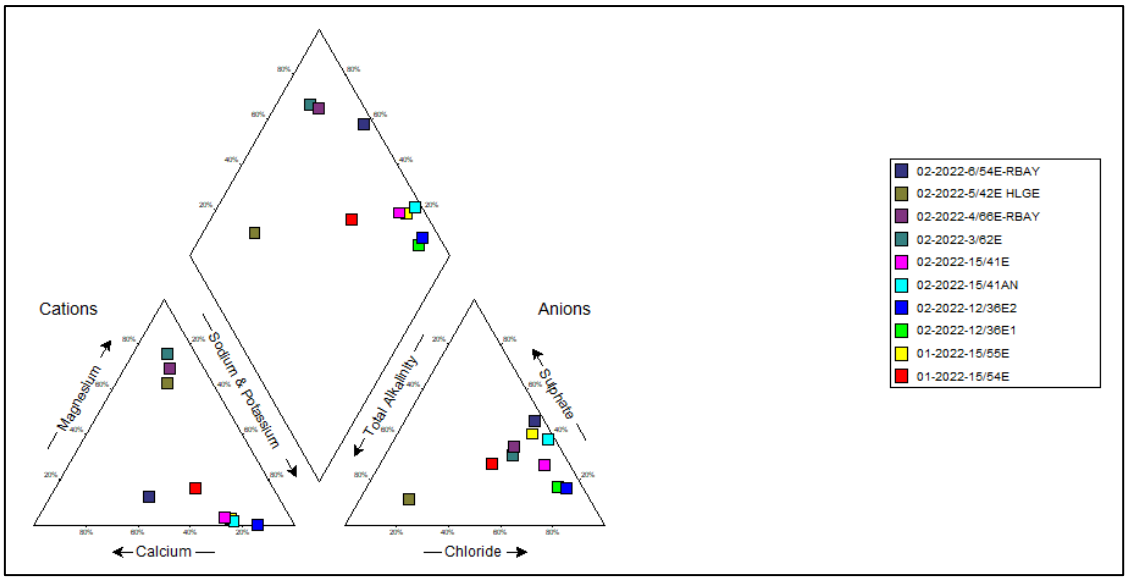

Figure 53: Piper diagram showing chemistry results from the different underground samples.

In the Durov diagram, the cations and anions are plotted separately in milliequivalents (meq) as a percentage, each adding up to 100%. The Expanded Durov diagram shows the major ionic species and show the cations and anions together to make up 100% (Durov, 1948; Burdon and Mazloum, 1958). Figure 54 shows the layout of the Expanded Durov diagram while Figure 55 shows the results of the current investigations plotted on an Expanded Durov diagram.

Based on the results, the 15/55E, 12/36E and 15/41E samples are predominantly old water that is at the end of the hydrogeological cycle. The 5/42E water sample is the freshest and most uncontaminated sample. The 15/54E sample shows a rare type of water with possibly a sulphate or sodium contamination. The 4/66E and 6/54E samples show a mixed type, with 4/66E dominated by sulphate and 6/54E by nitrate and/or chloride contamination.

Stiff diagrams are a graphical representation of water chemical analyses (Stiff, 1951). A Stiff diagram helps visualise ionically related waters. The cations are plotted on the left and the anions on the right of a centre axis. The farther away from the centre a point is, the higher the concentration.

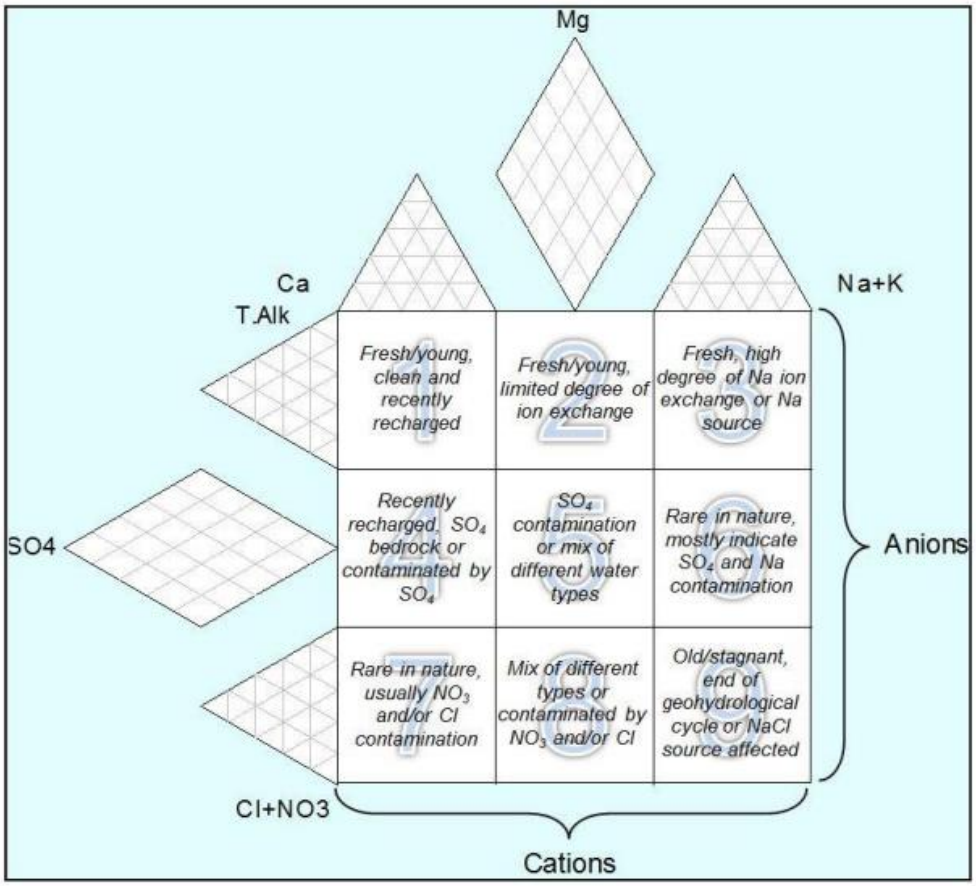

Figure 54: Fields of the Expanded Durov diagram.

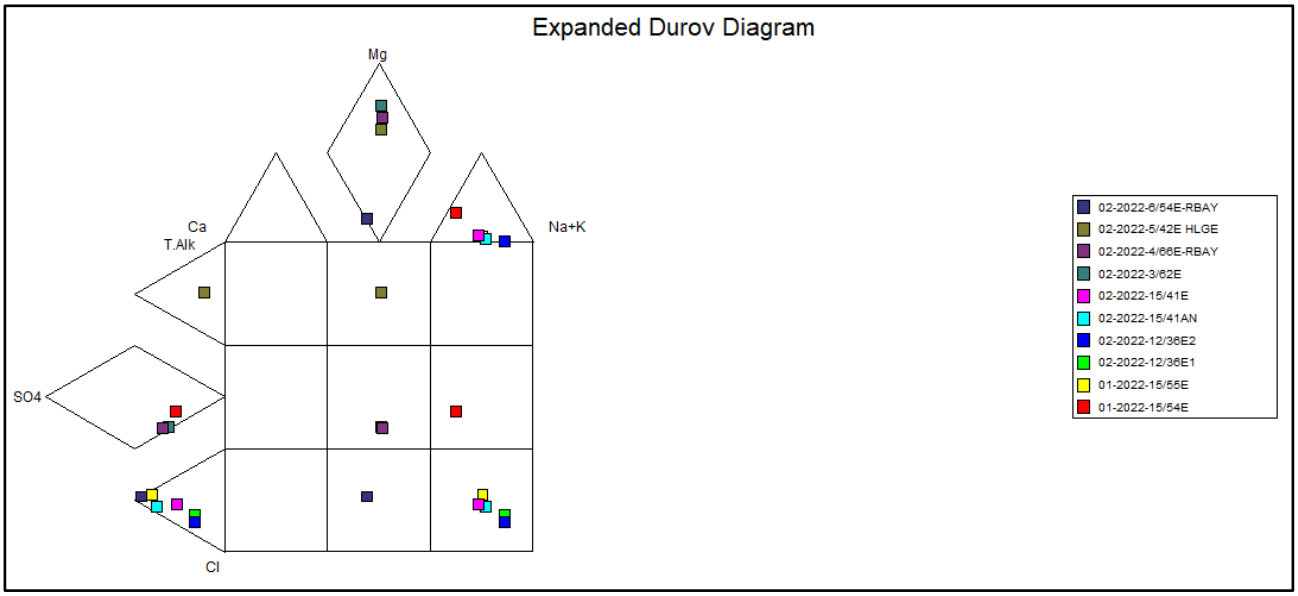

Figure 55: Expanded Durov diagram showing the results from the underground samples from Dishaba Mine.

Figure 56 shows the Stiff plot for the water samples from Dishaba Mine. Looking at the results, samples from neighbouring areas show good similarity. The following pairs of samples are most similar: the 15/54E and 15/55E samples, the 12/36E samples, the 15/41E samples and the 3/62E and 4/66E samples. The 5/42E and 6/54E samples are relatively unique and differ quite significantly from the rest of the samples.

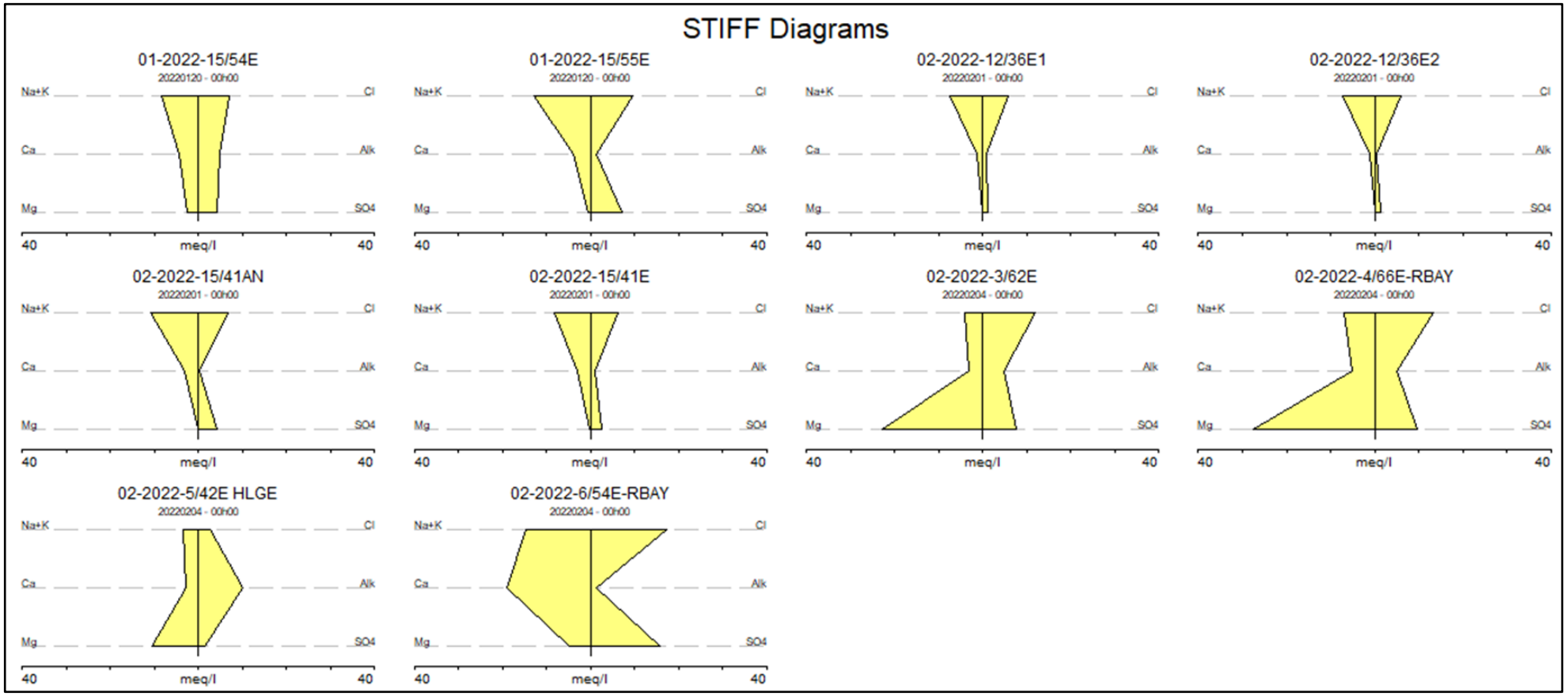

Figure 56: Different concentrations shown on a Stiff diagram.

The Schoeller diagram is a semi logarithmic plot that represents the major ion analysis in meq/L (Schoeller, 1962). The plots show patterns in the ratios of particular anions and cations. The results for the water samples from Dishaba Mine are plotted in Figure 57.

The samples from the deeper levels i.e., 12/36E, 15/41E, 15/54E and 15/55E, generally show a relatively similar trend in the Schoeller diagram. The samples from the shallower levels also show similar chemical trends i.e., 5/42E, 3/62E and 4/66E. There is, however, a prominently high alkalinity in 3/62E. The sample from 6/54E is from a shallow level but shows a similar trend to the deep levels, most closely resembling 15/54E. Overall the deep-level samples have low magnesium content with high and almost equal calcium, sodium, chloride, and sulphate content. The shallower-level samples have far higher magnesium content with lower calcium content. Similar to the deep-level samples, the sodium, chloride and sulphate content is almost equal. The alkalinity is higher in the shallow-level samples than in the deep-level samples.

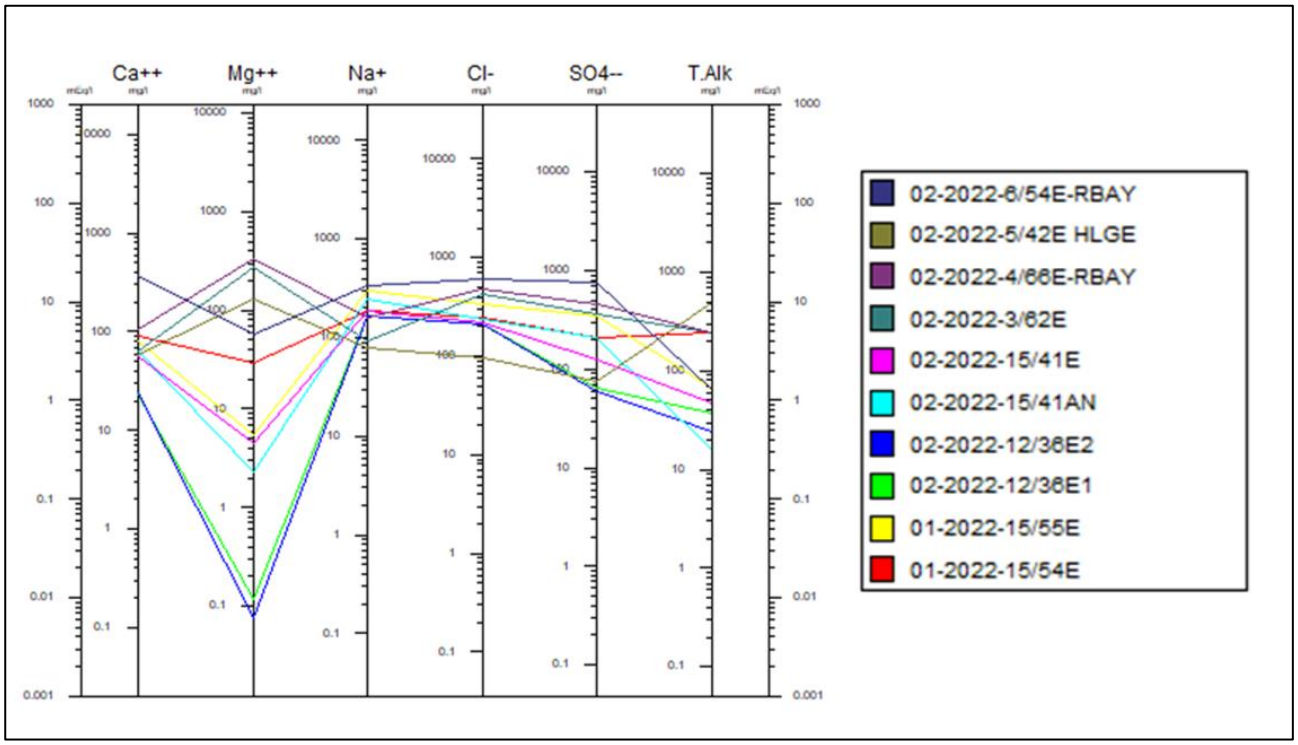

Figure 57: Chemistry results shown on a Scholler diagram.

4.4.3 Isotopes

The analytical results are presented in the common delta-notation:

$$\delta^{18}O\ (‰) = \left[\frac{\left({}^{18}O/{}^{16}O\right)_{sample}}{\left({}^{18}O/{}^{16}O\right)_{standard}} - 1\right] \times 1000 \qquad 1$$

The analytical precision is estimated at 0.5‰ for O and 1.5‰ for H. The results are shown in Table 8 and presented graphically against the Global Meteoric Water Line (GMWL) (Craig, 1961) in Figure 58.

Table 8: Isotope results.

Sample ID	δD (‰)	$\delta^{18}O$ (‰)
02-2022-3/62E	-4.7	-0.49
02-2022-4/66E-RBAY	-8.7	-1.50
02-2022-5/42E HLGE	-18.4	-3.00
02-2022-6/54E-RBAY	-6.0	-1.01
02-2022-12/36E1	-27.4	-4.22
02-2022-12/36E2	-28.0	-4.12
02-2022-15/41E	-24.7	-3.58
02-2022-15/41AN	-23.5	-3.26
01-2022-15/54E	-9.4	-1.49
01-2022-15/55E	-11.5	-1.92

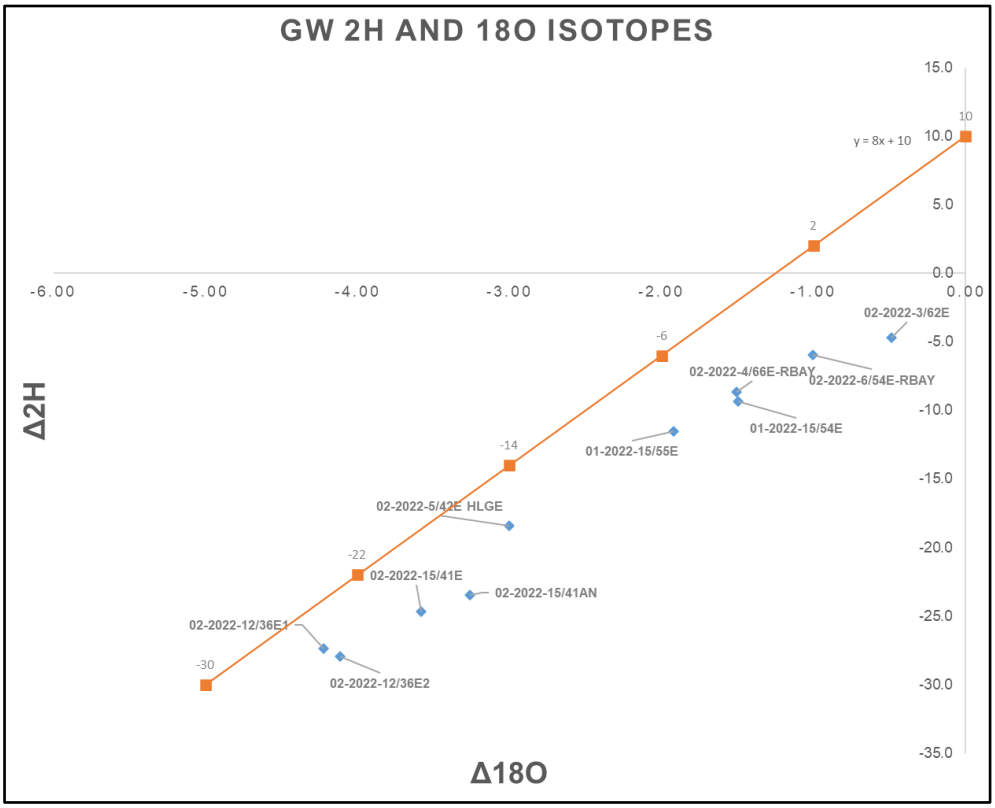

Figure 58: Stable isotope results plotted against the Global Meteoric Water Line.

Isotope samples need to be understood as combining the effects of source variation, mixing, and fractionation (Benettin *et al.*, 2018). A trend line through the samples relative to the Global Meteoric Water Line (GMWL) reveals the effects of source variability and evaporation variability. The closer the samples are to each other on a plot against the GMWL the more likely they are to

have the same source and the further away below the GMWL the samples plot the more likely to have been exposed to high evaporation (Figure 59).

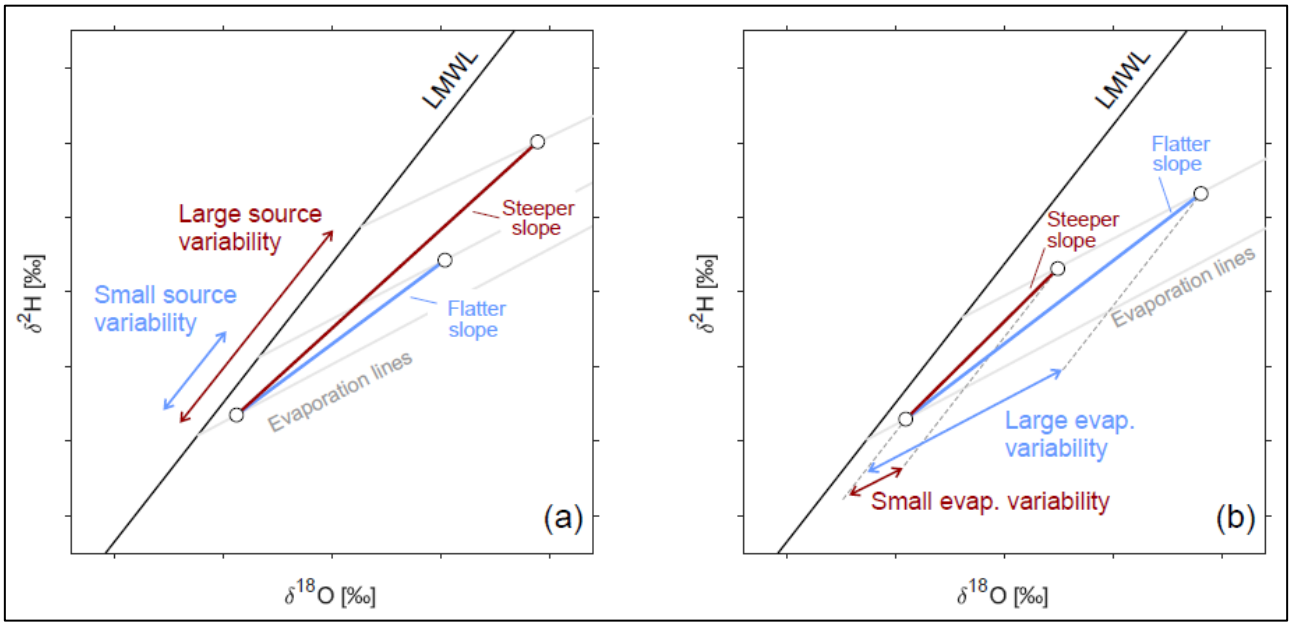

Figure 59: Effects of (a) precipitation source variability and (b) evaporation variability on the location of samples in a δ^2H vs $\delta^{18}O$ plot (from Benettin *et al.*, 2018).

The $\delta^2H/\delta^{18}O$ plot for the groundwater samples from Dishaba Mine is shown in Figure 60. The samples from the shallower levels (from 3, 4, and 6 Levels) plot farthest from the GMWL and on the up-side of the GMWL relative to the samples from the deeper levels (from 12 and 15 Levels). The 5/42E sample and the 15/54E sample, however, appear to be going against this apparent trend. The 5/42E sample plots closer to the 15/41E samples. The 41E and 42E Lines are roughly parallel to the Show-Stopper Fault which could explain the apparent relationship between the 5/42E and 15/41E samples. Interestingly, the samples from the western section of the mine (36E to 42E Lines) plot closer together, i.e., closer to and on the down-side of the GMWL with the samples from the eastern section (54E - 66E Lines) plotting on the opposite end. The 15/55E sample plots between the two clusters.

Looking at Figure 60, the trend line through the samples in this project is slightly flatter than the GMWL. This suggests the shallower level samples are from a source more exposed to evaporation than the deeper level samples. Overall, the samples have a wide distribution throughout the plot, suggesting a large variability in their sources.

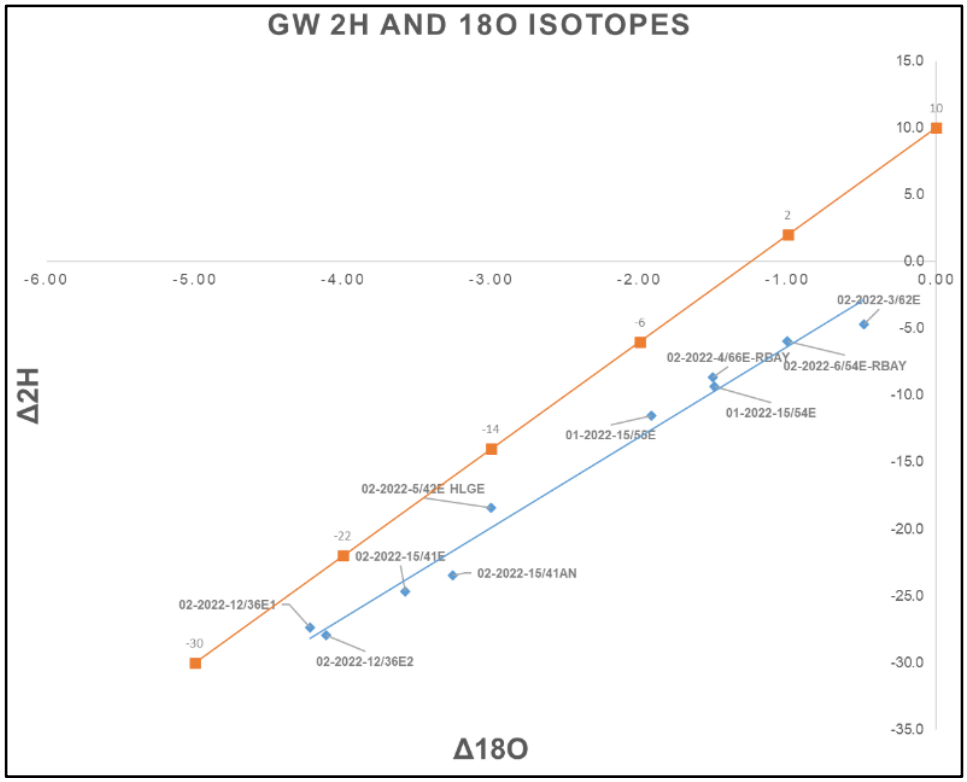

Figure 60: A plot of the isotope results with the GMWL in orange and the trend line in blue.

CHAPTER 5:
ASSESSMENT OF GROUNDWATER INGRESS

5.1 INTRODUCTION

This chapter discusses the possible causes and implications of the findings and results in the previous chapter. The chapter also looks into the significance of the results in relation to the study objectives.

5.2 DISCUSSIONS

It is widely accepted that rocks of the BIC have extremely low primary porosity (Golder, 2018). Fractures in the rock therefore play a highly dominant role in the transmission and storage of groundwater in the rocks of the BIC. To understand the groundwater regime at Dishaba Mine, it is important that a critical analysis of the fracture networks be undertaken.

Fracture networks at Dishaba Mine consist of faults, joints, shears, veins and dykes. From underground mapping and historical mapping data, it is evident that not all major faults found within the Dishaba Mine are water transmitting. A closer look at the faults shows that NW-SE striking faults tend to be the most prone to groundwater ingress. These faults are classified as the "Pongola" extensional fault zones according to Friese (2004). These faults tend to be normal faults, with near vertical dips and range in displacement between 0.1 m to over 200 m in the Middellaagte Graben.

When looking at fracture networks it is tempting to focus only on faults; however, joints also play a critical role in groundwater ingress into the mine workings. The joints most prone to groundwater ingress were found to be calcite filled, in leucocratic rocks. These joints have similar trend to the "Pongola" extensional fault zones as described above. The calcite infill could be from historical water flows and precipitates from presently flowing water. It must be noted though that field observations found the most prominent calcite precipitates to be emanating from water with pH of about 8. This is generally the best pH level for calcite precipitation (Koutsoukos and Kontoyanni, 1984).

Even though certain faults and joints have been found to have water flow, the flow is generally not consistent along the whole fracture plane or even along the strike of the fracture. This can possibly be explained by multi-scale heterogeneity due to variation in geometrical features such as surface roughness, fracture apertures, fracture density and connectivity (Titus *et al.*, 2009; Zhou *et al.*,

2023). This possibly leads to the development of preferential flow paths within the rock mass and the fracture surface itself.

In addition to the geometrical features described above, groundwater flow in faults is also influenced by: (1) the frequency of fracturing, (2) the infill or material within the fault, (3) the amount of displacement, and (4) the stress regime (Faunt, 1997). These are largely dependent on the lithology and how it responds to deformation or changes in the stress regime (Jager and Ryder, 1999).

The leucocratic lithologies (mainly norite and anorthosite) were found to be the most susceptible to groundwater flow. It was also observed that the leucocratic rocks were dominated by calcite-filled joints which is evidence of historical groundwater flow. The reason for the higher frequency of water-prone fractures in leucocratic rocks possibly lies in the geo-mechanical properties of these rocks. Table 9 shows the geo-mechanical properties of various rocks found across Dishaba Mine. Note that the Merensky Reef is a feldspathic pegmatoidal pyroxenite and the UG2 is a chromitite.

The norite and anorthosite have relatively higher Young's moduli, which translates to more brittle deformation (Jager and Ryder, 1999) and the production of more fractures, as opposed to the more ductile deformation response of the melacratic rocks (pyroxenite and harzburgite).

Table 9: Typical elastic constants and material properties of lithological units at Dishaba Mine (Gerber, 2022).

Rock Type	Young's modulus (GPa)	Poisson's ratio	UCS (MPa)	Tensile strength (MPa)	Cohesion (MPa)	Internal friction angle (°)	Shear modulus (GPa)
Anorthosite	90	0.2	190	10	5	30	38
Pyroxenite	50	0.25	150	10	5	30	20
Norite	70	0.2	170	7	5	30	29
Merensky	50	0.25	130	10	5	30	20
UG2	30	0.2	75	7	3	50	13

Rock mass classification systems attempt to define the characteristics of rock mass by following a simple assessment of certain critical rock mass parameters (Jager and Ryder, 1999). The components most commonly found in rock mass classification systems include strength of intact rock samples, the number and spacing of joints, effect of groundwater and frictional properties of natural joints. The rock mass rating (RMR) is a commonly used rock mass classification system. Based on RMR values, rock mass is classified into five categories:

- Very good (RMR = 100–81),
- Good (RMR = 80–61),

- Fair (RMR = 60–41),
- Poor (RMR = 40–21), and,
- Very poor (RMR <20).

Table 10 shows the typical RMRs of the different lithologies at Dishaba Mine at various depths relative to the Merensky Reef. The lithologies across Dishaba Mine generally rank in the "Fair" category with an RMR value of between 40 and 60. The chromitites of the UG1 and UG2 have RMR values of 30 and 35, respectively. This puts them in the "Poor" category. Interestingly, the anorthosite below the UG1 has a value of 30, which is far below the 50-55 values elsewhere in the stratigraphy. This potentially means the UG1 footwall has a more prominent fracture network than all other lithologies.

Table 10: Typical RMR values for different lithologies relative to the Merensky Reef at Dishaba Mine (Gerber, 2022).

Distance from Merensky (m)	Rock Type	Typical UCS (MPa)	Typical RMR
0 - 5	Anorthosite	190	50
5 - 18	Norite	170	55
18 - 20	Harzburgite (P2)	80	40
20 - 29	Norite	170	55
29 - 30	Pegmatoidal Pyroxenite(P1)	130	45
30 - 40	Pyroxenite	130	40
40 - 42	Chromitite (UG2)	70	35
42 - 55	Pyroxenite	150	40
55 - 57	Chromitite (UG1)	80	30
57 - 60	Anorthosite	190	30
60+	Norite	170	60

The quantity of groundwater ingress into the mine varies over time (refer to Section 4.3) and the average groundwater ingress may have changed significantly over the historic life of the mine. The estimated groundwater ingress is currently far lower than the 16 000m^3 that was estimated during the COVID times. This could be because of intersections drying up or, more significantly, errors in the recording of groundwater estimates. Obvious errors can be seen in the highly erratic ingress volumes, as shown in Figure 50 and Figure 51.

Considering the erratic nature of the estimated ingress, it is safe to assume that the best estimates are those captured during the mine "down-times" where the effects of mining activities are greatly reduced. Between 2021 and 2022, the groundwater ingress volumes are therefore estimated to be between 5000 m^3/d and 9000 m^3/d. This is specifically groundwater coming out of #2 Vertical Shaft and excludes the ingress from the shallow weathered zone which gets into the mine through the decline shafts in the Upper Section of the mine. This water from the shallow weathered zone is

handled via infrastructure associated with the decline shafts and will therefore generally not mix with water from the deeper levels that is reported at #2 Vertical Shaft.

It was observed that certain intersections, whether through boreholes or mining faces, dry up over a long period of time while others dry up or display significantly reduced flows in less than a 24-hour period. An example of an intersection that dried up over a long period of time is the 13/55E Raise which stood still from 2010 due to significant water intersection that made mining impossible (M. Moyo, personal communication, 2022). Mining only resumed in 2015 when the raise was completely dry. During the course of this study, a new water intersection at 15/41EA was reported to the Geology Department by the diamond drilling crew. However, the following day when a geologist went to investigate, it was completely dry. This possibly means drilling intersected a *pocket* of groundwater with no continuous recharge and the pocket got drained quickly (within 24 hours). These examples show that the spikes in estimated groundwater ingress in Figure 50 and Figure 51 cannot be completely dismissed and warrant further investigation.

Areas that are known to currently have consistent flows and have been flowing for a long period of time are 53-55E Lines, the Show-Stopper Fault area, the UG1 footwall south of the Bongani Fault, and the western end of the mine towards the Middellaagte Graben (Figure 61). An analysis of historical intersections relative to fault systems shows that these areas fall within four possible groundwater compartments. These compartments are shown in Figure 61 and have the following structural/lithological boundaries:

- Middellaagte Graben to the Tsholo Fault,
- SM Fault to Show-Stopper Fault,
- UG1 Footwall and MER Hangingwall Anorthosite South of the Bongani Fault, and,
- MER Hangingwall Anorthosite along the 54E-55E Lines.

The upper levels of the mine are likely experiencing ingress from leakages from the mined-out open cast operations. The old pits are not lined and therefore likely have water losses into the underground mine workings.

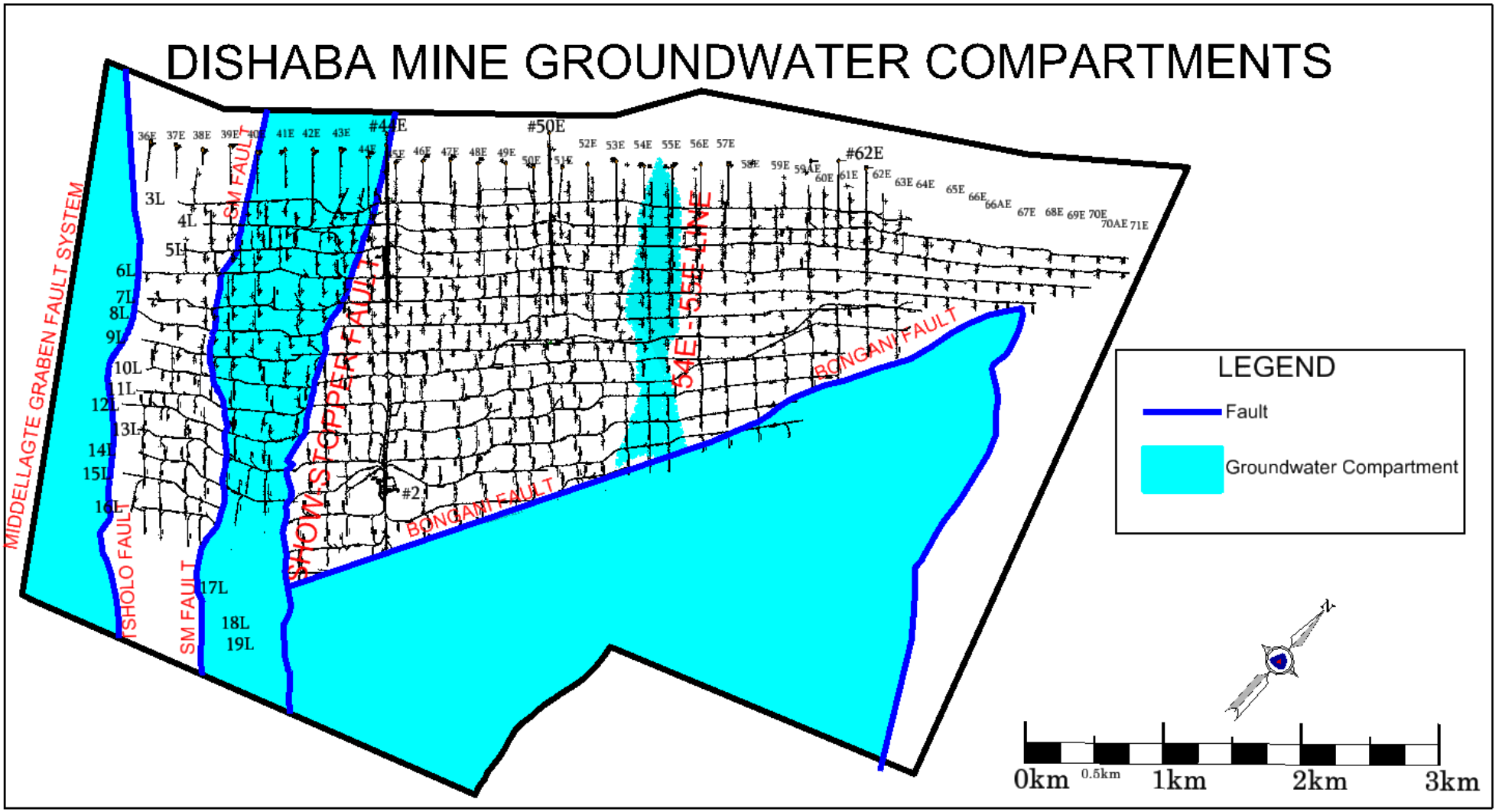

Figure 61: Groundwater compartments at Dishaba Mine.

No water ingress was observed below the Crocodile River in the eastern-most section of the mine. Interestingly, this is closer to surface on 4-6 Levels which sit at 189 mbgl to 332 mbgl. The farthest eastern intersection was found at 12/58E with a flow of 600 L/h.

The groundwater chemistry results generally show a trend of similarities amongst the deeper levels of the mine (15/41E, 15/55E and 12/36E) and similarities amongst the shallower levels (3/62E, 4/66E and 6/54E). Overall, there are two dominant clusters of water types, i.e., the calcium-magnesium-sulphate (shallower samples) and the sodium-chloride facies (deeper samples).

The 5/42E sample plots apart from the other samples in the Piper diagram. This sample seems to be typical shallow fresh groundwater. This means that the sample represents recently recharged water from precipitation and/or water that has travelled a relatively short distance from its source to the point where it was sampled. The deeper samples are typical of ancient groundwater that is reaching the end of its hydrological cycle. This means the water was infiltrated into the ground a long time ago and has potentially travelled a long distance from its source to the point where it was sampled. The shallow samples are waters typical of gypsum groundwater and mine drainage. These samples are possibly mixed fresh water and mine-related discharges.

The 15/54E sample appears to be mixed with no dominant type. This possibly implies that the water originates from more than one source and may have possibly undergone chemical reactions that altered the original chemical signature. In the area where the sample was taken, the water in the 54E-55E compartment possibly mixes with water in the south of Bongani Fault compartment (Figure 61).

Groundwater chemistry plots from previous studies are shown in Figure 26, Figure 27 and Figure 28. These plots broadly confirm the findings of this study that the deep level water samples are largely sodium-chloride facies. The shallow level sample from 5/55E as depicted in Figure 29 is consistent with the shallow level samples from this study. Interestingly, the Crocodile River, Tailings Storage Facility, and the shallow surface water monitoring holes all have a similar facies type (calcium-magnesium-sulphate) as the shallow level samples from this study. The 5/41E sample was also previously found to be from a dolomitic aquifer. These historic plots suggest a link between the surface water bodies, shallow weathered zone and the shallow level groundwater ingress into the mine workings.

The Durov diagram largely corroborates the findings of the Piper diagram. It indicates the deeper samples as being old groundwater, 5/42E fresh water and mixed water from the shallower samples. It further gives insight into the different mixing or contaminating agents for 6/54E and 4/66E being nitrate and/or chloride as well as sulphate, respectively.

The Stiff diagrams show clear relationship and similarities in samples from relatively close areas i.e., 12/36E, 15/54E, 15/55E and 3/62E and 4/66E. This potentially confirms the existence of compartments with different hydrogeological characteristics. The 5/42E and 6/54E samples are relatively unique and differ quite significantly from the rest of the samples. The two samples are almost complete opposites in terms of their ionic concentrations of Ca, Alk, Cl, SO_4 and Na+K; where one is high the other is low.

In the Schoeller diagram, the deep level samples continue to show similar trends and the shallower samples also show similar trends consistent with observations in the piper diagram. The most notable difference between the shallower and the deeper samples is the Mg+. The deeper samples have far lower Mg+ concentration compared to the shallower samples and other ions. The 5/42E sample shows a unique trend in that it has the highest total alkalinity compared to all samples. The 15/54E sample appears to be in the mid-point between the deeper samples and the shallower samples as it has almost equal amounts of all ions shown on the diagram.

None of the isotope results plot on the GMWL which suggests groundwater at Dishaba Mine is probably old and not directly feeding from the rain. The sparse distribution relative to the GMWL suggests a variety of groundwater sources across the mine. Shallow level samples appear to be from a source more exposed to evaporation than the deep level samples. Potential sources for the shallow level samples are the mined-out pits and groundwater in the weathered zone that is feeding from surface water bodies.

The source of the groundwater intersected in the deep levels of Dishaba Mine has been a subject of several studies. Titus *et al*. (2009a) concluded that mine water ingress is driven by vertical leakages through fracture networks from the surface weathered aquifer and direct rainfall recharge. They further concluded that the major source and largest contributor to the mine ingress is regional flow from various sources through major fracture systems. Re-circulation from mine discharges was found to be a minor contributor to the overall groundwater ingress into the mine.

Morrow (2015) concluded that the groundwater ingress is from meteoric water that underwent water-rock interaction through the BIC and the Transvaal Supergroup sediments. Golder (2018) concluded that the BIC on its own was unlikely to be capable of storing large amounts of water due to the low porosity of its lithological units; instead, three aquifers around the Dishaba Mine area were identified as contributing to the groundwater ingress in the mine. These are the BIC (fractured aquifer), the Transvaal Supergroup (dolomites and sediments) and the Crocodile River alluvial sediments.

Considering the low porosity of lithological units across the mine, it is undisputable that fractures indeed play a critical role in the transmission and storage of groundwater at depth. The most likely

source to continuously feed the mine recharge is the Transvaal Supergroup sediments and dolomites. Interestingly though, the neighbouring Tumela Mine is relatively dry and hardly experiences any groundwater ingress into deep mine workings. This is despite the fact that the mine has a similar lithological makeup (Figure 10), mining method and goes to a depth of just below 1 km. This is the case pretty much across the western limb with mines hardly intersecting water below the weathered zone.

At Tumela Mine, the NW-SE striking major fault systems, locally named the Train Smash and the Little John fault systems, are predominantly the only ones with any significant groundwater ingress (O. Chingobo, personal communication, 2022). These faults extend into Northam Platinum's Zondereinde Mine, located south of Tumela Mine and have also been reported to bring groundwater ingress into that mine workings (O. Chingobo, personal communication, 2022).

The outcrop of the Transvaal Supergroup lies north of Dishaba Mine, just outside the BIC. A clear contrast between the BIC and the Transvaal Supergroup can be observed on surface with the landscape over the BIC being relatively flat and featureless (Lageat,1997; Wagner, 1925), in contrast to the mountainous Transvaal Supergroup. At Dishaba Mine, the Transvaal Supergroup is located some 2 km below the Critical Zone of the BIC (Golder, 2018). Considering the close proximity of the Tumela and Dishaba Mines, it is assumed that the location of the Transvaal Supergroup relative to the mines is generally similar. Considering the dryness of Tumela and the rest of the Western Limb mines, the outcrop side of the Transvaal Supergroup is likely not the major source of groundwater at depth. If it were, by fault extension and similarity in geology, Tumela Mine (and certainly other mines on the Western Limb) would likely have experienced similar groundwater issues as Dishaba Mine.

To better understand the relatively large volume regional flow, one has to question what makes the Dishaba Mine block more conducive to groundwater flow. Two possible answers are proposed:

1. The mine lies between two major faults systems. The Middellaagte Graben on the west and the Crocodile River Fault on the east (Figure 12). These major faults are associated with many relatively smaller but also significant faults with displacements above 10 m, such as the locally named Show-Stopper Fault. These synthetic faults also tend to have a generally NW-SE strike. These fault systems have possibly created a highly connected and extensive fault network capable of transmitting large volumes of water from outside the BIC. As a result of the synthetic faults, there is possibly numerous groundwater compartments across the mine.
2. The major faults described in Point 1 above extend into and past the Crocodile River Fragment which is located south of the mine (Figure 12). The Crocodile River Fragment is one of the most

prominent and highly deformed Transvaal Supergroup inliers that occur in the BIC (Hartzer, 1995). The Crocodile River Fragment consists of dolomites, sandstones and other sedimentary rocks of the Transvaal Supergroup. This makes it an excellent aquifer and potential recharge zone that feeds the major faults that bound and extend into Dishaba Mine.

A detailed geological description of the Crocodile River Fragment can be found in Hartzer (1989). Of the various theories on the structural relationship between the BIC and the Crocodile River Fragment, and the formation of the fragment, Hartzer (1989) and Hartzer (1995) concluded that the up-doming and faulting model is the most plausible. This up-doming of the Transvaal Supergroup exacerbated by the intrusion of the BIC is said to have resulted in extensive folding of the Crocodile River Fragment (Figure 62).

According to Hartzer (1989) there are three phases of folding in the fragment. The first are folds with an axial trend that varies from north-east to north-west in the northern to the southern parts of the fragment. Secondly, folds with an east-north-east striking axis, and thirdly, folds with a north-west to south-east striking axis. Two major faults with a south-east to north-west strike are said to be the last major deformational event that took place in the fragment. These faults cut across both the BIC and the Transvaal Supergroup and have been traced as far as the Brits Graben. These major faults are the Middellaagte Graben and the Crocodile River Fault.

Straskraba and Effner (1998) describe grouting and drainage as the two most common methods for groundwater control in underground mines. The advantages and disadvantages of the different water control methods for underground mines are listed in Table 11.

At Dishaba Mine, the current practice for dealing with groundwater ingress in the mine is diamond drilling and grouting. This practice is generally simple and with the application of common cement, it is relatively cost effective. The two main disadvantages are that grouting is not very effective over a large area of water ingress and it closes the conduits through which water is flowing and displaces it. Where the water gets displaced to when the conduits are closed, is not known. In the past there has been cases where grouting takes place in one mining end and water starts coming out in another (M. Moyo, personal communication, 2022). This shows how unpredictable and uncontrollable the grouting method is.

Another disadvantage of grouting is that it makes it difficult to harvest the groundwater in a controlled manner. This is because the known water-bearing fractures are sealed and the water flowing in them is displaced into an unknown location or fracture, thereby changing the known flow path that may have been determined through mapping and drilling.

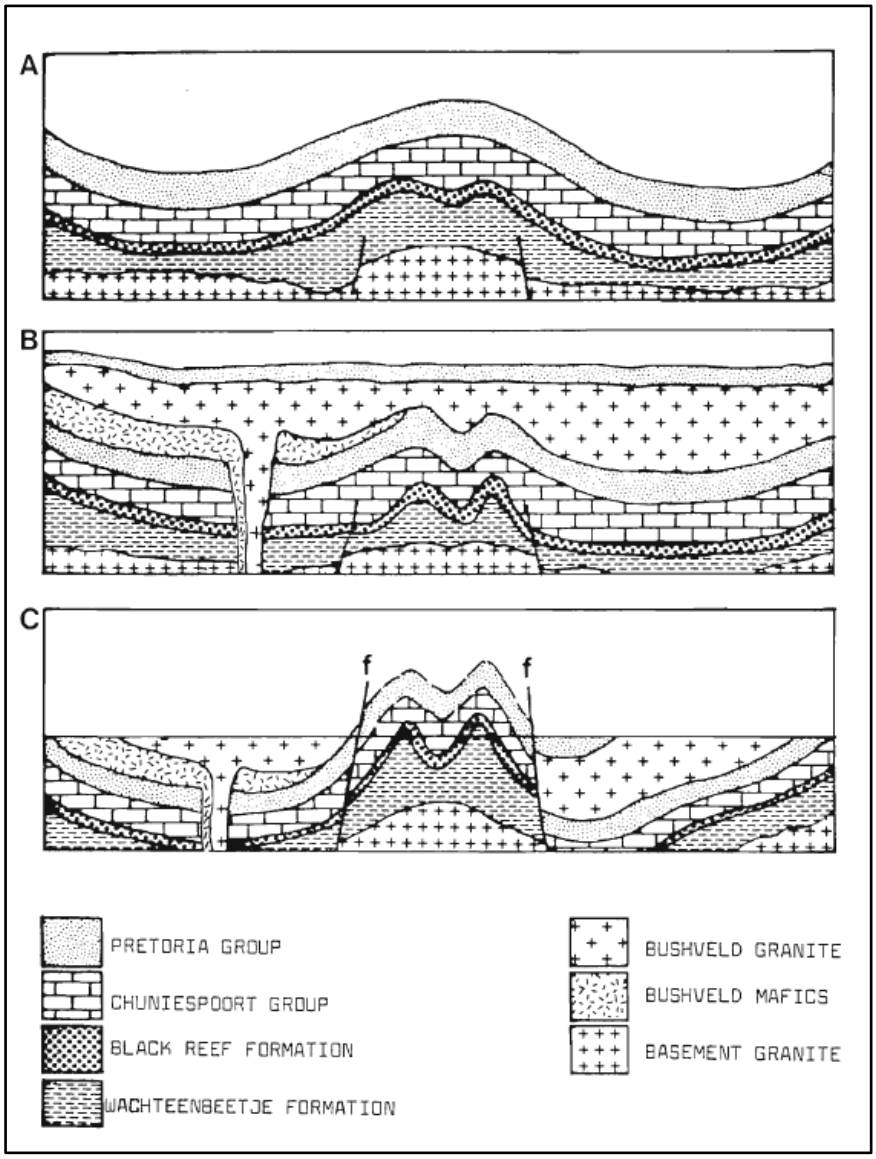

Figure 62: Tectonic-stratigraphic model for the Crocodile River Fragment (from Hartzer, 1995). Up-doming (A) started during the deposition of the Pretoria Group and folding took place along pre-existing structural lineaments. The intrusion of the BIC (B) enhanced the deformation in the fragment, which acted as a barrier to the mafic suite (or was covered with it). The resulting isostatic imbalance was corrected through two major faults (C), which caused the fragment to rise sharply on the eastern side, relative to the surrounding stratigraphy.

Dewatering in the mine is largely passive, this means there is no active seeking and removal of groundwater in the rock mass across the mine. Due to economic reasons, the mine changed the extraction strategy from predominantly mining the Merensky Reef to exclusively mining the UG2 Ref underground. This mostly eliminated the need for routine cover drilling because the UG2 Reef is mined from below the mined-out Merensky stopes. The assumption is that the Merensky Reef stopes will have exposed any water- and gas-bearing fractures, allowing gasses and water to drain out, thereby reducing the risk of gas and water intersections on the UG2 Reef horizon. Essentially, without cover drilling there is no dewatering, except when water is intersected by blasting and supporting activities.

Table 11: Water control methods for underground mines (Straskraba and Effner, 1998).

Water control method	Advantages	Disadvantages	Examples of practical application
Surface stream sealing and relocation	Prevents inflow into mine. Limits impacts on surface streams. Good for limited areas and small streams.	Can be costly for major streams. Cost of maintenance after spring run-off.	Neves - Corvo, Portugal Konkola - Zambia
Ground freezing	Highly efficient in aquifers with primary permeability. Most applications in shaft sinking.	Not practical in fractured rock. Most applications temporary only.	Many potash and coal mines in Europe and Canada.
Grouting	Highly effective to reduce flows and improve ground stability. Highly effective for smaller areas (faults). Can be used in materials with both primary and secondary permeability (granular materials and fractures). Variety of types of grout (cement, bentonite, microfine and chemical grouts) enables grouting of materials with wide range of permeability. Used for shaft sinking and underground mines.	Can be costly if large areas are to be grouted. Grouting boreholes must be typically spaced at 1.5 to 10 m. Groutingof low permeable materials with microfine or chemical grouts is expensive. Potential impacts on water quality. Difficult in high pressure, high permeability conditions.	Many shaft sinking projects in a form of pre-grouting or cover grouting. Grout cover during drift mining in water-bearing strata. Used as major water control method at many mines: Quirke 11 Mine, Canada; Deep Creek Mine, Canada; Southeatst Missouri Lead district; Konkola Mine, Zambia; Lamefoot Mine, Washington.
Wells from ground surface	Dewatering accomplished before mining. Large volume of water from wells up to 1 000 m deep. Pumped water not impacted by mining activities. Efficient in certain hydrogeological conditions for shaft sinking. No interference with the mining operations.	High cost of drilling deep wells. Not efficient in areas with many low permeable faults. High cost of pumping large volumes of water. Maintenance and power costs. Not efficient in low permeable strata and in rock with vertical fractures.	Several new gold mines in Nevada, USA (Meikle Mine, Turquoise Ridge Mine, West Leeville Mine). Homer Wauseca Mines, Michigan.
In-mine drainage boreholes	Low cost if combined with definition drilling. Gravity flow, no pumps or power necessary. Can be oriented to intersect major fractured systems. Boreholes can be used for drainage or grouting. Size of boreholes can be adapted for range of discharge rates.	Drainage possible only at later stage of mining. Plugging of boreholes in weathered or highly fractyred ground. Discharge from typical size of boreholes is limited.	Exclusively used for mine drainage in many mines: Konkola, Mulfira, Nkana Nchanga, Chambishi in Zambia; Kipushi, Kambove, Kamoto in Republic of Congo; Lamefoot and K-2 in Washington; Deepstar and Rosebud in Nevada; Kensington in Alaska; Henderson in Colorado; Hamilton in Australia.

When dealing with groundwater, options available to mine management are dewatering, diversion, sealing or a combination of methods (Morton and Mekerk, 1993). An active dewatering strategy coupled with a monitoring network aimed at the four critical compartments (Figure 61) would be a better suited strategy for the mine to follow and would ensure water supply and dry mining conditions. Drilling for dewatering should target NW-SE striking fractures and norite and anorthosite layers.

Cintolesi *et al*. (2020) give a detailed six-step framework for the development and implementation of a dewatering strategy (Figure 63). Steps 1 to 4 can be applied to studies and operations but Steps 5 and 6 are purely for operations. Step 5 puts emphasis on having specific dewatering targets and having alignment with mine planning. Specific lithologies and fracture networks have been identified as dewatering targets in this study. Step 6 emphasises monitoring and reporting. This is an area that needs improvement at Dishaba Mine.

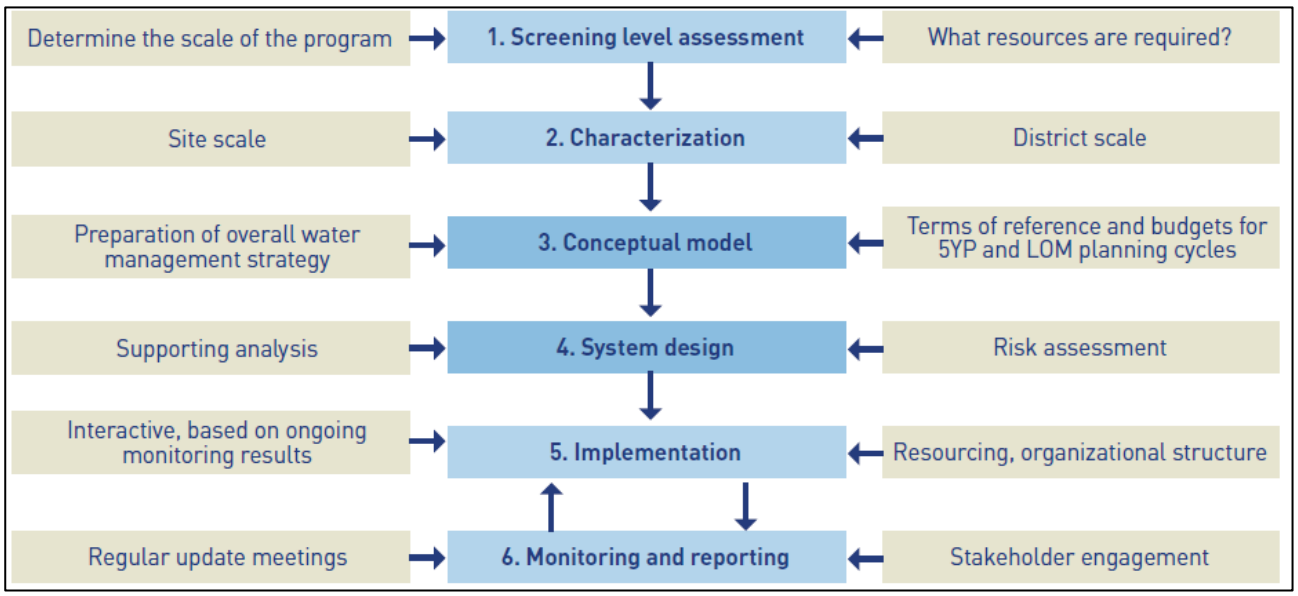

Figure 63 Steps for preparing and implementing the strategic dewatering plan (Cintolesi *et al*., 2020).

The groundwater chemistry results show a total of three potential water facies. Previous studies show that a dolomitic source is likely the biggest contributor to groundwater ingress at depth in the mine. Considering the discussion on the Crocodile River Fragment above, the following components of the conceptual model are hereby proposed:

1. Groundwater recharges through the Crocodile River Fragment. This is due to its favourable geology, i.e., dolomite and other porous sedimentary rock layers.
2. The groundwater then travels through the major fault systems (The Crocodile River Fault and Middellaagte Graben) and associated fracture networks to reach the mine. These fracture

systems are mainly NW-SE trending as observed underground. Titus *et al*. (2009) observed high inflow volumes in a mine in the Brits area, which (similar to Dishaba Mine) lies between the Crocodile River Fault and the Brits Graben, an extension of the Middellaagte Graben.

3. Additional groundwater rises up from the Transvaal Supergroup in the footwall of the BIC via young faults that cut across the BIC and the Transvaal Supergroup (Golder, 2018). This is largely water observed to be coming from the footwall of mine excavations, particularly below the UG1 horizon.

4. The leucocratic rocks (norite below UG1, anorthosite above the P1 and anorthosite below and above the Merensky Reef) deform in a relatively more brittle manner and as a result have more pronounced fracture networks making them the most suitable lithological layers in the Upper Critical Zone for groundwater flow and storage.

5. Due to the low primary porosity across the BIC, fractures are the main conduits through which water flows (Evans *et al*., 1997; Bense *et al*., 2013) The fractures create distinct compartments with different hydrogeological behaviours. These can be likened to the compartmentalisation model of a basin as proposed by Garven (1995) and modified by McCaffrey (1998) (Figure 64). There is potential for connectivity of the different compartments by structures that cut across the various compartments.

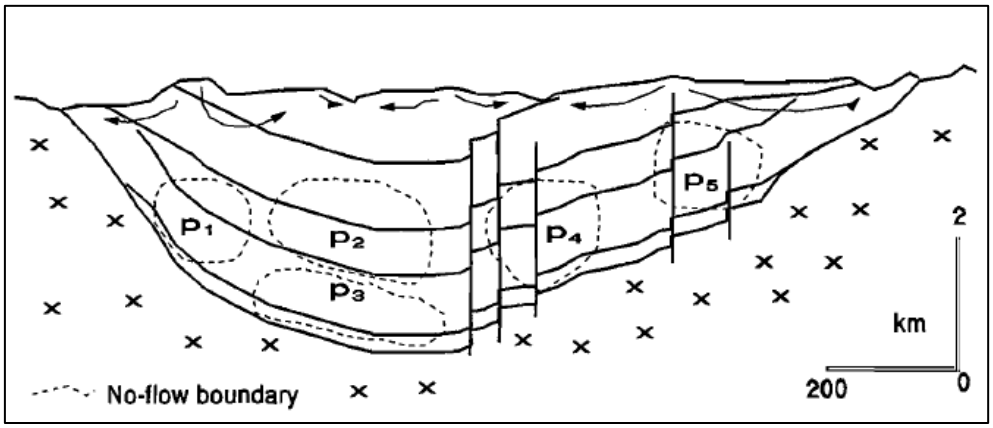

Figure 64: Compartmentalisation of a basin with compartments P1-P5 (Garven, 1995).

6. The differences in the compartments can also be ascribed to the different hydrogeological behaviour of faults. Underschultz *et al*. (2018) stated the following about faults:
    i. Faults can be both a barrier and a conduit,
    ii. Faults can have different hydraulic properties at different locations along the fault plane,

iii. The hydraulic behaviour of faults is a result of a combination of the geometry and architecture of the fault complex, the rheology of the host rocks that the fault cuts across, the distribution and orientation of in-situ stress, and,

iv. Fault hydraulic properties can depend on pressure, temperature, depth and stress; both at the time when the fault was formed and the present time.

7. Dykes at Dishaba Mine are dry or have no significant groundwater ingress associated with them. This is possibly due to dykes penetrating open fractures and therefore sealing them and displacing whatever water that could have been in the fracture. Since there is extremely low primary porosity, the dykes block off any potential recharge.

CHAPTER 6:
CONCLUSIONS AND RECOMMENDATIONS

6.1 INTRODUCTON

This chapter looks at the conclusions that may be drawn from the study and makes recommendations for future work to further improve the understanding of groundwater ingress at Dishaba Mine.

6.2 CONCLUSIONS

From this study, it can be concluded that there is between 5 and 9 ML/d of groundwater ingress. The groundwater is found across the mine; however, there are four compartments that clearly have significant volumes. These zones are:

- The Middellaagte Graben area located on the western side of the mine,
- The Show-Stopper Fault area,
- The 54E Line across all levels, and,
- The deep-most levels of the mine (17-19 Level).

Water ingress is predominantly associated with fractures that have a NW-SE strike and the leucocratic lithologies in the upper critical zone of the BIC. Dewatering as opposed to grouting in the compartments will result in better control and monitoring of groundwater and likely lead to dry mining conditions, particularly of the UG2 reef within the compartments. Mining of the Merensky Reef in the compartments remains a high risk for groundwater ingress as the norite and anorthosite are relatively closer to the reef, in some cases less than 3 m from the bottom and top contacts of the reef. Mining activities, e.g., support with 3 m cable anchors, can therefore expose or tap into the norite/anorthosite resulting in groundwater ingress into the stopes.

Drilling and grouting do not allow for effective monitoring and control of water ingress. Targeted active dewatering with monitoring will allow for better control and harvesting of the groundwater thereby increasing the groundwater supply for other activities in the mine and continuously provide data for hydrogeological modelling. Active dewatering should however be done well ahead of mining to minimise disturbance of mining activities, this can be achieved through effective planning and alignment of mining and dewatering activities.

The dolomitic source of groundwater is the Transvaal Supergroup dolomites, both located north of the mine and south of the mine in the Crocodile River inlier. The Crocodile River Fault and the Middellaagte Graben form a structurally complex compartment that is abnormally conducive to groundwater flow in the Bushveld Igneous Complex. This possibly explains the water issues being experienced in Dishaba Mine and the mine in Brits described by Titus *et al*. (2009).

6.3 RECOMMENDATIONS

Further studies to numerically understand the hydrogeological properties of the different compartments across the mine are required. These studies could include but not limited to packer tests, shut-in tests and continuous monitoring of groundwater flow. A compilation of groundwater related data into a formal database will greatly assist in collecting, storing, arranging and accessing data for future studies and improvement of groundwater models.

Active dewatering targeting specific compartments and lithologies will result in drier mining conditions and maintain groundwater supply for mining related activities. Having a larger groundwater quality assessment will assist in designing a pumping system that will separate clean water from mine service water. This may potentially allow for cost saving in relation to pumping water out from underground as the water can rather be used underground without having to be pumped out to be cleaned.

An expanded isotopic study that looks beyond the mine boundaries and covers the surface water bodies and groundwater from the Transvaal and Crocodile River inlier is required to trace the recharge to the mine and track the recharge flow path. The neighbouring Tumela and Zondereinde Mines could also provide valuable information on regional groundwater flow systems.

Closer collaboration between the hydrogeology, geotechnical and water management disciplines is required. There are several projects and studies that have groundwater components in different disciplines across the mine complex. Collection of data from these projects will help build up the groundwater database. Since hydrogeology is a recent addition to the Geosciences Department of Dishaba Mine, the application of this field is still in its infancy at the mine, and there is large scope for improvement.

REFERENCES

Anglo Platinum, 2009. Platinum, A precious metal for a precious planet. 2009 Annual report. Financial, social and environmental performance. Available at: https://www.angloamericanplatinum.com/~/media/Files/A/Anglo-American-Group-v5/Platinum/report-archive/2009/ar2009.pdf (Accessed 28/06/2023).

Bamisaiye, O.A., Eriksson, P.G., Van Rooy, J.L., Brynard, H.M., Foya, S., Billay, A., Nxumalo, V., and Adeola, A.M., 2016. Subsurface geometry of the northwestern Bushveld Igneous Complex, South Africa. Canadian Journal of Tropical Geography, Issue 3(1), pp. 28-36.

Basson, I., 2019. Cumulative deformation and original geometry of the Bushveld Igneous Complex. Tectonophysics, Volume 750, pp. 177-202.

Benettin, P., Volkmann, T.H., Von Freyberg, J., Frentress, J., Penna, D., Dawson, T.E. and Kirchner, J.W., 2018. Effects of climatic seasonality on the isotopic composition of evaporating soil waters. Hydrology and Earth System Sciences, 22(5), pp.2881-2890.

Bense, V.F., Gleeson, T., Loveless, S.E., Bour, O. and Scibek, J., 2013. Fault zone hydrogeology. Earth-Science Reviews, 127, pp.171-192.

Bromley, J., Mannström, B., Nisca, D., and Jamtlid, A., 1994. Airborne Geophysics: Application to a ground-water study in Botswana. Groundwater, 32(1), pp.79-90.

Buchanan, D.L., 1987. Platinum-group element exploration: targets and guidelines. Institution of Mining and Metallurgy Transactions. Section A. Mining Industry, 96.

Burdon. D.J. and Mazloum. S., 1958. Some chemical types of groundwater from Syria. UNESCO symp. Teheran, pp 73-90.

Cawthorn, R.G., 1999. The platinum and palladium resources of the Bushveld Igneous Complex. South African Journal of Science, pp. 481-489.

Cawthorn, R.G. and Lee, C., 1998. Field excursion guide to the Bushveld Igneous Complex. In 8th International Platinum Symposium. Geological Society of South Africa and The South African Institute of Mining and Metallurgy.

Cawthorn, R.G, Cooper, G.R.J., and Webb, S.J., 1998. Connectivity between the western and eastern limbs of the Bushveld Igneous Complex. South African Journal of Geology. 101 (4). 291-298.

Cawthorn, R.G., Eales, H.V., Walraven, F., Uken, R., and Watkeys, M.K., 2006. The Bushveld Igneous Complex. In: The geology of South Africa. Johannesburg/Pretoria: Geological Society of South Africa/Council for Geosciences, pp. 261-281.

Chingobo, O., 2022. Conversation with Dumakude S.K., 9 July.

Cintolesi, C., Beale, G., Dowling, J., Kotze, J., Rowland, A. and Mansell, S., 2020. Anglo American framework for strategic dewatering plans. In Slope Stability 2020: proceedings of the 2020 international symposium on slope stability in open pit mining and civil engineering (pp. 1291-1304). Australian Centre for Geomechanics.

Cook, P.G., 2003. A guide to regional groundwater flow in fractured rock aquifers. CSIRO Land and Water, Glen Osmond, SA, Australia.

Craig, H., 1961. Isotopic variations in meteoric waters. Science, 133, 1702–1703.

Dumakude, S.K., Moyo, M., and Mokoka, T.D., 2022. Structure model update note for the record. Anglo Platinum internal report. Not published.

Durov S.A., 1948. Natural waters and graphic presentation of their compositions. Dokl Akad Nauk SSR 59:87-90

DWA, 2013. Climate Change Adaptation Strategy for Water. DWA report Number: P RSA 000/00/18012/5. Department of Water Affairs, Pretoria, RSA. April 2013.

DWAF, 2008. Best Practice Guideline - A6: water management for underground mines. South African Department of Water Affairs and Forestry. Pretoria. South Africa.

Eales, H.V., and Cawthorn, R.G., 1996. The Bushveld Igneous Complex. In layered Intrusions, Edited by Cawthorn R.G. Elsevier, Amsterdam. p 181-229.

Evans, J.P., Forster, C.B. and Goddard, J.V., 1997. Permeability of fault related rocks, and implications for hydraulic structure of fault zones. Journal of Structural Geology, 19, 1393-1404.

Faunt, C.C., 1997. Effect of faulting on ground-water movement in the Death Valley region, Nevada and California (No. 95). US Department of the Interior, US Geological Survey.

Ferreira, S.J.S., 2012. A trade-off study between down-dip and breast mining on the Merensky Reef at Khomanani 2. Journal of the Southern African Institute of Mining and Metallurgy, 112(4), 257-266.

Friese, A., 2004. Assessment of the structural geology and its impact on mining of Business Area 3 (#2 Shaft Area), Amandelbult Section. Anglo Platinum. Internal Document, Not Published.

Garven, G., 1995. Continental-scale groundwater flow and geological processes. Ann. Rev. Earth planet sci. 23. 89-117.

Gebrekristos, R. and Cheshire, P., 2012. Hydrogeological properties of the UG2 pyroxenite aquifers of the Bushveld Igneous Complex. In Proceedings of the 5th Platinum Conference of the Southern African Institute of Mining and Metallurgy (pp. 143-152).

Gerber, R., 2022. Combat rockfall and rockburst accident in tabular metalliferous mines underground. Internal Mandatory Code of Practice, Dishaba Mine. Not published.

Golder, 2016. Assessment of the hydrochemical and environmental stable isotope (ESI) signatures from a set of water samples from the Anglo American Amandelbult platinum mine area. Anglo American Platinum internal memorandum. Not Published.

Golder, 2018. Updated Amandelbult groundwater modelling report. Anglo American Platinum internal report. Not published.

Golder, 2018a. Amandelbult Groundwater Management Project. Hydro(geo)chemistry assessment. Anglo American Platinum Internal Presentation. Not Published.

Groundwater Complete. 2021. Annual assessment of groundwater monitoring results for 2020. Anglo Platinum Amandelbult Platinum Mine Internal Report. Not published.

Hartzer, F.J., 1989. Stratigraphy, structure, and tectonic evolution of the Crocodile River Fragment. South African journal of geology, 92(2), pp.110-124.

Hartzer, F.J., 1995. Transvaal Supergroup inliers: geology, tectonic development and relationship with the Bushveld Igneous Complex, South Africa. Journal of African Earth Sciences, 21(4), pp.521-547.

Jager, A.J., and Ryder, J.A., 1999. (Editors). A handbook on rock engineering practice for tabular hard rock mines. The Safety in Mines Advisory Committee (SIMRAC). Johannesburg.

Koutsoukos, P.G., and Kontoyanni, C.G., 1984. Precipitation of Calcium Carbonate in Aqueous Solutions. Journal of the Chemical Society Faraday Transactions. I,80, 1181-1192

Kruger, F., 2005. Filling the Bushveld Igneous Complex magma chamber: lateral expansion, roof and floor interaction, magmatic uncomformities, and the formation of giant chromite, PGE and Ti-V-Magnetite deposits. Mineralium Deposita, pp. 451-472.

Kruger, F.J., 1990. The stratigraphy of the Bushveld Igneous Complex: a reappraisal and the relocation of the Main Zone boundaries. South African Journal of Geology, pp. 376-381.

Kruger, F.J., 1992. The origin of the Merensky cyclic unit: Sr-isotopic and mineralogical evidence for an alternative orthomagmatic model. Australian Journal of Earth Sciences, 39(3), pp.255-261.

Lageat, Y. 1997. Geomorphology of the Bushveld Igneous Complex. Coruña. Vol. 22, pp. 209-227

Lonergan, A.J. and Cange, J.B., 1994. Cation and Anion Analysis: Application s to Enhance and Expedite Site-Level Hydrogeological Investigations: Proceedings of the 1994 Focus Conference on Eastern Regional Ground Water Issues. The National Ground Water Association, pp.619-630.

Maakamedi, R. and Moyo, M., 2018. Dishaba 62E Thrust Fault System. Anglo American Platinum Internal Presentation. Not published.

Maier, W.D and Walters, B.M., 1994. The UG2-Merensky Reef interval at Amandelbult Section, Rustenburg Platinum Mines: patterns of lateral variation in lithology. South African Journal of Geology., 1994,97(1),45-51

McCaffrey, L.P., 1998. Distribution and causes of high fluoride groundwater in the western Bushveld area of South Africa. University of Cape Town. PhD Thesis.

Meteoblue, 2022. Simulated historical climate & weather data for Thabazimbi. Available at: https://www.meteoblue.com/en/weather/historyclimate/climatemodelled/thabazimbi_south-africa_949683 (accessed 13/05/2022)

Mitchell, A.A., 1990. The stratigraphy, petrography and mineralogy of the Main Zone of the northwestern Bushveld Complex. South African Journal of Geology, 93(4), pp.818-831.

Mitchell, A.A., Scoon, R.N. and Sharpe, M.R., 2019. The Upper Critical Zone in the Swartklip Sector, north-western Bushveld Complex, on the farm Wilgerspruit 2JQ: II. Origin by intrusion of ultramafic sills with concomitant partial melting of host norite-anorthosite cumulates. South African Journal of Geology 2019, 122(2), pp.143-162.

Mofomme, P., 2021. Conversation with Dumakude S.K., 18 February.

Mohlahlana, N., 2019. Structural analysis and tectonic interpretation of the Thabazimbi Kumba Iron Mine region, using the Operational Land Imager (OLI), Landsat 8 satellite imagery. MSc Thesis. University of Pretoria.

Mohulatsi, T., 2022. Dishaba Mine Isopachs for geotechnical considerations. Anglo American Platinum Internal Presentation. Not Published.

Morton, K.L. and Van Mekerk, F.A., 1993. A phased approach to mine dewatering. Mine Water and the environment, 12(1), pp.27-33.

Morrow, M., 2015. Geochemical and geothermal contributions to thermal springs associated with the Bushveld and Waterberg area, Limpopo. BSc Hons. Thesis. University of the Witwatersrand. Not published

Moxham, K A., 2004. A hard rock narrow reef mining machine – ARM 1100, in Proceedings of the First International Platinum Conference: 'Platinum Adding Value', Sun City, South Africa, 3rd – 7th October 2004, The South African Institute of Mining and Metallurgy, pp207-214.

Moyo, M., 2020. Conversation with Dumakude S.K., 2 March.

Moyo, M., 2022. Conversation with Dumakude S.K., 8 July.

Naldrett, A.J., Wilson, A., Kinnaird, J. and Chunnett, G., 2009. PGE tenor and metal ratios within and below the Merensky Reef, Bushveld Igneous Complex: implications for its genesis. Journal of Petrology, 50(4), pp.625-659.

Ngubane, S.E., Maakamedi, R., Mademutsa, C., and Malenga, S., 2015. Impacts of groundwater in business planning at Dishaba Mine. SAIMM. MPES 2015. Johannesburg. South Africa.

Nxiweni, N., 2020. Conversation with Dumakude S.K., 02 June.

Piper, A.M., 1944. A graphic procedure in the geochemical interpretation of water-analyses. Eos, transactions American geophysical union, 25(6), pp.914-928.

Sami, K. and Hughes, D.A., 1996. A comparison of recharge estimates to a fractured sedimentary aquifer in South Africa from a chloride mass balance and an integrated surface-subsurface model. Journal of Hydrology, 179(1-4), pp.111-136.

SANS., 2015. South African National Standard 241-1. Drinking water quality. South African Bureau of Standards.

Schoeller, H., 1962. Groundwaters. Paris: Mas-son and Cie.

Sibiya, B., 2017. AMB Strat Code Sign Off. Anglo American Platinum Internal Report. Not Published

Stiff Jr, H.A., 1951. The interpretation of chemical water analysis by means of patterns. Journal of petroleum technology, 3(10), pp.15-3.

Straskraba, V., and Effner, S., 1998. Water control in underground mines – Grouting or drainage? Proceedings of IMWA Symposium. Johannesburg. p195-212.

Titus, R., Witthüser, K., Bumby,. A., Holland, M., and Rossouw, T., 2009. Integrated groundwater management for Amandelbult. Anglo Platinum Internal Report, Not published.

Titus, R., Witthüser, K. and Walters, B., 2009a. Groundwater and mining in the Bushveld Igneous Complex. Proceedings of the International Mine Water Conference, Pretoria, South Africa, 2009, 178 – 184.

Underschultz, J., Esterle, J., Strand, J., and Hayes, S., 2018. Conceptual representation of fluid flow conditions associated with faults in sedimentary basins. Prepared for the Department of the Environment and Energy by The University of Queensland Centre for Coal Seam Gas, Queensland. 61p.

Viljoen, M.J., 1999. The nature and origin of the Merensky Reef of the western Bushveld Igneous Complex based on geological facies and geophysical data. South African Journal of Geology, 102(3), pp.221-239.

Viljoen, M.J. and Schurmann, L.W., 1998. Platinum group metals. In: Wilson, M.G.C and Anhaeusser, CR. (Eds.), The Mineral Resources of South Africa. Coun. Geosci., S. Afr., Pretoria, S. Afr., 532-568.

Viring, R.G. and Cowell, M.W., 1999. The Merensky Reef on Northam Platinum Limited. South African Journal of Geology, 102(3), pp.192-208.

Wagner, P.A., 1925. Notes on the platinum deposits of the Bushveld Igneous Complex. Geological Society of South Africa.

Walters, B.M., Snyman, Q., and Theron, K., 2004. A guide to the geology of Amandelbult. Amandelbult Geology Internal Report. Not published.

Waring, C.L., Hankin, S.I. and Perl, T., 2004. Seismoelectric survey results from the south Australian riverland near Loxton and Berri: Australian Society of Exploration Geophysicists, Extended Abstracts, 1-6.

Weaver, J.M., Cave, L. and Talma, A.S., 2007. Groundwater sampling. Water Research Commission Report No. TT, 303(07).

WRC., 1998. Quality of domestic water supplies. Volume 1: Assessment guide. Water Research Commission Report No: TT 101/98.

Wyns R., Baltassat, J.M., Lahcassagne, P., Legchenko, A., Vairon, J., Mathieu, F., 2004. Application of SNMR soundings for groundwater reserves mapping in weathered basement rocks (Brittany, France). Bulletin de la Société Géologique de France, Vol. 175 (1), pp. 21-34.

Zhou, C.B., Chen, Y.F., Hu, R. and Yang, Z., 2023. Groundwater flow through fractured rocks and seepage control in geotechnical engineering: Theories and practices. Journal of Rock Mechanics and Geotechnical Engineering, 15(1), pp.1-36.

ABSTRACT

This study investigates groundwater ingress into an underground mine on the northern edge of the Western Limb of the Bushveld Igneous Complex (BIC). The water ingress occurs at depths ranging from less than 300 m to over 1000 m below ground surface and presents an opportunity for the mine to potentially use the groundwater and reduce reliance on potable water supplies. Striking the balance between keeping the mine dry and maintaining a water supply presents a challenge that can only be overcome by fully understanding the quantity, quality and source of the groundwater. These make up the conceptual model of the mine and therefore improving the conceptual model of the mine became imperative.

Underground mapping, hydrochemistry sampling and stable isotope analysis were undertaken to delineate the quantity, quality, and possible source of the groundwater. The BIC is known to have low primary porosity and groundwater occurrence is therefore largely associated with the fractures that make up the fractured rock aquifer. However, underground mapping and the diamond drilling database revealed that in addition to fractures, there are certain lithological units that are prone to groundwater ingress.

Groundwater chemistry showed three groundwater facies and a generally good water quality that can be largely classified as Class II as per SANS 241 standard. The stable isotopes showed a varied groundwater source between the shallower levels and deeper levels. The Crocodile River Fragment is proposed to be a major recharge source via the Crocodile River Fault and the Middellaagte Graben Fault systems.

A move away from grouting to a groundwater management system centred around active dewatering and monitoring is proposed to ensure a water supply, as well as dry and safe mining conditions. The continuous updating of the conceptual hydrogeological model with monitoring data is recommended. Further studies to numerically understand the hydrogeological properties of the different compartments across the mine are also required. The development of a groundwater database at the mine will lead to a better understanding and facilitate future studies into the water ingress at the mine.